

University of Southern Queensland
Faculty of Health, Engineering and Sciences

**Using a sprinkler infiltrometer and the GAML model to
predict moving sprinkler performance in the field**

A dissertation submitted by

Mr Simon Kelderman

0011120971

In fulfillment of the requirements of

Bachelor of Engineering (Agricultural)

October 2015

Abstract

The Green-Ampt (1911) equation has been regarded as one of the foremost infiltration models. Mein and Larson's (1971) work extended its use to modelling infiltration under rainfall conditions, known as the GAML model, and Chu (1987) further extended its use to time-varying application rates such as occurs under moving sprinkler systems. However, Chu only demonstrated the efficacy of his work using simple, idealised application patterns that are not seen in the real world. This project, then, sought to extend Chu's work by testing it in the field using real sprinkler performance data.

Sprinkler performance data, using Nelson brand centre-pivot S3000 sprinkler heads, was collected for the project in the hydraulics laboratory at USQ, Toowoomba. A sprinkler infiltrometer was used in the field to determine modified GAML model parameters, per Chu (1986). A computer program written in Matlab, based on the graphical methods of Chu (1987), used the laboratory sprinkler data and the modified GAML parameters to make a prediction of the runoff that would be generated from a specified time-varying application rate. A mobile sprinkler rig was constructed to deliver the time-varying application rate of water in the field.

A new concept for a sprinkler infiltrometer was tested in the course of the project. Initial work in the laboratory appeared promising but the concept failed to meet expectations in the field, principally due to wind interference. Consequently a small droplet-forming sprinkler infiltrometer was constructed and used for all of the field testing.

The process of determining the modified GAML model parameters was reasonably successful. However, predictions of runoff by the computer model were consistently far larger than that measured. This was believed to be for two key reasons. Firstly, whilst Chu's (1987) method worked well for simple application patterns, it appeared to struggle with real data and so the predicted runoff by the computer program could only be regarded with suspicion. Secondly, there were significant difficulties collecting all of the runoff from the soil plots in the field. These two reasons for the disparity between predicted and measured runoff meant that this project was not able to conclusively affirm or reject Chu's (1987) method for applying the GAML model as being suitable for use with real moving sprinkler systems in the field.

Limitations of Use

The council of the University of Southern Queensland, its Faculty of Health, Engineering and Sciences, and the staff of the University of Southern Queensland, do not accept any responsibility for the truth, accuracy or completeness of material contained within or associated with this dissertation.

Persons using all or any part of this material do so at their own risk, and not at the risk of the Council of the University of Southern Queensland, its Faculty of Health, Engineering & Sciences, or the staff of the University of Southern Queensland.

This dissertation reports an educational exercise and has no purpose or validity beyond this exercise. The sole purpose of the course pair entitled 'Research Project' is to contribute to the overall education within the student's chosen degree program. This document, the associated hardware, software, drawings, and other material set out in the associated appendices should not be used for any other purpose: if they are so used, it is entirely at the risk of the user.

Dean

Faculty of Health, Engineering & Sciences

Candidate's Certification

I certify that the ideas, designs and experimental work, results, analyses and conclusions set out in this dissertation are entirely my own effort, except where otherwise indicated and acknowledged.

I further certify that the work is original and has not been previously submitted for assessment in any other course or institution, except where specifically stated.

Simon Kelderman

0011120971


.....
Signature

15 - October - 2015
.....

Date

Acknowledgements

I was advised some time ago (I forget by whom) that I should choose a project topic in an area that I would like to know a lot about. Hydraulics and irrigation science have been the two areas of study during this undergraduate degree that I have enjoyed the most, and it made sense to select a topic related to these. Dr Joseph Foley, my project supervisor, lectured in both of these areas of study and the quality of his teaching and his encouragement were significant in setting me on this path. So I wish to express my appreciation and thanks for his influence as well as his project supervision.

My thanks goes to the Cotton Research and Development Corporation for the financial assistance received. Thank you also to the USQ technical staff at the hydraulics laboratory who allowed me to take over a good part of the laboratory for the sprinkler testing and provided support in various ways.

And thank you to Rebecca, my wife, who has cheered me on all along.

Simon Kelderman

October 2015

Contents

Abstract	iii
Limitations of Use	v
Candidate’s Certification	vii
Acknowledgements	ix
List of Figures	xv
List of Tables	xix
Nomenclature and Modelling Parameters	xxi
Modelling parameters and variables	xxii
Chapter 1 - Introduction	1
1.1 Background to the Project.....	1
1.2 Objectives of the Project	2
1.3 Outline of the Project.....	3
Chapter 2 – Literature Review	5
2.1 Significance of Sprinkler Irrigation	5
2.2 The Infiltration Process.....	7
2.3 Modelling Infiltration	10
2.3.1 Numerical Models	10
2.3.2 Empirical Models.....	12
2.3.3 Analytical Models.....	15
2.3.4 Factors that affect infiltration models.....	16
2.4 Infiltrimeters	20
2.4.1 Poned Ring Infiltrimeters.....	20
2.4.2 Sprinkler and Rainfall Infiltrimeters.....	21
2.5 The Green-Ampt Infiltration Model	24
2.5.1 Model Concept.....	25
2.5.2 Assumptions	27
2.5.3 Advantages.....	28
2.5.4 Limitations and Difficulties.....	29
2.5.5 Developments upon the Green-Ampt Equation	36
2.6 Approximating Sprinkler Patterns for Use in Infiltration Models.....	44
2.7 Literature Review Summary.....	48

Chapter 3 – Methodology	49
3.1 Determining an Infiltration Characteristic and Predicting Runoff	49
3.2 STEP ONE: Determine GAML Parameters with Sprinkler Infiltrometer	50
3.2.1 The Sprinkler Infiltrometer.....	51
3.2.1.1 The SHCAZ Sprinkler Infiltrometer.....	51
3.2.1.2 A Reserve Sprinkler Infiltrometer: The ‘Bucket Infiltrometer’	56
3.3 STEP TWO: A Computer Model to Predict Runoff and Infiltration	57
3.3.1 Part 1 of the Computer Model: Determine the Infiltration Characteristic	57
3.3.2 Part 2 of the Computer Model: Estimating Runoff under Sprinklers.....	59
3.3.3 Desktop Testing of the Computer Model.....	61
3.4 STEP THREE: Field Measurements of Runoff	61
3.4.1 Mobile Sprinkler Rig.....	61
3.4.2 Collecting Runoff	64
Chapter 4 – Results and Analysis	69
4.1 Preparatory Work and Computer Model Testing	69
4.1.1 Laboratory Sprinkler Testing.....	69
4.1.2 Desktop Testing of Computer Model	76
4.2 Field Observations and Model Predictions	82
4.2.1 The SHCAZ Sprinkler Infiltrometer.....	82
4.2.2 The Bucket Infiltrometer	83
4.2.3 Mobile Sprinkler Rig.....	85
4.2.4 Detailed Results for a Single Pair of Tests	88
4.2.5 Summarised Results for All Tests	93
4.3 Summary of Results	95
Chapter 5 – Discussion	97
5.1 Sprinkler Data Collection	97
5.2 Field Testing	100
5.2.1 Sprinkler Infiltrometers.....	100
5.2.2 Mobile Sprinkler Rig.....	102
5.2.3 Measuring Runoff.....	103
5.2.4 Difference between Predicted and Measured Runoff Values	104
Chapter 6 – Conclusions	109
6.1 Achievement of Project Objectives	109
6.2 Further Work and Recommendations	111
List of References	113

Appendices	123
Appendix A – Project Specification	125
Appendix B - Chu’s Method for Determining GAML Parameters	127
Appendix C - Matlab Code Used in Part 1 and Part 2 of Computer Model.....	131
C1. Code for Part 2 of Computer Model.....	131
C2. Code for Part 1 of Computer Model.....	134
C3. Further Code for User Written Functions	137
Appendix D - Selected Laboratory Sprinkler Data.....	141
Appendix E: Field Data	173
Appendix F - Project Administration.....	185
F1. Project Risk Management.....	185
F2. Project Planning: Timelines, Resource Requirements	187
F3. Consequential Effects of the Project	189

List of Figures

Figure 2–1: Irrigation in Australia by area watered, 2013-14 (ABS 2015).....	6
Figure 2–2: Infiltration under ponded conditions (Williams et al. 1998, Fig. 1, p.2).....	8
Figure 2–3: The change of infiltration rate with time where the soil is not ponded at time $t = 0$ (Ravi & Williams 1998, Fig.2, p.3)	9
Figure 2–4: A double-ring infiltrometer featuring Mariotte tubes (ASTM 2009, Fig.2, p.3)	20
Figure 2–5: A photo of a small droplet forming rainfall simulator (Singh et al. 1999, Fig.2a, p.172)	22
Figure 2–6: A portable rainfall simulator using a single pressurised nozzle. The plot area is 1.5m x 2.0m (Humphrey et al. 2002, Fig.1, p.201).....	22
Figure 2–7: A sprinkler infiltrometer in operation (Tovey & Pair 1966, Fig.1, p.359)..	24
Figure 2–8: Illustration of the Green-Ampt parameters and the concept of the 'piston flow' water movement down through the soil profile (Ravi & Williams 1998, Fig.3, p.7)	26
Figure 2–9: An example of an $S - k_r$ curve (capillary suction vs relative conductivity) for selected soils (Mein & Larson 1971, Fig.13, p.33)	32
Figure 2–10: Variation of capillary suction, h_f , with moisture content (Mein & Larson 1971, Fig.7, p.11). Curve (1) is typical of a sandy soil, and curve (2) is typical of a clay soil.....	33
Figure 2–11: The total infiltration flows and the matric sub-components of the total infiltration flows obtained using the Green-Ampt equation with constant and time- dependent h_f (Kunze & Shayya 1993, Fig.1, p.1095).	34
Figure 2–12: An example of the variability of h_f with time, for three different initial soil moisture conditions (Kunze & Shayya 1993, Fig.3, p.1096).....	34
Figure 2–13: A 'typical textbook infiltration curve' (Mein & Larson 1971, Fig.4, p.8)	37
Figure 2–14: Infiltration curves for three different cases of infiltration behaviour (Mein & Larson 1973, Fig.1, p.385). Curve D is the case when the soil is saturated from time $t = 0$. Curve A is the case when rainfall is always less than K_s . Curve BC is the case when rainfall is greater than K_s but initially less than infiltration capacity.....	38

Figure 2–15: An illustration of Mein & Larson's (1973) Case 'C' where ponding or runoff is generated because infiltration capacity has become less than rainfall intensity (Williams et al. 1998, Fig.2, p.3).	38
Figure 2–16: Example of when there are multiple occasions when application rate exceeds infiltration capacity.....	41
Figure 2–17: An illustration of the graphical method proposed by Chu (1987, Fig.2, p.159) to solve the generalised Mein-Larson model.	43
Figure 2–18: An example sprinkler application rate curve showing a triangular approximation to the observed data (Slack 1980, Fig. 1, p.598)	44
Figure 2–19: An example sprinkler application rate curve (Slack 1980, Fig.2, p.599) that demonstrates that in some cases the chosen triangular or elliptical approximation poorly reflects the observed data.	45
Figure 2–20: A variable rainfall pattern of an idealised elliptical form (Hachum 1978, Fig.2, p.504).....	45
Figure 2–21: An example of a more 'typical' rainfall pattern (Morel-Seytoux 1978, Fig. 3, p.563).	46
Figure 2–22: An example of the commonly assumed elliptical irrigation application pattern (DeBoer 2001, Fig. 1, p.1217).	46
Figure 2–23: An example of trapezoidal and elliptical approximations of measured sprinkler data (DeBoer 2001, Fig.3, p.1218).....	47
Figure 3–1: An example of a sprinkler radial leg profile. This example is of a Nelson S3000 with #21 nozzle, 10 PSI, height 2.44m, red plate. There is no zone of constant application rate in this profile.	51
Figure 3–2: An example of a sprinkler radial leg profile that exhibits a zone of constant application rate. This example is of a Nelson S3000 #44 nozzle, 25 PSI, height 2.44m, red plate.	52
Figure 3–3: Illustration of the SHCAZ infiltrometer concept. From the data shown in Figure 3-2 this Soil Test Plot would be expected to receive a uniform 27mm/hr. .	52
Figure 3–4: Nelson S3000 Spinner head assembly with yellow plate and #18 nozzle (www.nelsonirrigation.com).	53
Figure 3–5: Sprinkler head set-up, with the pressure line to primary pressure gauge and the secondary pressure gauge shown.	54
Figure 3–6: Schematic of the layout for the sprinkler radial leg data collection.	55
Figure 3–7: A Cornell Sprinkler Infiltration Meter in use (Molacek et al. date unknown). ..	56

Figure 3–8: The ‘bucket infiltrometer’ used as a reserve sprinkler infiltrometer,	57
Figure 3–9: Flowchart describing the process used in Part 1 of the computer model.....	58
Figure 3–10: Flowchart describing the process used in Part 2 of the computer model. .	60
Figure 3–11: The mobile sprinkler rig that was constructed for Step 3 of the project....	61
Figure 3–12: Sketch of the mobile sprinkler rig showing key dimensions. Not drawn to scale.	62
Figure 3–13: The mobile sprinkler rig as used in the static role as a sprinkler infiltrometer. The other 3 sprinkler heads have been removed and capped off.....	63
Figure 3–14: A schematic drawing showing how the water supply hose was repeatedly divided in an identical manner for each of the sprinklers.	64
Figure 3–15: Sketch of side profile of the soil plot sloping down to the trench with an inlaid PVC half-pipe.	65
Figure 3–16: Sketch of end-view of PVC trough sitting in soil trench and sloping down to collection container.	65
Figure 3–17: One of the soil plots. The adjacent soil plot, the diverting trench (upslope) and protective cover have not been prepared yet and are not shown.	66
Figure 4–1: Naming format for sprinkler test results.....	70
Figure 4–2: Plots of the catch-can data for the Sred25_44 sprinkler test. The second plot includes the catch-can directly beneath the sprinkler head.	73
Figure 4–3: Plots of the catch-can data for Sred6_44 sprinkler test.....	76
Figure 4–4: Output from desktop testing of Part 1 of computer model using the first set of Chu's (1986) infiltration data.	78
Figure 4–5: Output from desktop testing of Part 1 of computer model using second set of Chu's (1986) infiltration data.	79
Figure 4–6: Example of the iterative process used per Chu (1987) for Part 2 of the computer model. These plots correspond to the Silt Loam of Table 4-7. The red dashed line has been added in for illustrative purposes.....	81
Figure 4–7: Photo of the mobile rig with sprinklers running. Note the flowmeter and pressure gauge at the bottom right.	85
Figure 4–8: Photo of the rig before sunrise. Note the reflective ropes used to stabilise the structure and reduce sagging of the horizontal bar.	85
Figure 4–9: Screen-shot of video of sprinkler rig www.youtube.com/watch?v=8fFEglt_iJg	86

Figure 4–10: Plots produced by the computer model for the Sred6_44 sprinkler. The top two plots are for the single sprinkler, and the bottom two are for four overlapping sprinklers.....	87
Figure 4–11: Cumulative infiltration (I) versus time (t) for Test 6A.....	89
Figure 4–12: Plots from Part 1 of computer model for Test 6A.	91
Figure 4–13: Cumulative infiltration versus time (<i>I vs t</i>) for all of the sprinkler infiltrometer tests.....	94
Figure 4–14: Comparison of predicted runoff volumes (red squares) from the sprinkler infiltrometer tests and the measured runoff volumes (blue diamonds) using the mobile sprinkler rig.....	95
Figure 5–1: Sprinkler test data for a Nelson Sred6_44 when measured at 0.25m intervals.....	98
Figure 5–2: Sprinkler test data for the same Nelson Sred6_44 when measured at 1.0m intervals.....	98
Figure 5–3: Chu’s (1987) iterative graphical method failing to settle on stable values for a complex sprinkler application pattern (Compare Figures 2-17 and 4-6).	105

List of Tables

Table 2-1: Comparison of estimated ponding time, t_p , calculated from four methods (Chu 1987, Table 1, p.161)	43
Table 4-1: Suitable sprinkler configurations for SHCAZ Sprinkler Infiltrometer concept.	70
Table 4-2: Catch-can data for Sred25_44 test.....	71
Table 4-3: Test conditions for the Sred25_44 test.....	72
Table 4-4: Catch-can data for Sred6_44 test.	74
Table 4-5: Test conditions for the Sred6_44 test.	75
Table 4-6: Cumulative Infiltration (I) vs time (t) data from Chu (1986).	77
Table 4-7: Comparison of predicted time-to-ponding for two different soils by different approaches. The numerical solution to Richard's equation and Chu's graphical method are both per Chu (1987).....	80
Table 4-8: Bucket Infiltrometer performance parameters.	83
Table 4-9: Details of test conditions common to all pairs of tests.	84
Table 4-10: Example data (from Test 6A) collected when using sprinkler infiltrometer.	89
Table 4-11: Summary of results for the 9 pairs of field tests.	93

Nomenclature and Modelling Parameters

In this project, the term ‘model’ is used as per the Oxford English Dictionary to mean a simplified description, especially a mathematical one, of a system or process, to assist calculations and predictions (Oxford 2015). Generally the term will not be used to refer to a computer model; when it is necessary to do so, the term ‘computer model’ or ‘computer algorithm’ will be used explicitly.

Matric potential, soil water pressure, capillary tension, capillary pressure, and capillary suction are sometimes used as though they were synonymous, even though there are differences between these terms. In this project the term ‘capillary suction’, which is a positive value, has been preferred.

Runoff and ponding are both phenomena that occur as a consequence of the situation where the rate of water application to a soil surface exceeds the infiltration capacity of the soil (see Section 2.2). Pondered water does not flow laterally, and runoff does flow laterally. However, in this project, when the term ‘runoff’ is used it is usually to represent both phenomena, unless explicitly stated otherwise.

Similarly, the term ‘rainfall’ is sometimes used in this project to represent water applied by either rainfall or sprinkler irrigation, except when the context makes it clear otherwise. This is just to save having to repeatedly say ‘rainfall and sprinkler irrigation’.

Modelling parameters and variables

θ_0	initial (antecedent) soil moisture content (L^3/L^3)
θ_s	saturated soil moisture content (L^3/L^3), equal to porosity
$\Delta\theta$	change in soil moisture content (L^3/L^3), equal to $\theta_s - \theta_0$
h_f	capillary suction, a positive value whose magnitude is equal to capillary pressure which is a negative value (L)
i	instantaneous infiltration rate (L/T)
I	cumulative infiltration (L)
K	hydraulic conductivity (L/T)
K_e	effective hydraulic conductivity (L/T), approximately equal to $0.5K_s$
K_s	saturated hydraulic conductivity (L/T)
r	rainfall (or sprinkler) application rate (L/T)
R	cumulative rainfall (or sprinkler) application (L)
t	time (T)
t_p	time to ponding (T)
t_s	pseudotime (T), a concept used by Chu (see Section 2.5.5.2)
z	depth to wetting front (L)

Chapter 1 - Introduction

1.1 Background to the Project

Irrigation is an important part of agriculture around the globe, and sprinkler irrigation is playing an increasing role within that. However, sprinkler irrigation tends to be capital and energy intensive and its design and management should be undertaken holistically. In particular, a reasonable match between the soil properties, crop requirements and sprinkler performance should be sought. However, it has often been the case that this has not been done, or that data used in the design process was generated by methods that are unrepresentative of sprinkler irrigation. Thus the sprinkler irrigation system may be operated inefficiently to the detriment of water use efficiency, crop productivity, environmental protection, and financial profitability. Considering the large financial investment that is generally needed to undertake sprinkler irrigation, it is arguably worthwhile to have an appropriate assessment done of the sprinkler-soil system.

One aspect of a sprinkler-soil system assessment is to determine the behaviour of infiltration for the soils in question. Sometimes this is not done at all; at other times it may be determined in a laboratory or perhaps in the field typically using ponded infiltrometers. None of these scenarios are ideal because they do not give a good representation of the infiltration process that is occurring under sprinkler irrigation.

The Green-Ampt-Mein-Larson (GAML) model was developed in the 1970's in response to this need for a suitable method to estimate the infiltration and runoff properties of a system under sprinkler or rainfall conditions. The GAML model was the theoretical basis for this project.

1.2 Objectives of the Project

The primary objective of this project was to investigate an alternative method for estimating runoff that will be generated from a sprinkler irrigation event that has a time-varying application rate. The method under investigation was based upon the work of Green and Ampt (1911), Mein and Larson (1971), and Chu (1986, 1987). Chu's work appeared promising but was not tested against real sprinkler data in the field; this project sought to make that next step.

The project was an attempt to apply the GAML-plus-Chu model to the case of a simple moving sprinkler system (purpose-built for this project) to predict its performance in terms of infiltration and runoff generation. Rather than separately attempt to predetermine the soil hydraulic properties for the field where the sprinkler system will operate, as is generally done, a sprinkler infiltrometer was used to estimate modified forms of the GAML parameters immediately before the irrigation event. These, in turn, were used to make a prediction of the surface runoff that would be generated from the field from a given irrigation event.

Successful attainment of this objective was, admittedly, always going to be a difficult prospect because there were many possible confounding factors. It was hoped, however, that by predetermining the GAML parameters of the field using a sprinkler infiltrometer (to mimic the sprinkler irrigation process), in the immediate vicinity of the sprinkler system, and immediately before running the sprinkler-system, that some of the confounding factors could be mitigated against.

1.3 Outline of the Project

The project was comprised of seven phases.

- Phase 1. A literature review of 91 books and papers was undertaken.
- Phase 2. 67 sprinkler performance tests, each of about 30min to 60min duration, were undertaken to search out and find suitable data for use in subsequent phases.
- Phase 3. Writing of a computer program (590 lines in Matlab) to apply the data from Phase 2 using a GAML-based model.

Phase 2 and Phase 3 were undertaken concurrently.

- Phase 4. Desktop testing of the computer algorithm by using the methods of Chu (1986, 1987) to compare against two sets of published results in the literature.
- Phase 5. Construction of a sprinkler rig capable of use as both a sprinkler infiltrometer and as a moving sprinkler system.
- Phase 6. Field testing (9 tests) using the sprinkler rig as a static infiltrometer to gather infiltration versus time data and determine GAML parameters for use by the computer model.
- Phase 7. Field testing (9 tests) using the sprinkler rig as a moving system to compare the computer model's predictions against observed results.

Phase 6 and Phase 7 were necessarily undertaken together.

The literature review is contained in *Chapter 2*. Descriptions of the computer model and the field and laboratory test procedures are included in *Chapter 3*. The results and analysis from Phases 2, 4, 6 and 7 are included in *Chapter 4* and the discussion of these results and issues that arose follows in *Chapter 5*.

Chapter 2 – Literature Review

91 papers and books were reviewed or referred to in the undertaking of this project. The key ideas have been summarised in this chapter.

2.1 Significance of Sprinkler Irrigation

Irrigation is becoming increasingly important for agriculture around the world, especially as arid and semi-arid regions seek to increase crop productivity, crop diversification and stability of food supply (Rossi 2015, Postel 1999). Sprinkler irrigation already comprises a significant proportion of irrigated land, and surface irrigated lands are steadily being converted to sprinkler irrigation due to labour and water concerns (Kincaid 2005). Nearly one third of irrigated land in the United States is already irrigated by centre-pivots (Kincaid 2005). Figure 2-1 shows that 29% of Australian irrigation is under sprinklers of all forms (ABS 2015), of which 45% is irrigated by centre-pivots or lateral-move (CPLM) machines. Some growers have been reluctant to convert to sprinkler irrigation because of misinformation regarding the extent of evaporative losses; Uddin et al. (2014) showed that additional evaporative losses due to use of sprinklers are actually only about 4% rather than up to 45% as is sometimes cited. In Queensland's Murray Darling Basin, 66% of CPLM operators are irrigating on heavy clay soils, and a further 31% are irrigating on clay loam soils (Wigginton 2011). Among these operators, the primary drivers for adopting CPLM irrigation are to save labour, save water and reduce waterlogging (Wigginton 2011).

There are a number of difficulties that are sometimes experienced with sprinkler irrigation. Travelling laterals can have very high application rates, sometimes exceeding the soil's intake rate, which can lead to runoff and/or ponding in lower parts of the field (Addink et al. 1975). Some sprinkler systems have been designed to use low-pressure nozzles with high peak application rates, which means the wetted diameters of the sprinklers are too small, in order to save energy (Luz 2011). However, again, this may cause surface runoff, especially on low-infiltration soils such as the heavy clays of the Murray Darling Basin mentioned above. Surface runoff and / or ponding are undesirable

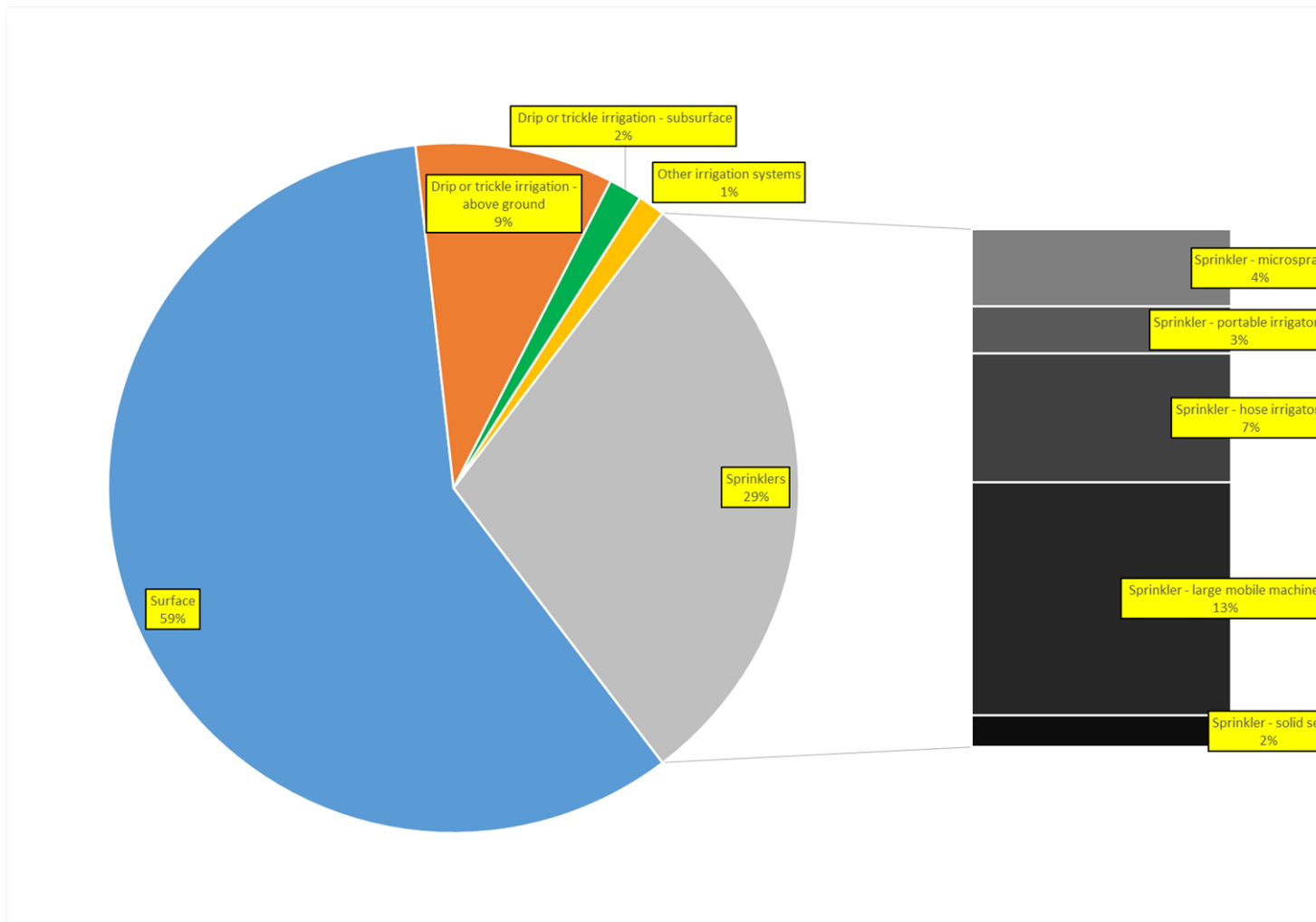


Figure 2-1: Irrigation in Australia by area watered, 2013-14 (ABS 2015)

for several reasons. They lead to reduced uniformity of water application across a field (Kincaid 1969); they waste resource inputs (DeBoer 2001), both of water and the energy used to move the water; they may promote surface sealing and crusting (Jennings et al. 1988); and may lead to reductions in crop yields (DeBoer 2001). The runoff may also carry fertilisers and soil components off the field and detrimentally affect the water quality of downstream receiving waters (DeBoer 2001).

2.2 The Infiltration Process

There has been great interest in studying and modelling infiltration from a diversity of disciplines, including agriculture, irrigation design, hydrology, soil science, civil engineering and environment sciences (Assouline 2013; Ravi & Williams 1998). In particular, there has been a concerted effort on the part of hydrologists to understand infiltration because it has the largest influence on the volume of catchment runoff generated from a given rainfall event (Mein & Larson 1973).

Infiltration can be defined as ‘the entry of water into the soil surface and its subsequent vertical motion through the soil profile’ (Assouline 2013, p.1755). This is a process under the influence of gravity (although gravity may not necessarily be the primary driver) in contrast to when water moves as horizontal flow in the absence of gravity forces, a process known as ‘sorption’.

The following description of the infiltration process is, for the most part, per Assouline (2013), Williams & Ouyang (1998), and Ravi & Williams (1998). Water supplied to a permeable soil surface will enter down through that surface (unless the soil volume is confined by impermeable barriers or is already fully saturated). The rate at which the water will enter the soil will decrease as the volume of water entering the soil increases until eventually a limiting rate is reached (which has usually been taken to be the soil’s ‘saturated hydraulic conductivity’, K_s). Bower (1969) argued that $0.5K_s$ should be used instead of K_s when modelling infiltration due to various effects (see Section 2.5.4.1). The rate of water entry at the soil surface is driven predominantly by capillary forces, or matric potentials. When the water has entered the soil, then both gravitational and capillary forces are important in moving the water down through the soil profile. Capillary forces

vary inversely and non-linearly with the soil moisture and can exhibit enormous variation between soil types and within soil types under different management regimes.

Figure 2-2 shows the zones in the soil profile as the infiltration process occurs under ponded conditions. In the saturated zone the pores are all filled with water (this may only extend to a few millimetres depth). The transition zone features a rapid decrease in water content with depth, extending perhaps only a few centimetres. The transmission zone makes up the majority of the soil moisture profile and features nearly uniform water content with depth. The wetting zone has a steep decrease in water content and sits between the transmission zone and the wetting front, and the wetting front is the boundary between the 'dry' and wetted soil. Water flow in the wetting front and wetting zone is driven predominantly by capillary forces, whereas flow in the top three zones is driven predominantly by gravity forces.

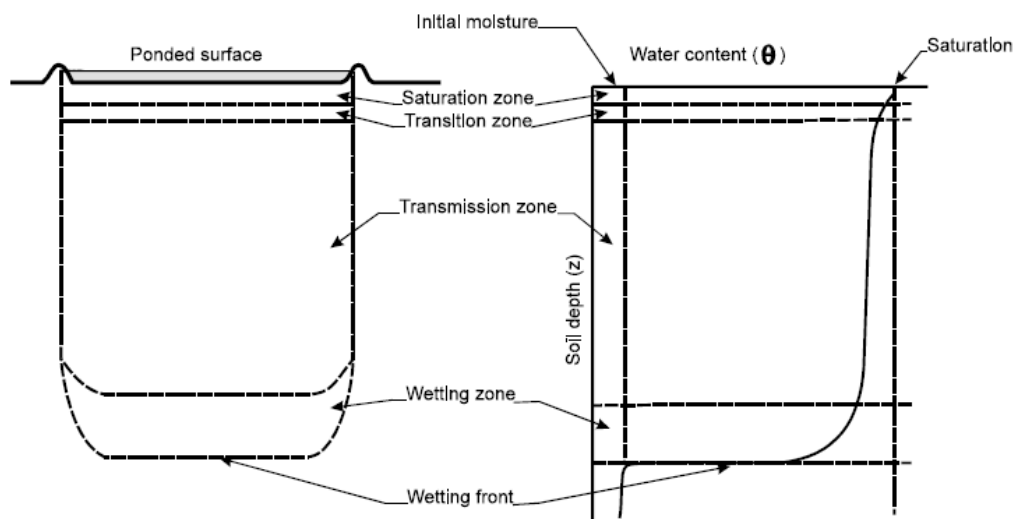


Figure 2-2: Infiltration under ponded conditions (Williams et al. 1998, Fig. 1, p.2)

There are many factors that affect the infiltration process. These include the water supply rate and the pattern of application; the elapsed time since the onset of water application; the hydraulic properties of the soil, including porosity, conductivity, antecedent moisture content, sorptivity, and connectivity of pores; the depth of the soil; the presence of impermeable sub-layers such as the rock bed or plough pans; the chemical properties of the soil and water; water and soil temperature; and biological activity.

While the soil surface is ponded the water supply rate and application pattern are of no consequence. However, if the surface is not ponded then these factors become critical. If the water is supplied at a greater rate than the soil's ability to allow the water to enter, the excess water will accumulate on the soil surface and/or become runoff (Figure 2-3). The 'infiltration capacity' (i) of a soil is the maximum rate at which the water can enter through the soil surface, often expressed in units of mm/hr or cm/hr. It depends on the initial soil moisture content of the soil and on the temporal pattern of application of water. Under ponded conditions the infiltration capacity will always decrease monotonically to K_s as infiltration continues.

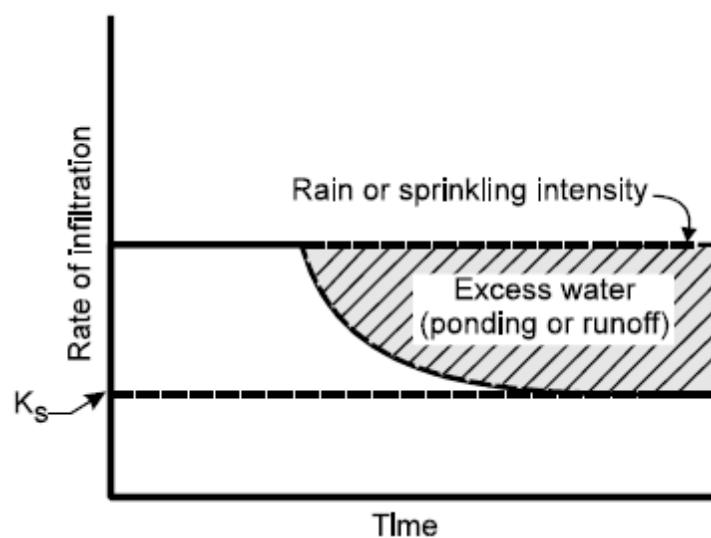


Figure 2–3: The change of infiltration rate with time where the soil is not ponded at time $t = 0$ (Ravi & Williams 1998, Fig.2, p.3)

Under sprinkler irrigation or rainfall, if the application rate is less than K_s then it can continue indefinitely and no ponding or runoff will occur. This scenario is generally of little interest to hydrologists (Morel-Seytoux 1978) but may be of interest to irrigators, especially those operating fixed sprinkler systems (Tovey 1966). Hillel (1982) termed this type of infiltration process as 'supply controlled'. If the application rate is greater than K_s then initially the applied water will be imbibed by the soil until such a time when the soil becomes saturated, termed the 'ponding time' (t_p). Thence the sub-surface water movement will govern the infiltration capacity ('profile controlled' per Hillel 1982), which will decrease with continuing water application. If the infiltration capacity becomes less than the application rate then water will accumulate on the surface or runoff.

2.3 Modelling Infiltration

In this project, the term ‘model’ is used as per the Oxford English Dictionary to mean a simplified description, especially a mathematical one, of a system or process, to assist calculations and predictions (Oxford 2015). Generally it will not be referring to a computer model; when it is necessary to do so, the term ‘computer model’ or ‘computer algorithm’ will be used explicitly.

‘There is of course no such thing as an equation of infiltration in general’ (Morel-Seytoux & Khanji 1974, p.795). Indeed, there are a plethora of techniques to estimate water infiltration into soil. For the purposes of this project, however, the infiltration models can be divided into the following three categories per Ravi & Williams (1998): empirical models; analytical models (principally Green-Ampt models); and numerical models based on the Richards equation. These categories will be briefly surveyed below. Williams et al. (1998) noted that the selection of a model should be subject to the model’s suitability for intended use, the model’s efficiency, the model’s reliability, and the model’s credibility. With regard to the model’s credibility they stated that:

“The credibility of the model, and that of the theoretical framework represented, is based on the model’s proven reliability, and on its acceptance by users. Model credibility is a major concern in model use. Therefore, special attention should be given in the selection process to ensure the use of qualified simulation models which have undergone adequate review and testing.” (Williams et al. 1998, p.16)

2.3.1 Numerical Models

Numerical modelling of infiltration is usually about finding solutions to the Richards equation. The Richards equation (Richards 1931) is based upon the Darcy-Buckingham law (which is analogous to Darcy’s law):

$$q = -K(\theta)\nabla\Psi(\theta) \quad (2-1)$$

where

q	water flux
θ	volumetric water content (as a function of time and location)
K	unsaturated hydraulic conductivity of the soil (as a function of θ)
ψ	total soil water head (as a function of θ)

The Darcy-Buckingham law is combined with the continuity equation to get the general Richards equation:

$$\frac{\partial \theta}{\partial t} = \nabla(K(\theta)\nabla h(\theta)) - \frac{\partial K(\theta)}{\partial z} \quad (2-2)$$

where h is the capillary head. Because the vertical infiltration of water can be treated as a one-dimensional problem, the general Richards equation can be simplified to:

$$\frac{\partial \theta}{\partial t} = \frac{\partial}{\partial z} \left(K(\theta) \frac{\partial h(\theta)}{\partial z} \right) - \frac{\partial K(\theta)}{\partial z} \quad (2-3)$$

The variables h and θ are dependent on each other and so the one-dimensional Richards equations can be rewritten in terms of either h or θ . This version of the Richards equation assumes isothermal conditions, homogenous isotropic soil, and a rigid porous medium that allows air to freely escape (Assouline 2013). It also requires that the relationship between θ and ψ be known, which is the water retention curve, or soil moisture characteristic.

Numerical solutions to the Richards equation are not only used ‘to solve the partial differential equations of porous media flow and thus provide a model... ..they can be used in designing infiltration experiments and interpreting infiltrometer results’ (Smith 1976, p.507). They are also frequently used as a benchmark against which to evaluate empirical or analytical models. Mein & Larson (1973, p.385) stated that ‘though the Richards equation... ..is not suitable for general application, it is considered the best method available for computing vertical flow of soil moisture’ and thus invaluable for evaluations and comparisons.

The Richards equation is a nonlinear, parabolic partial differential equation and generally analytical solutions are not possible. Numerical methods are thus used but convergence and stability remain ongoing problems and the equation continues to be a challenge to solve (Assouline 2013). Furthermore, the results tend to come in sets of numbers and there is difficulty in generalising the results or understanding the mechanics of the process (Hachum & Alfaro 1978). The requirement for large amounts of data about soil hydraulic parameters makes the use of Richards equation impractical except for research use (Ravi & Williams 1998; Morel-Seytoux & Khanji 1974; Mein & Larson 1973).

2.3.2 Empirical Models

Empirical models are equations that have been formed by curve-fitting to actual measured data. They are generally relatively simple and seek only to describe input-output relations (Smith 1975). They feature parameters that are specific to particular data and have no apparent physical basis (Ravi & Williams 1998). The emergence of empirical models that related infiltration rate to time came about, in part, because of ‘the importance of infiltration and the need to describe it quantitatively on one hand and the high non-linearity of the [Richards] flow equation on the other’ (Assouline 2013, p.1757).

Several of the more significant empirical models used for modelling of infiltration are highlighted below.

2.3.2.1 Kostiakov’s Equation

The Kostiakov equation (also referred to as the Kostiakov-Lewis equation) is of the form:

$$i(t) = \alpha t^{-\beta} \quad (2-4)$$

$$I(t) = \frac{\alpha}{1-\beta} t^{(1-\beta)} \quad (2-5)$$

where

- i infiltration rate [mm/hr] at time t [hr]
- I cumulative infiltration [mm] at time t [hr]
- α, β empirical constants to be fitted ($\alpha > 0, 0 < \beta < 1$)

Because $i(t) \rightarrow 0$ as $t \rightarrow \infty$ the equation for $i(t)$ is usually modified to:

$$i(t) = i_f + \alpha t^{-\beta} \quad (2-6)$$

where i_f is the steady final infiltration rate [mm/hr] as $t \rightarrow \infty$ (Assouline 2013, p.1757). The Kostiakov equation is often used in modelling of surface irrigation (Assouline 2013) and whilst it generally performs well at small time values, it becomes less accurate at large times (Ravi & Williams 1998). Also, the equation does suggest that the infiltration rate is infinite at the beginning of the test, which clearly is not true. On a side note, Swartzendruber (1993) pointed out that Kostiakov never wrote the power-of-time equation $i = \alpha t^{-\beta}$; rather, his contribution was to propose that $K_t = K_0/t^\alpha$ where K_t is the coefficient of absorption at time t, and K_0 is the coefficient of absorption responding to the air-dry condition of the soil. Swartzendruber argues that it was not possible to get from the equation for K_t to the equation for $i(t)$ without making ruthless assumptions that Kostiakov never would have taken. Instead, there is ‘a historical basis for an unambiguous attribution of [the equation for $i(t)$] to Lewis (1937)... ..I now propose and recommend that [the equation for $i(t)$] be called the Lewis equation.’ (Swartzendruber 1993, p.2456).

2.3.2.2 Horton’s Equation

The Horton equation is the most widely used empirical equation in hydrology (Ravi & Williams 1998). It is of the form:

$$i(t) = i_f + (i_o - i_f)e^{-\gamma t} \quad (2-7)$$

$$I(t) = i_f t + \frac{1}{\gamma}(i_o - i_f)(1 - e^{-\gamma t}) \quad (2-8)$$

where i_0 , i_f and γ are the empirical constants to be fitted. Unlike Kostiakov's equation, the infiltration rate is finite at the beginning of the test. For the purposes of predicting ponding time (t_p) under sprinkler irrigation, Gencloglan et al. (2005) found the Horton equation to perform much better than the Kostiakov equation.

2.3.2.3 Philip's Two-Term Model

The Philip's two-term model is the truncated version of Philip's (1957) Taylor series solution (Williams et al. 1998):

$$i(t) = \frac{1}{2}St^{-\frac{1}{2}} + A \quad (2-9)$$

$$I(t) = St^{\frac{1}{2}} + At \quad (2-10)$$

where S is the sorptivity [$\text{mm/hr}^{1/2}$] and A is an empirical constant to be fitted. The Philip's two-term model is equivalent to the Kostiakov equation for particular sets of parameters. The model assumes a homogenous soil; uniform and constant soil water content; and that water content near the surface is constantly near saturation. The model is suited to early stages of infiltration into a relatively dry soil (Assouline 2013) but there is an assumption of an excess water supply at the surface and thus the model does not handle a time lag between onset of water application and ponding as well as other models (Williams et al. 1998; Mein & Larson 1973).

2.3.2.4 Other Empirical Models

Other significant empirical infiltration models include, without explanation here, Mezencev's equation, the Soil Conservation Service (SCS) method, Boughton's equation, and Holtan's equation. Interestingly, like the Green-Ampt equation, Holtan's equation is not a function of time but, in Holtan's case, of the unoccupied pore space in the soil (Mein & Larson 1973). A major difficulty with the Holtan model is that the

estimated infiltration capacity is highly dependent on the arbitrarily selected control depth of soil (Mein & Larson 1971). Smith (1976) further argued that Holtan's equation did not agree with hydraulic principles, but maintained nonetheless that it was still superior to the SCS method that required that the infiltration predicted by the SCS be proportional to the rainfall rate.

Empirical models are used for their simplicity and low computing demands. However, some significant difficulties detract from their use. They need to be fitted to observed data or to data extrapolated from other fields or catchments (Wilson et al. 1982). Without specific data, the parameters are difficult to predict or calculate because they are obscure and have no physical significance (Mein & Larson 1973, Smith 1976). There is difficulty of correlating regression constants with governing physical parameters (Jennings et al. 1988), and they 'do not consider the changes in the initial water content without obtaining a new flooded infiltration rate curve' (Hachum & Alfaro 1978, p. 500). They are, essentially, spatially and temporally restricted and they are dependent on infiltrometer testing having been done.

2.3.3 Analytical Models

Analytical models are theoretically derived from a physical law, such as Darcy's Law, and as such tend to be more general and enable a better understanding of the phenomena involved (Hachum & Alfaro 1978; Mein & Larson 1971). A key advantage of the analytical models is that they often use physical parameters that can be determined by experiments or inferred from other data obviating the need for curve-fitting and, perhaps, site-specific field experiments (Slack 1980). However, the derivation of analytical models frequently involves making simplifying assumptions that can be critical under certain conditions (Hachum & Alfaro 1978).

The Australian scientists W.H. Green and G.A. Ampt (1911) were the first to derive a physically-based analytical model to describe infiltration, since known as the Green-Ampt equation. It has been the subject of great scrutiny and many developments thereupon, particularly within the hydrology disciplines. The Green-Ampt equation continues to be the model of choice for estimating infiltration in many physically-based

hydrology models (Ravi & Williams 1998). Section 2.5 below will discuss the Green-Ampt model in more detail.

Analytical models can become mathematically very complex. Some authors have complained of such models becoming ‘mathematical overkill’, subject to such an array of parameters that, though being physically determinable, require such extensive time and effort in the laboratory or field to measure that is unjustifiable given the approximate nature of infiltration equations (Smith 1975, p.762). Some authors have advocated the use of graphical methods to solve analytical infiltration models (Luz 2011; Chu 1987), sometimes producing results identical to the more accurate, but demanding, Richards equation (Chu 1987). However, these graphical methods can be cumbersome and are generally not easily included into computer-based algorithms for modelling infiltration.

2.3.4 Factors that affect infiltration models

There are many factors to account for when modelling infiltration, some of which have been mentioned already. Empirical equations avoid the need to directly address these factors by simply fitting a curve to the measured data to determine the equation’s parameters; the trade-off, however, is that it becomes very difficult to know how the model’s parameters might apply to, or be modified for, different field condition from whence they were determined.

Besides the pattern of water application, some of the more significant factors for infiltration modelling are as follows below.

2.3.4.1 Crusting and surface sealing

A surface seal and a soil crust, which may only be in the order of 0.1mm and 1-3mm thick, respectively, can reduce infiltration by up to an order of magnitude (Brakensiek & Rawls 1983). Jennings et al. (1988) found that puddling following rainfall impact on unprotected soil surfaces, especially those with small soil aggregates, could cause a surface crust to form upon drying which is responsible for up to a 107 fold decrease in

the hydraulic conductivity for subsequent water application events. Philip (1998) argued that the Green-Ampt model is ill-fitted for the analysis of crusted soils.

2.3.4.2 Chemical and physical properties

Soil swelling during wetting due to high clay contents; soil sodicity and electrolyte concentrations of the irrigation water; and thermal effects of the soil and water were all cited by Assouline (2013) as impacting upon the hydraulic properties of soil and will consequently affect infiltration.

2.3.4.3 Macropores

When a soil surface is generating runoff, or is ponded, macroscopic channels such as cracks, root holes or worm holes can conduct water and enhance its vertical transfer. This has been termed ‘preferential flow’ or ‘bypass flow’ (Crescimanno et al. 2007). However, this will not occur when the water application rate is less than the infiltration capacity of the soil (Davidson 1985). Davidson (1985) cites several studies that confirm that infiltration is increased by the presence of macropores and that the water may infiltrate laterally at depth bypassing the unsaturated zone (Beven & Germann 1982).

2.3.4.4 Dynamic nature of soils (temporal variability)

‘Predicting runoff generation on arable land is inherently difficult due to the rapidity with which soil and crop conditions change’ (Van den Putte 2013, p.343). Rawls et al. (1983) discussed how surface roughness and porosity of the soil can change within a growing season due to natural and operational processes.

2.3.4.5 Surface storage of water

The amount of runoff will depend on the amount of water that can accumulate in the depressions of a rough soil surface and on the slope (Rossi 2015; Gencloglan et al. 2005). This amount is termed the ‘retention capacity’ of the soil (Chu 1978). Luz (2011) found that his models had a general trend of runoff over-prediction and suggests that surface storage factors might have contributed to this result. Smith (1976) cautioned that modellers must understand that the time to ponding (t_p) is not a depression storage phenomenon and that such depression storage of water can result in significant lag of response. Rossi (2015, p.3) found that there has not been a lot of investigation into the ‘effect of micro-topographic surfaces and the related hydrological connectivity on the spatial distribution of surface water and infiltration flows.’

2.3.4.6 Entrapped soil air and air viscosity

Assouline (2013, p.1766) said that infiltration is

“basically a problem of immiscible movement of water and air. Under natural conditions, the movement of air is generally small... ..However, under conditions of flood irrigation, intense rainfall, and soil column experiments, air can be compressed at the wetting front and beyond and reduce significantly the infiltration rate until it could find a way to escape and release the pressure build-up.”

Jarret and Fritton (1978) observed that soil air could become entrapped and compressed ahead of the wetting front. This has the effect of reducing the gradient head that is driving the infiltration. The air pressure may eventually become sufficiently large that the air can escape via the larger pores to the surface, and infiltration will then proceed at an increased rate (Jarret & Fritton 1978), which may mean that the infiltration capacity function is not always monotonically decreasing. Wilson et al. (1982) found that the largest soil pores, which are the most efficient at conducting water, were often occupied by air that can become entrapped. Thus the hydraulic conductivity can actually be much less than K_s determined in the laboratory (Wilson et al. 1982).

Morel-Seytoux (1978) pointed out that most of the major studies that had been undertaken toward predicting ponding time and infiltration rates had neglected the air viscous effect. Morel-Seytoux and Khanji (1974) formed an infiltration equation based on the GAML model that accounted for air viscosity. They found that neglecting the air viscosity term could cause errors in predicted infiltration rates of 10% – 40%. Similarly, Jarrett and Fritton (1978) found that air-trapped treatments showed a reduction in infiltration rates of 45%. ‘Even without air compression effects, the mere air viscous resistance to flow can affect infiltration rates significantly (Morel-Seytoux 1975, p.763). Bouwer (1969) recommended that the K value required for the Green-Ampt model should be half that of the fully saturated K_s value, which appears consistent with the models that factor in air-entrapment and air viscosity.

In conclusion, the great number of infiltration models is due, in part, to the inclusion or exclusion of these and other influencing factors. Rossi and Ares (2015, p.2) conceded that ‘complex interactions of runoff generation, transmission and re-infiltration over short temporal scales... ..add difficulties in the estimation of infiltration and overland flows.’ Thus many of these factors are simply ignored by the major infiltration models.

“Perhaps this and other easily improved infiltration models have been perpetuated because they are most often used (or evaluated) in hydrologic situations which are either insensitive to errors of infiltration pattern, or where other uncertainties override.” (Smith 1976, p. 507).

Mein & Larson (1971, p. 7) commented that

“It follows then that a simple infiltration model which will be accurate for natural soils is not possible, for the complete description of the soil itself is impracticable. One can only hope to produce a model which will give a reasonable estimate of the infiltration behaviour.”

Van den Putte et al. (2013, p.333) concurred, remarking that

“The [modelling] approaches vary in complexity with respect to the (assumed) description of the factors controlling infiltration and hence also with respect to the information that is required. It is, however, still unclear whether the incorporation of

additional effects through a more refined model description and/or through more refined parameter estimation methods do indeed result in better predictive capabilities.”

2.4 Infiltrometers

Infiltrometers are a means of applying water to a field soil so that soil hydraulic data can be measured or inferred. The two main methods are ponded infiltrometers and sprinkler/rainfall infiltrometers.

2.4.1 Ponded Ring Infiltrometers

Ponded ring infiltrometers can be single-ring or double-ring. The latter is preferable as it simplifies calculations and reduces bias that can result from the three-dimensional flow that will occur near the outer boundary of the wetting zone (Smith 1976; McQueen 1969). Indeed, lateral movement of water past the outer boundary of the soil plot is generally considered to be a primary source of error (McQueen 1969). The double-ring ponded infiltrometer has been used extensively in infiltration research. It consists of concentric rings that have been driven into the soil and often a set of Mariotte tubes to maintain a constant water depth within the rings (Figure 2-4). The volume of water infiltrated into the soil from the inner ring is measured against time and plotted to produce the infiltration capacity function. The test method for use of double-ring ponded infiltrometers on soils is specified by ASTM D3385-09 (ASTM 2009).

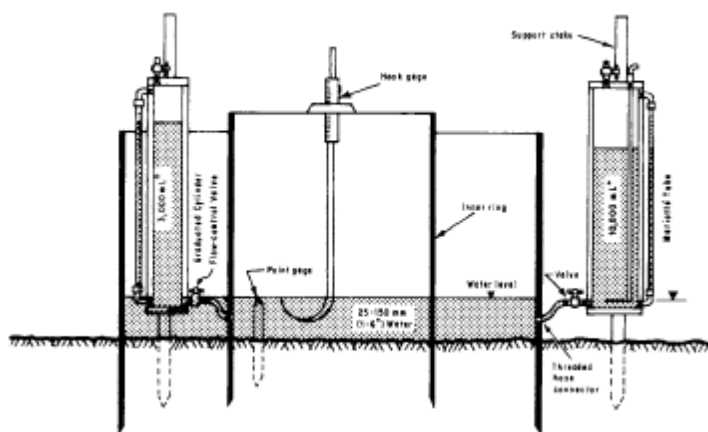


Figure 2-4: A double-ring infiltrometer featuring Mariotte tubes (ASTM 2009, Fig.2, p.3)

Ponded ring infiltrometers can be convenient and generate data well suited to empirical models (Kincaid 1969). However, McQueen (1969, p.2) cautioned against use of the ponded ring infiltrometers. He pointed out that ‘any ring, tube, or plot frame forced into the soil surface to delimit an infiltrometers plot will disturb a part of the plot area. Water movement into the disturbed zone may be increased to several times the natural infiltration rate.’ He concedes that this may not be such an issue for ploughed or cultivated agricultural soils. A further issue is that the ponded surface may poorly model the soil behaviour under sprinkler irrigation or rainfall (Gencoglan et al. 2005).

2.4.2 Sprinkler and Rainfall Infiltrometers

Sprinkler and rainfall infiltrometers can be used to determine the infiltration capacity function for a soil (Gencoglan et al. 2005). Sprinkler and rainfall infiltrometers have generally been of two forms: simulators that use drop formers, and simulators that generate ‘rainfall’ from nozzles. The former generally use arrays of hanging yarn, coiled hollow wire, capillary tubes, drawn glass, tubing tips or hypodermic needles that allow water from a reservoir above to generate arrays of droplets of known diameters and intensities (Humphrey et al. 2002; Singh et al. 1999). The Dripolator, also known as the Stalactometer, was developed by the US Soil Conservation Service and was one of the first such devices (Hall 1970). A number of techniques have been developed to allow the operator to vary the droplet sizes and/or intensity of application, or to promote randomness in terms of where the droplets land on the soil (Humphrey et al. 2002; Singh et al. 1999).

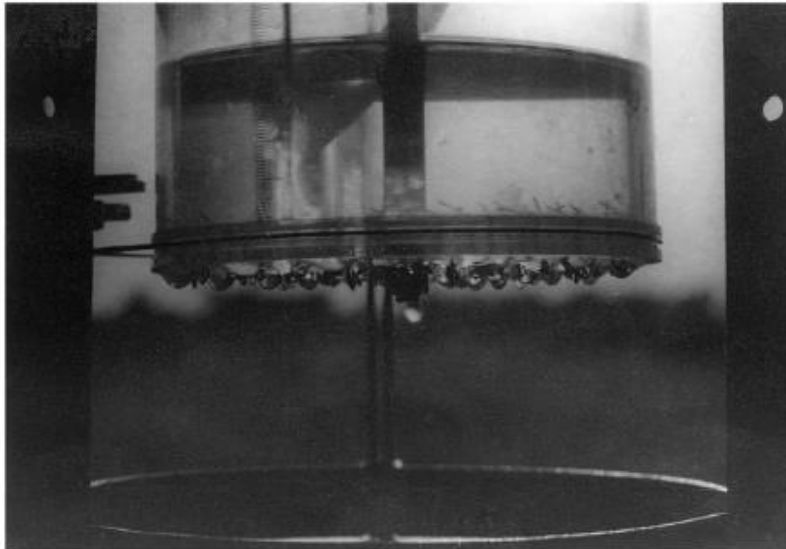


Figure 2-5: A photo of a small droplet forming rainfall simulator (Singh et al. 1999, Fig.2a, p.172)

Simulators that use nozzles to generate ‘rainfall’ come in many forms (Hall 1970). Mostly they consist of a frame that suspends a singular nozzle (Figure 2-6), or an array of nozzles, above the test plot. The nozzle/s may be fixed, rotating or reciprocating, but the effect of the frequency of intermittent applications must be taken into account in the latter two cases (Hall 1970). An important advantage of nozzle-based sprinkler infiltration tests is that the simulation can be performed over much larger ground surface areas than the double-ring infiltrometers or droplet formers (Gencoglan et al. 2005).



Figure 2-6: A portable rainfall simulator using a single pressurised nozzle. The plot area is 1.5m x 2.0m (Humphrey et al. 2002, Fig.1, p.201).

Chu (1986) noted that sprinkler or rainfall infiltrometers have seldom been used to model infiltration under sprinkler irrigation. He cited difficulties with a) droplet impact energy, and b) the initial period when all of the water is imbibed into the soil, as historical disincentives to their adoption. But Singh et al. (1999) cites these very factors as one of the reasons for the recent growth in popularity of sprinkler infiltrometers. The ability to replicate the processes of droplets impacting the soil and absorbing into it, which a ponded infiltrometer cannot do, is a key advantage of sprinkler infiltrometers. Furthermore, if a soil crust is to be avoided, because crusted soil infiltration models are not convenient for parameter evaluation, then use of a sprinkler infiltrometer with at least 50% vegetation cover on the soil surface should suffice (Chu 1986). Smith (1976, p.508) argued that it is 'important to treat infiltration under rainfall [or sprinklers] as significantly different from infiltration from sudden ponding.' McQueen (1969) also identified the value of sprinkler infiltrometers in not having to disturb the surface soil through driving large steel cylinders or plot frames deep into the soil.

Kincaid et al. (1969) conceded that the assumptions in their analysis of potential runoff were probably invalid under the moving sprinkler systems; they had used ponded ring infiltrometers where the soil is suddenly flooded to determine their parameters, rather than sprinklers where the soil is gradually saturated. Mein and Larson (1971), two years on, published their model that separated the pre-ponding phase from the ponded phase of infiltration, thereby avoiding altogether the convoluted process that Kincaid et al. (1969) took to adjust the data by the methods of Cook (1946).

Perhaps the simplest sprinkler infiltrometer design come across in the literature was that presented by Tovey and Pair (1966). The concept was simply to position an irrigation sprinkler on a representative field (Figure 2-7), whose moisture content was near field capacity, with an array of catch-cans spaced out on a radial leg. The soil was observed during the irrigation and the times at which surface ponding first occurred at various distances along the radial leg were recorded. The application rates for each of the corresponding distances were determined by dividing the volume of water in the catch-cans at those distances by the elapsed time. Thus the times to ponding (t_p) for given application rates could be estimated, as could the maximum application rate that should be used so that runoff will not be generated on this field. However, no further information

on the infiltration capacity function or even on how t_p might change with different antecedent soil moisture conditions is obtained.

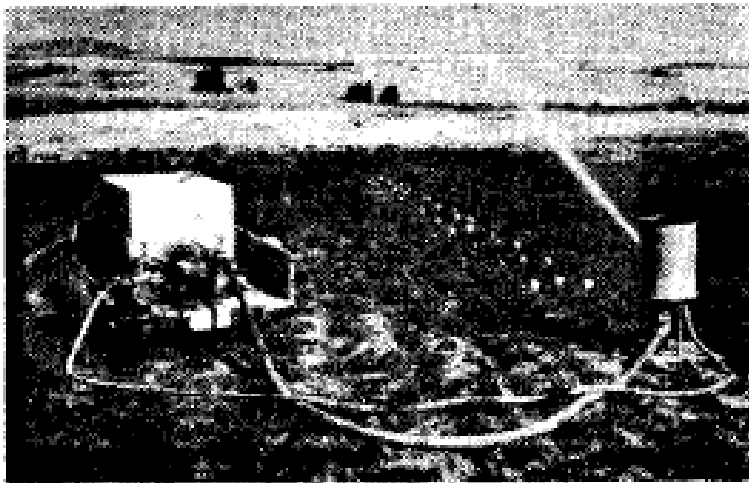


Figure 2–7: A sprinkler infiltrometer in operation (Tovey & Pair 1966, Fig.1, p.359)

2.5 The Green-Ampt Infiltration Model

W. Heber Green and G.A. Ampt, who were chemists in Victoria, Australia, published their seminal paper *Studies on Soil Physics – Part 1: The Flow of Air and Water through Soils* in 1911 (Green & Ampt 1911). The paper pointed out that commonly performed mechanical analyses of soils whereby percentages of various sized particles were determined were, at best, giving only a qualitative understanding of the drainage properties of the soils. For example, a soil with a large percentage of clay was known to be only slightly permeable to water. Green and Ampt sought to create a quantitative model of movements of water and air through the soil. The result of their work came to be known as the Green-Ampt equation. Green and Ampt thence recommended that soils be classified in terms of the parameters of permeability, capillary potential, and porosity. Such information would have become invaluable for soil hydraulic modelling; unfortunately, this advice has generally not been taken (Mein & Larson 1971).

Over 100 years have elapsed since the publication of the Green-Ampt equation and it continues to be the most widely used analytical infiltration model, especially in the fields of hydrology and erosion modelling (Van den Putte 2013; Chu 1995). Chu (1978, p.461) believed the Green-Ampt model, despite its highly simplified representation of the

infiltration process, to be ‘by far one of the best models available to describe infiltration during a rainfall event.’ Brackesiek et al. (1979) found the Green-Ampt equation to satisfactorily simulate an observed infiltration rate curve under a portable droplet-forming infiltrometer in the field. Whisler and Bouwer (1970) compared the Philips equation and the Green-Ampt equation with field data and found that the Green-Ampt equation was superior for practical reasons. Smith (1976, p.506) even went so far as to remark that ‘...the Green-Ampt formula is the most elegant approximation that exists today’.

2.5.1 Model Concept

The Green-Ampt model was the first infiltration model to be theoretically derived from physical principles (Ravi & Williams 1998). The Green-Ampt model assumed that the soil could be treated as a bundle of capillary tubes and took its derivation from Darcy’s Law (Green & Ampt 1911), which is also referred to as the Darcy-Buckingham equation (Narasimhan 2005):

$$q = -K \frac{\partial h}{\partial z} + K \quad (2-11)$$

where

- q flux [mm/hr]
- K hydraulic conductivity [mm/hr]
- h capillary pressure head [mm]
- z vertical co-ordinate [mm], taken as positive downward.

In the development of the Green-Ampt equation, the soil water was considered to be ponded at the surface and to move downward as a unit with a sharp front (Figure 2-8), sometimes referred to as ‘piston flow’. The pressure gradient at the wetting front was considered to be the sum of the capillary tension of the soil immediately ahead of the front and the height of the water column behind the wetting front (Smith 1976).

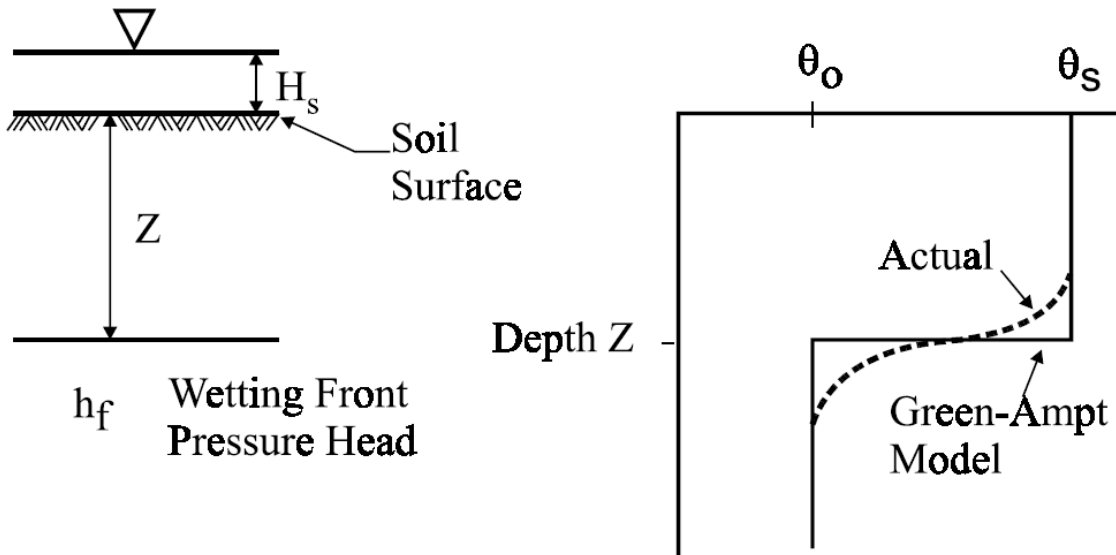


Figure 2-8: Illustration of the Green-Ampt parameters and the concept of the 'piston flow' water movement down through the soil profile (Ravi & Williams 1998, Fig.3, p.7)

The full derivation of the Green-Ampt equation can be found in Green and Ampt (1911, pp. 2-8). Its final form is as follows:

$$I = K_s t - (h_f - h_s)(\theta_s - \theta_0) \log_e \left[1 - \frac{I}{(h_f - h_s)(\theta_s - \theta_0)} \right] \quad (2-12)$$

where

- I cumulative infiltration [mm] and is a function of time
- K_s soil's hydraulic conductivity [mm/hr]
- T time [hr]
- h_f wetting front pressure head, a negative value [mm]
- h_s pressure head at the soil surface under ponded conditions [mm]
- θ_s saturated volumetric water content of the soil [m^3/m^3]
- θ_0 antecedent volumetric water content of the soil ahead of the wetting front [m^3/m^3]
- \log_e the natural logarithm

Using the relation $I(t) = Z(\theta_s - \theta_0)$, where Z is the depth of the wetting front, then:

$$i = \frac{dI}{dt} = -K_s \left(\frac{h_f - (h_s + Z)}{Z} \right) \quad (2-13)$$

where $i(t)$ is the rate of infiltration [mm/hr]. Often a negligible ponding depth is assumed and so h_s is taken to be zero. The equation then takes the familiar form:

$$i = K_s \left(1 + \frac{h_f \Delta \theta}{I} \right) \quad (2-14)$$

where h_f is now treated as a positive *suction* head [mm], and $\Delta \theta$ is the difference between saturated volumetric water content [m^3/m^3] and the antecedent volumetric water content [m^3/m^3]. Often the saturated volumetric water content is assumed to equal the porosity of the soil.

2.5.2 Assumptions

Smith (1976, p.505) reiterated that ‘The key to utilising approximations [such as the Green-Ampt equation] lies in understanding the sensitivity of their assumptions, and in appreciating the accuracy needed for their use.’ The Green-Ampt model makes some significant assumptions, either explicitly or implicitly. The model’s piston displacement profile (Figure 2-8) is very rough and takes liberties with significant factors such as gravity and viscosity effects (Morel-Seytoux & Khanji 1974). Water flow is assumed to occur only downwards with a well-defined wetting front (Ravi & Williams 1998), and there is no effect of diffusion. The Green-Ampt model assumes that the soil is homogenous and without macropores that would allow preferential flow, or bypass flow (Green & Ampt 1911). The model assumes that the surface is ponded from time $t = 0$, thus ensuring that the surface is always saturated. The model also assumes that the antecedent soil moisture content is uniform throughout the soil profile ahead of the wetting front, and that the soil is uniformly saturated behind the advancing wetting front (Green & Ampt 1911). It is also implied that the soil is isothermic; that the supplied water is not changing the physical properties of the soil, such as shrink-swell phenomena or sodicity effects; that the soil surface is not sealed or crusted such that the hydraulic conductivity of the surface is markedly different to the subsoil; and that the soil pores are continuous and are not occluded by air. Many models have been developed upon the original Green-Ampt equation to specifically deal with some of these assumptions.

And yet, given all of these assumptions, when compared against measured data, empirical models, and solutions of the Richards equation, the performance of the model is ‘astonishingly good’ (Morel-Seytoux & Khanji 1974, p.795). Indeed, it can be shown that the Green-Ampt equation can be obtained as an exact analytical solution of the Richards equation (Craig 2010; Raats et al. 2006; Ravi & Williams 1998).

Mein and Larson (1971) and Broadbridge and White (1987) pointed out that some of the assumptions are not really as restrictive as they appear. The assumptions of soil homogeneity and of uniformity of soil moisture content are reasonable because it is only the upper layer that determines the soil’s infiltration behaviour, possibly as shallow as 5cm for heavy clays (Mein & Larson 1971). In particular, the long-term effects of tillage are known to homogenise the upper soil layer (Mein & Larson 1971). Furthermore, wetting fronts seldom go deeper than 10cm before ponding occurs in many rainfall events, and soil cracks and macropores do not become fully operative until after the surface has become saturated (Broadbridge & White 1987; Davidson 1985).

2.5.3 Advantages

There are several important advantages associated with the Green-Ampt equation. The equation itself, particularly in its time-derivative form for i , is conceptually easily understood, relatively simple to apply, and exhibits satisfactory performance across a broad scope of problems (Ravi & Williams 1998). Also, the parameters required for the equation have physical significance and thus are better able to be predicted (Luz 2011; Mein & Larson 1973), and do not require calibration unlike the empirical models (Wilson et al. 1982).

Luz (2011) reported that the Green-Ampt model is increasingly being used, particularly after Mein and Larson’s (1971) work to allow for non-ponding conditions at time $t = 0$. Morel-Seytoux and Khanji (1974) described the Green-Ampt equation as an ‘efficient’ equation in that, by assuming a priori the piston displacement profile of water advance, the need to find a solution to a partial differential equation for flow is obviated.

An outstanding feature of the Green-Ampt model, as presented in its Equation 2-14 form, is that the infiltration capacity, i , is a function of the accumulated infiltration, I , rather

than time (Foley 2015). This is a somewhat unique characteristic among infiltration models (the Holton model is also a non-time based infiltration model - refer 2.3.2) and is a different way to understand infiltration. It may also become advantageous when the water being supplied to the soil surface and the water infiltrating through the surface are being measured on different time scales or are being measured as functions of volume (instead of time).

2.5.4 Limitations and Difficulties

Several difficulties with the Green-Ampt equation will be discussed here, namely its implicit form; that it does not account for many significant influencing factors; the need for ponded conditions; and determination of parameter values. Because of the attention that the issue of Green-Ampt parameters has received in the literature, they will be discussed separately in Section 2.5.4.1.

Historically, the implicit form of the Green-Ampt equation had caused difficulties because it required an iterative procedure to determine the time, t , for different values of cumulative infiltration, I (Nasseri et al. 2008). Thus various explicit, approximate solutions have been proposed, some yielding less than 2% error compared to the implicit form (Williams et al. 1998). Srivastava et al. (1996) pointed out that the speed advantages from using explicit, approximate, solutions may become significant when performing simulations of multiple scenarios with fine resolutions of space and time. In recent years, fast modern computers have become ubiquitous which has meant that the difficulty of solving the implicit form has generally been limited to instances of hand calculations.

Another limitation to the original Green-Ampt model is that it did not account for some significant influencing factors such as entrapped air (Wilson et al. 1981; Jarret & Fritton 1978; Morel-Seytoux & Khanji 1974); viscosity changes such as occur with temperature changes (Bodman & Coleman 1943); the effect of consecutive irrigation or rainfall events, especially upon bare soil (Jennings 1998); or, indeed, any of the other factors listed in Section 2.3.4. Wilson et al. (1982) reported that there were some discrepancies in the literature as to the importance of these factors on the outputs of the Green-Ampt model. Broadbridge and White (1987), who neglected soil swelling, entrapped air and

raindrop impact phenomena reported that the time to ponding (t_p) was substantially overestimated by the Green-Ampt model.

Until the work of Mein and Larson (1971) the assumption of ponded conditions for the entire duration of the infiltration event was a significant limitation for the Green-Ampt equation. Particularly under sprinkler or rainfall conditions, researchers resorted to other methods that were generally modifications of empirical equations [see, for example, Kincaid's (1969) use of methods proposed by Cook (1946)].

2.5.4.1 Parameters in the Green-Ampt Equation

Perhaps the most significant difficulty with using the Green-Ampt model is to correctly determine the value of the parameters. Brackensiek et al. (1981, p.338, italics added) wrote that 'Use of the Green and Ampt infiltration equation for computing surface runoff for a constant rainfall rate is fairly simple, *once the parameters are known*'. Mein and Farrell (1974) and Luz (2011) stated that some of the Green-Ampt parameters, whilst having a physical basis, are not easily obtained, except by exacting and time consuming procedures.

Bard (1974, p.11) explained what is meant by the term 'parameters':

"Usually a model is designed to explain the relationships that exist among quantities which can be measured independently in an experiment; these are the variables of the model. To formulate these relationships, however, one frequently introduces "constants" which stand for inherent properties of nature (or of the materials and equipment used in a given experiment). These are the parameters."

Accordingly, in the Green-Ampt equation the required *variables* are depth of ponding, h_s , and antecedent soil moisture, θ_o . There are well established techniques for determining the soil moisture (Schmugge et al. 1980). The Green-Ampt *parameters* requiring determination are the soil porosity, which is assumed equivalent to the soil moisture content at saturation, θ_s ; saturated hydraulic conductivity, K_s ; and the capillary suction, h_f (Morel-Seytoux & Khanji 1974). The processes for determining the latter two are not altogether clear and established values of these parameters are not available for many

soils (Ahuja et al. 1989). Empirical relations or estimation procedures for the Green-Ampt parameters in terms of easily-measured variables were developed, particularly following extensive efforts by the USDA's Agricultural Research Service (Luz 2011; Ravi & Williams 1998). Rawls et al. (1983) published tables of K_s and h_f that were estimated from soil texture, bulk density and organic content by empirical regression equations. However, published tables of 'typical' values for the K_s and h_f parameters for representative soil classes vary enormously between authors [See the comparison by Williams et al. (1998, pp.25-28) of tabulated data from Carsel & Parrish (1988), Pajian (1987), and Brackensiek et al. (1981)]. Ravi and Williams (1998) appended to their report an annotated bibliography containing 44 papers that deal with the issues of estimating various soil hydraulic parameters, including those required for the Green-Ampt equation.

The saturated hydraulic conductivity, K_s , of a soil is frequently determined in the laboratory using vertical columns of (disturbed) soil or in field using a ponded infiltrometer or permeameter. However, Bouwer (1966) argued that the hydraulic conductivity parameter that should be used in models where there is a positive capillary suction, such as the Green-Ampt model, should be $0.5K_s$ to allow for entrapped air. This is consistent with the findings of Morel-Seytoux and Khanji (1974) and Jarret and Fritton (1978).

The capillary suction parameter, h_f , has proved more difficult to both define (Skaggs et al. 1983) and to determine. Hillel (1980) defined matric potential, which is almost synonymous with capillary suction, as the affinity of water to the whole soil matrix. For a long time it was considered that h_f did not have any direct relation to measurable soil characteristics (Neuman 1976) and this was a great impediment to the use of the Green-Ampt model. Morel-Seytoux and Khanji (1974) stated that the Green-Ampt equation might even have been forgotten but for the work of Bouwer (1964) who, 53 years after Green and Ampt (1911) published their work, was the first to suggest a way to link h_f to measurable soil characteristics based on an analogy with horizontal flow (Neuman 1976). Bouwer (1969) also proposed an alternative approach to estimating h_f by taking it as one-half of the soil air-entry value, where the air-entry value had already been defined by Bouwer (1966, p.730) as 'the pressure head of the soil water when air of zero gauge pressure enters soil with a continuous water phase'. Following on from Bouwer, Mein and Larson (1971) showed that the average capillary suction could be determined from integrating the $S - k_r$ curve, i.e. the suction versus relative conductivity curve (Figure 2-

9). Note that k_r is defined by $k_r = \frac{K(\theta)}{K(\theta_s)}$ where $K(\theta)$ is the absolute conductivity and $K(\theta_s)$ is the absolute conductivity at saturation. Mein and Larson (1971) conceded, however, that 'it is very difficult to experimentally determine this relationship even for an ideal soil' (Mein & Larson 1971, p.49). Smith (1975) and Morel-Seytoux and Khanji (1974) both found that Mein and Larson's method for determining h_f generally under-predicted infiltration. Estimation of capillary suction is particularly difficult for clay soils (Mein & Larson 1971) where small changes in soil moisture can cause large changes in suction (Figure 2-10).

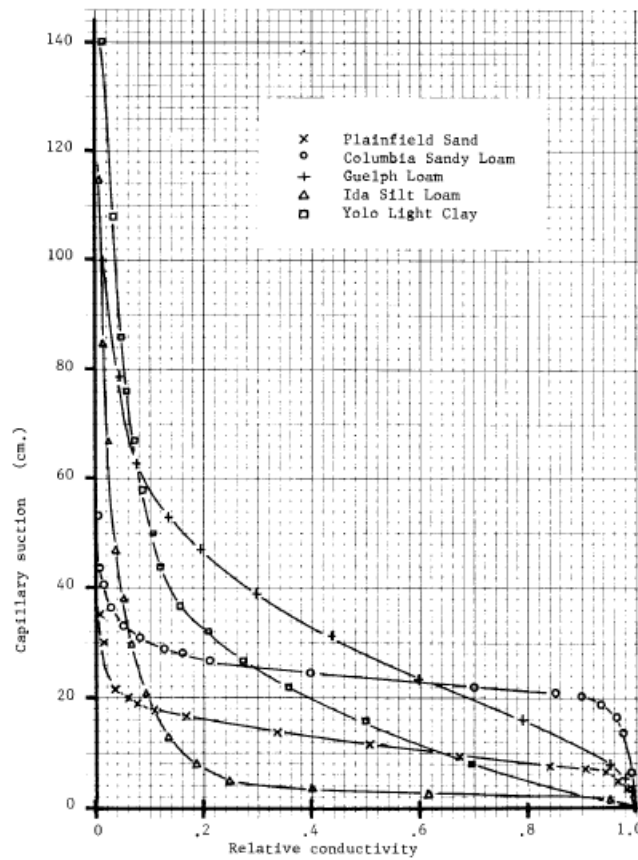


Figure 2-9: An example of an $S - k_r$ curve (capillary suction vs relative conductivity) for selected soils (Mein & Larson 1971, Fig.13, p.33)

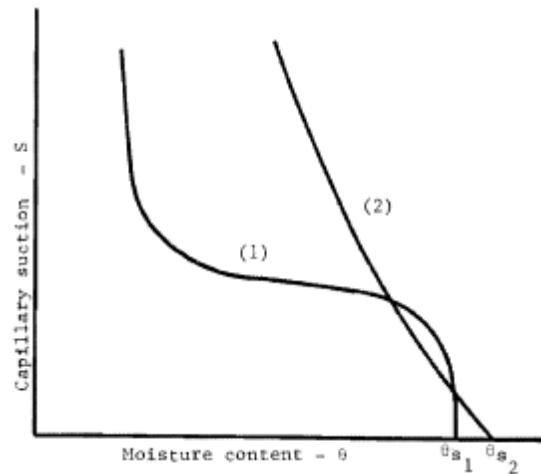


Figure 2–10: Variation of capillary suction, h_f , with moisture content (Mein & Larson 1971, Fig.7, p.11). Curve (1) is typical of a sandy soil, and curve (2) is typical of a clay soil.

Smith (1976) said that the Green-Ampt equation could be used as an empirical formula and have it fitted to data to accurately find the parameters, but ‘the laboratory work necessary makes the procedure absurd if a practical use is intended’ (Smith 1976, p.508). This is because not only is significant spatial variability in the Green-Ampt parameters frequently observed (Brackensiek & Onstad 1977), but the parameters are not necessarily even constant for a given site. Van den Putte et al. (2013) noted, for example, that a decrease in K_s might be observed over time because of surface sealing secondary to rainfall impact. Kunze and Shayya (1993) also found that, regardless of the initial and boundary conditions, the value of h_f was time-dependent and that it tended to decrease (when it was taken as a positive suction value) to about 70% of its initial value; they found that there was, on average, an overall reduction on cumulative infiltration of about 5% when the decreasing h_f was accounted for (Figure 2-11). Chu (1995) reported that all three Green-Ampt parameters are affected by the initial water content, and Luz (2011, p.88) admitted that the assumption ‘that the soil water characteristics and saturated hydraulic conductivity relationships are not time variant’ may not always hold.

Then there is the question of the relative importance of each of the Green-Ampt parameters, and how sensitive the performance of the Green-Ampt equation is to each of its parameters.

The capillary suction, h_f , which is generally the more difficult parameter to determine, turns out to be the least important of the parameters. Because h_f only contributes to the matric flow component of total soil water flow, its influence becomes less and less as

infiltration time increases (Figures 2-11 and 2-12). Brackensiek and Onstad (1977) found that h_f is clearly the least sensitive parameter in the Green-Ampt equation. They reported that a 10% high estimate of h_f caused a 4.7% high estimate in surface infiltration, and a 10% low estimate of h_f caused a 9.4% low estimate of surface infiltration; thus an overly high estimate of h_f is preferable to an overly low estimate.

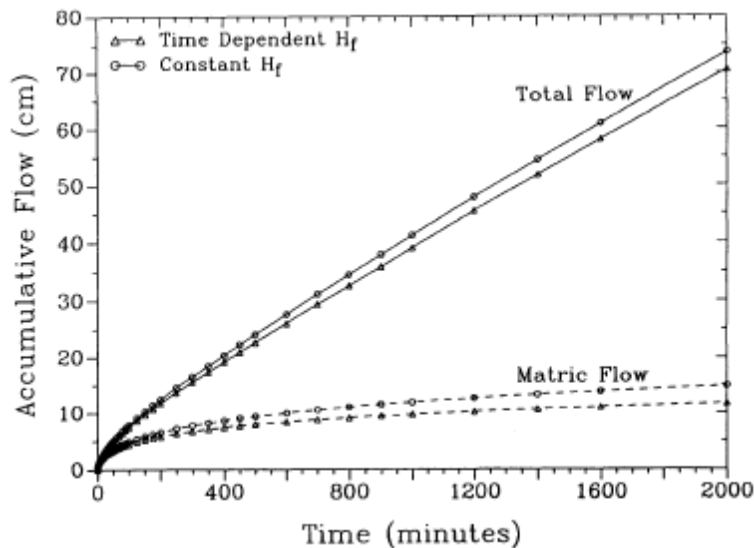


Figure 2-11: The total infiltration flows and the matric sub-components of the total infiltration flows obtained using the Green-Ampt equation with constant and time-dependent h_f (Kunze & Shayya 1993, Fig.1, p.1095).

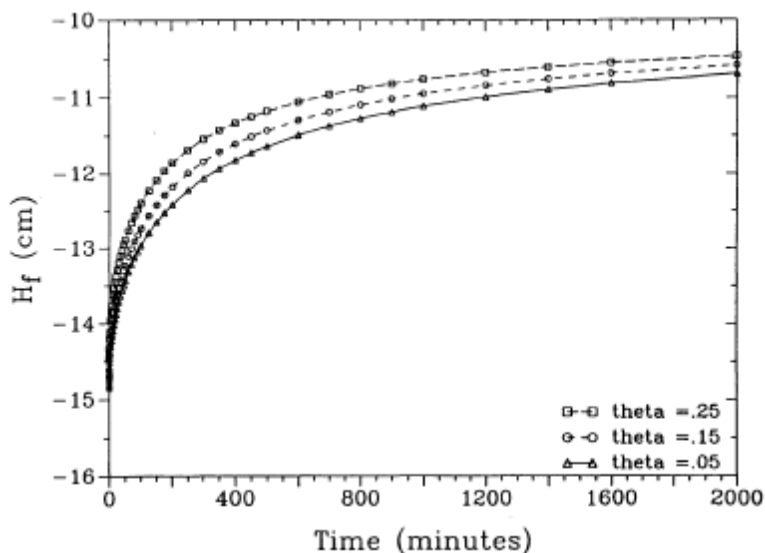


Figure 2-12: An example of the variability of h_f with time, for three different initial soil moisture conditions (Kunze & Shayya 1993, Fig.3, p.1096).

The soil porosity, or the *fillable* soil porosity, is a slightly more significant parameter than h_f . A 5% low estimate of fillable porosity was found to translate to an almost 29% overestimate of runoff (Brackensiek & Onstad 1977).

By far the most significant parameter in the Green-Ampt equation is the hydraulic conductivity, K . Brackensiek and Onstad (1977) preferred to use the term ‘effective conductivity’, K_e , because of the impacts of air viscosity and air entrapment on water flow. Kincaid (2002) found that K is the main soil parameter that affects infiltration and runoff predictions. Van den Putte et al. (2013) similarly noted that K is an especially sensitive parameter in the GAML model; indeed, they were able to optimise the GAML model in K alone, with the other parameters fixed at average values, and still obtain satisfactory results. Commonly used field techniques to estimate K are subject to major errors and variations (Brackensiek & Onstad 1977). McQueen (1963) argued against the use of ponded ring infiltrometers because of the need to hammer them into the ground; the shaking, cracking and disturbing of the soil that results will inevitably lead to errors in K . An error of 100% is reportedly not unreasonable (Brackensiek & Onstad 1977; Nielsen et al. 1973); Brackensiek and Onstad (1977) found that a 100% low estimate translated to a 441% overestimate of runoff volume, and a 100% high estimate translated to 281% underestimate of runoff volume. Broadbridge and White (1987) cautioned that, under ponded conditions, considerable preferential flow may occur. This may affect the accuracy of field determination of K , or the accuracy of predictions made when applying laboratory-determined K to a field environment; predicted results may be out by 100 times (Broadbridge and White 1977). McQueen (1963) advocated the use of sprinkler infiltrometers because preferential flow would not become a factor until the surface had become saturated.

There is some contention about whether or not having more parameters is better. Smith (1976, p.509), for example, reasoned that ‘to a certain extent, there should be a positive relation between accuracy (or fit to data) and number of model parameters in these approximate relations.’ Van den Putte et al. (2013, p.341) disagreed:

“...the predictive capability of the one parameter GAML model was clearly superior to that of model versions with more parameters, while still being somewhat lower than that of a multiple regression equation... ..Thus while allowing more parameters to be calibrated does increase the model’s ability to describe the data it actually decreases its predictive ability. This is because the two and four parameter calibration procedures result in parameter values that are poorly related to the measured variables. Optimisation of more than one parameter value allows the model to respond to variability in infiltration

dynamics that is not captured or controlled by the measured data, resulting in physically unrealistic parameter values for some experiments.”

But a one-parameter Green-Ampt model, in K, still requires an educated guess for capillary suction, h_f . Fortunately, as discussed earlier, h_f is the least sensitive of the Green-Ampt parameters. Smith (1976) was hopeful that eventually surveys and tabulations of soil parameters would be compiled and made available in support of ‘handbook’ approximations of soil infiltration calculations.

2.5.5 Developments upon the Green-Ampt Equation

There have been numerous models developed based upon the Green-Ampt equation. Some will be listed here without further explanation. Because of their direct relevance to this project, more attention will be given to the work of Mein and Larson, and then to Chu.

There are many Green-Ampt based models that have attempted to incorporate one or more of the factors noted in Section 2.3.4 (Kale & Sahoo 2011; Ravi & Williams 1998 pp.8-9). Van Duin (1955), Bouwer (1969), Childs and Bybordi (1969), and Bybordi (1973) extended the model to account for layered soils. Hillel and Gardner (1970) and Rawls et al. (1990) sought to account for a surface crust. Ahuja and Tsuji (1976) accounted for time-varying effective hydraulic conductivity, and Wilson et al. (1981) accounted for air viscosity and air entrapment effects. Chen and Young (2006) created a sloping surface variant of the Green-Ampt model, and Craig et al. (2010) sought to account for the spatial variability of the Green-Ampt parameters across a catchment. However, the Mein and Larson (1971, 1973) and Chu (1978) variants remain as the most implemented versions of the Green-Ampt model (Van den Putte 2013).

2.5.5.1 The Green-Ampt-Mein-Larson (GAML) model for steady rainfall

Mein and Larson (1971) pointed out that the typical textbook infiltration curve (Figure 2-13) assumes that the soil is saturated from time $t = 0$. This is an assumption of the Green-Ampt model and can occur for flood irrigation. It would, however, be a very unlikely occurrence for sprinkler irrigation or rainfall because there will likely be a period of time between $t = 0$ and $t = t_p$ when all of the rainfall is imbibed into the soil. Smith (1976, p.508) stated that it is ‘important to treat infiltration under rainfall as significantly different from infiltration from sudden ponding’.

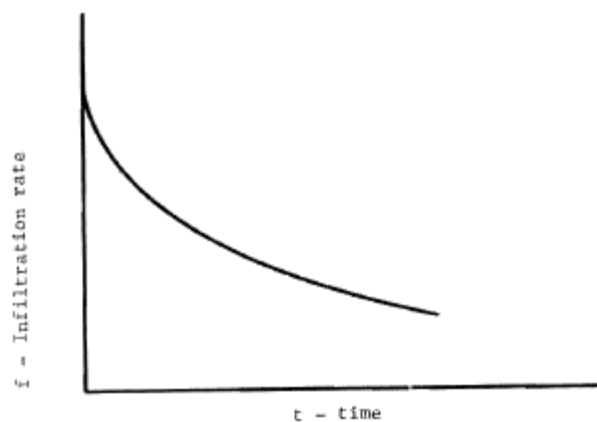


Figure 2–13: A 'typical textbook infiltration curve' (Mein & Larson 1971, Fig.4, p.8)

It was thus proposed by Mein and Larson (1971) that three general cases for infiltration could occur under rainfall or sprinkler irrigation:

Case ‘A’: $r \leq K_s$

The rainfall rate, r , is less than the saturated hydraulic conductivity of the soil, and ponding or runoff will never be generated. This corresponds with curve ‘A’ in Figure 2-14.

Case ‘B’: $K_s < r < i$

This case is when the rainfall rate is greater than saturated hydraulic conductivity but initially less than the soil’s infiltration capacity. It corresponds to the horizontal part (‘B’) of the infiltration curve ‘B-C’ in Figure 2-14.

Case 'C': $r > i$

When the rainfall exceeds the infiltration capacity, ponding or runoff will begin to occur. This will correspond to the decaying part ('C') of the infiltration curve 'B-C' in Figure 2-14. For a constant rainfall, the runoff can be estimated by the difference between the (flat) rainfall curve and the decaying infiltration curve (Figure 2-15)

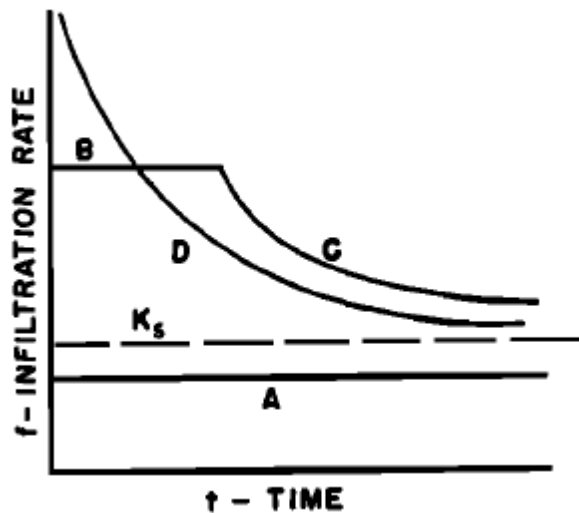


Figure 2-14: Infiltration curves for three different cases of infiltration behaviour (Mein & Larson 1973, Fig.1, p.385). Curve D is the case when the soil is saturated from time $t = 0$. Curve A is the case when rainfall is always less than K_s . Curve BC is the case when rainfall is greater than K_s but initially less than infiltration capacity.

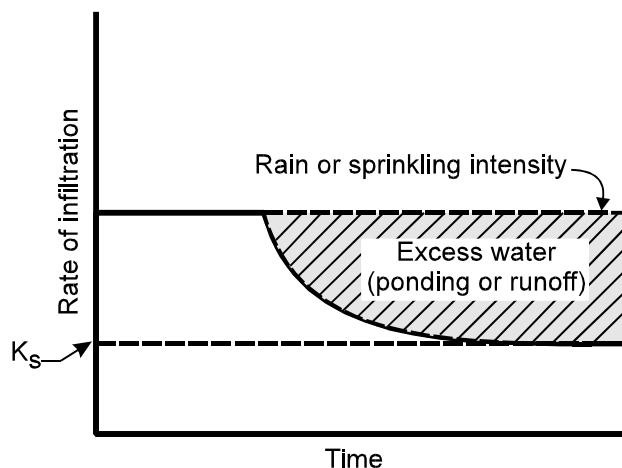


Figure 2-15: An illustration of Mein & Larson's (1973) Case 'C' where ponding or runoff is generated because infiltration capacity has become less than rainfall intensity (Williams et al. 1998, Fig.2, p.3).

Mein and Larson (1971) proposed that the infiltration event be divided into two distinct phases: pre-saturation and post-saturation. The post-saturation phase would be equivalent

to the Green-Ampt model, except that the value for time requires an adjustment equal to t_p . The pre-saturation phase assumes that all of the applied water is imbibed.

The so-called Green-Ampt-Mein-Larson (GAML) model is thus a two-part equation given as follows:

$$I(t) = \begin{cases} rt & \text{for } t \leq t_p \\ K_e(t - t_p) + I_p + h_f(\theta_s - \theta_0) \log_e \left(\frac{h_f(\theta_s - \theta_0) + I}{h_f(\theta_s - \theta_0) + I_p} \right) & \text{for } t > t_p \end{cases} \quad (2-16)$$

where

- r rainfall / sprinkler intensity [mm/hr]
- t_p ponding time [hr], which is when the surface has become saturated
- I_p accumulated infiltration [mm] at time t_p , and is found by $I_p = rt_p$
- K_e effective hydraulic conductivity [mm/hr] which is estimated by Bouwer (1966) as $K_e = 0.5K_s$.

All other components of the model are as defined for the Green-Ampt model in Section 2.5.1. Note that this model assumes that the rainfall intensity is constant (Mein & Larson 1971).

The cumulative infiltrated volume of water, I_p , is found by $I_p = rt_p$. It can also be calculated, per Mein and Larson (1971), as:

$$I_p = \frac{h_f(\theta_s - \theta_0)}{\left(\frac{r}{K_e}\right) - 1} \quad (2-17)$$

Equating the two expressions for I_p yields the following expression for determining t_p (Van den Putte 2013; Craig 2010):

$$t_p = \frac{K_e h_f(\theta_s - \theta_0)}{r(r - K_e)} \quad (2-18)$$

The infiltration rate, i , which is found by taking the time-derivative of I , is given by Craig et al. (2010) as:

$$i = \begin{cases} r & \text{for } t \leq t_p \\ K_e \left(1 + \frac{h_f(\theta_s - \theta_0)}{I} \right) & \text{for } t > t_p \end{cases} \quad (2-19)$$

Thus for time $t > t_p$ the form of the GAML model is exactly the same as the original Green-Ampt model.

Generally the same assumptions are made as for the Green-Ampt model (refer 2.5.2), however the ponded surface assumption is replaced with a constant rate rainfall that is greater than K_s and does not have an impact effect on the soil (Mein & Larson 1971). The raindrop non-impact assumption is significant (Jennings et al. 1988) and Chu (1987) and Slack (1980) have said that the GAML model shows promise for predicting surface ponding under time-varying application rates in the field when the soil surface is protected by vegetation. Van den Putte et al. (2013) cautioned that there is uncertainty about the performance of the GAML model under wet conditions because the piston flow assumption, which is quite reasonable under relatively dry conditions, may break down.

2.5.5.2 The Chu model for unsteady rainfall

The GAML model was limited to the case of a constant application rate, a situation rarely ever seen. Mein and Larson (1971) suggested that further study should be made to account for non-uniform rainfall; this was done by Chu (1978, 1986, 1987).

Chu followed Mein and Larson in recognising that infiltration under rainfall or sprinklers requires the process be modelled as two distinct phases: pre-ponding and ponded. Chu (1978) also used the Green-Ampt equation to model the ponded phase but introduced two time parameters, ponding time t_p and pseudotime t_s , to modify the Green-Ampt equation. He also supplied a rather detailed calculating procedure for estimating runoff that was quite suitable for use in a spreadsheet software package.

Chu (1978) recognised that modelling infiltration under unsteady rainfall is further complicated by the possibility that the ponding time, t_p , may not be unique for a rainfall event. There may be several periods when the rainfall exceeds infiltration capacity and the infiltration process may alternate between ponded and non-ponded phases (Figure 2-16).

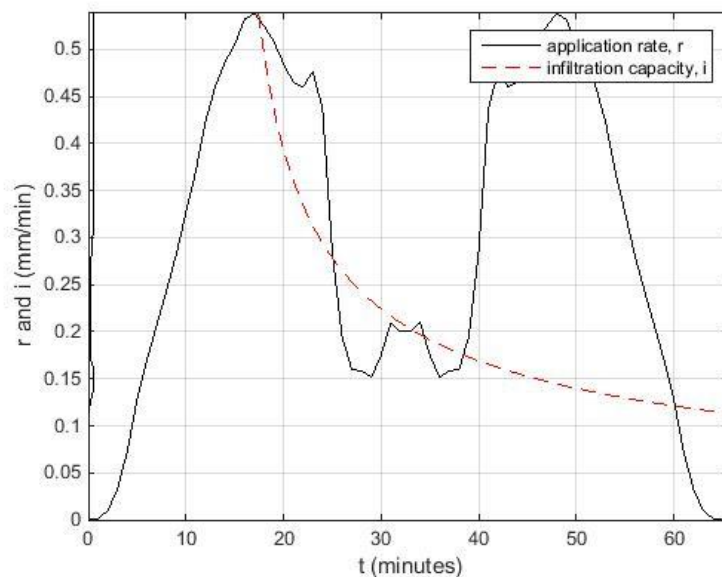


Figure 2–16: Example of when there are multiple occasions when application rate exceeds infiltration capacity.

A simpler generalised GAML infiltration model was proposed by Chu (1987). The intent was to retain the Mein-Larson technique of dividing the infiltration process into pre-ponding and ponded phases, and also to have the flexibility to replace the Green-Ampt equation for the ponded phase with any other infiltration model. This replacement model might be, for example, a Kostiaikov infiltration capacity curve as measured in the field, or a representative family curve from the Soil Conservation Service, or a modified form of the Green-Ampt model itself. As long as the soil has a unique infiltration capacity curve, which means that raindrop impact and soil crusting are of no influence, then the generalised Mein-Larson model can work (Chu 1987). A centre-pivot sprinkler irrigation over a vegetated soil surface is an example of where this model might work well.

The challenge with the Chu (1987) model is that there cannot be a general set of equations that will allow the determination of important values such as time to ponding, cumulative infiltration, runoff etc. This is because the ponded phase may be described by any one of

a considerable number of models. Additionally, the application curves and the infiltration curves might be on different time scales (Chu 1987) and this makes superimposition of the curves problematic because it first requires the determination of the time offset between the curves.

Chu's solution was to use a graphical technique (Figure 2-17). The time-based application patterns were plotted on the left, and the time-based infiltration patterns plotted on the right. The rate curves (application rate and infiltration capacity) were at the top, and the depth curves (cumulative rainfall and cumulative infiltration) were at the bottom. Starting at any point on the lower left curve, a vertical line is extended upward until it hits the application rate curve at point 'A₁', then turn right 90° and extend a horizontal line to the next curve 'A₂', then turn right 90°... and keep repeating until the points 'A₁', 'A₂', 'A₃', and 'A₄' at which the drawn lines intersect the four curves stabilise and the drawn lines form a rectangle. Then translate the infiltration capacity curve (on the right) to the left so that 'A₂' and 'A₃' coincide. As seen in Figure 2-17, the point 'B₂' is the second intersection of the application rate curve and infiltration capacity curve when they have been superimposed. Extending a horizontal line from 'B₂' to 'B₃', then down to 'B₄' allows the potential runoff from the event to be determined. The term 'potential runoff' is used because the Mein-Larson model does not attempt to account for factors that reduce the actual runoff, such as surface storage of water.

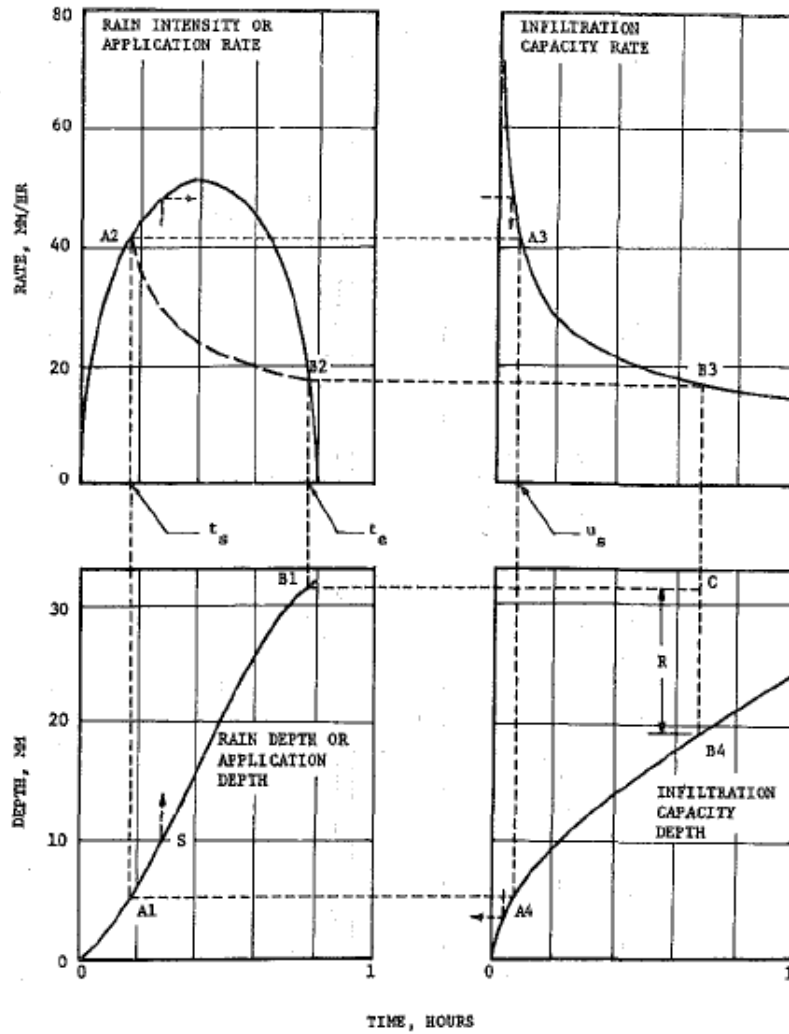


Figure 2-17: An illustration of the graphical method proposed by Chu (1987, Fig.2, p.159) to solve the generalised Mein-Larson model.

Table 2-1 shows that the graphical solution method of the Generalised Mein-Larson model fared very well against other modelling methods (Chu 1987).

Table 2-1: Comparison of estimated ponding time, t_p , calculated from four methods (Chu 1987, Table 1, p.161)

Soil (1)	Numerical solution ^a (days) (2)	Generalized Mein-Larson (days) (3)	Kincaid ^a (days) (4)	Dillon, et al. ^a (days) (5)
Loamy sand	0.043	0.043	0.050	0.032
Silt loam	0.018	0.018	0.018	0.015

^aData obtained from Heermann and Duke (6).

One of the difficulties with Chu's (1978, 1987) approach is that it presupposes that the infiltration capacity function is known and is unique for a given soil. Also, it may be that the sprinkler pattern is not a clean elliptical curve such as that used by Chu (1987) in Figure 2-17. Chu's method assumed that once t_p had been reached, that the application rate would remain greater than the infiltration capacity for the duration of the event. This assumption may not always hold true as Figure 2-16 illustrated and some further modification of Chu's methods may still be required to accommodate such scenarios.

2.6 Approximating Sprinkler Patterns for Use in Infiltration Models

Kincaid (2002) reported that reliable estimates of both K and the water application pattern were critical to predicting runoff. A common practice has been to approximate sprinkler or rainfall patterns with simple geometric shapes. Slack (1980) noted that elliptical or triangular approximations are generally used when modelling centre-pivot irrigation systems (Figure 2-18), even when the approximation bears little resemblance to the observed data (Figure 2-19).

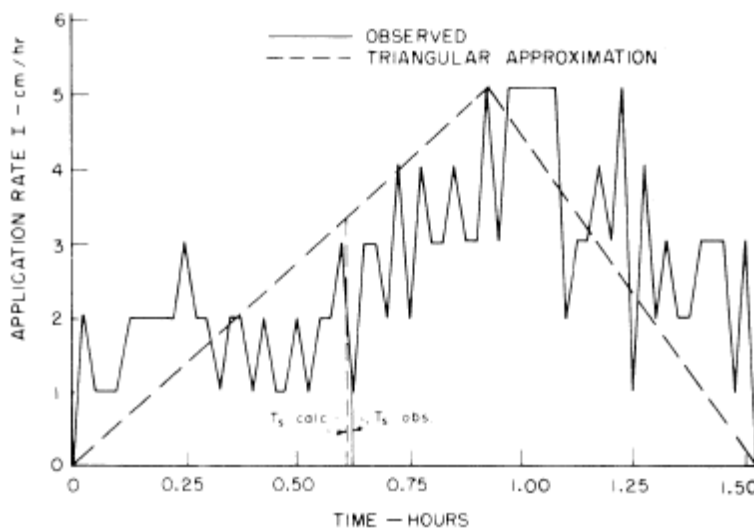


Figure 2-18: An example sprinkler application rate curve showing a triangular approximation to the observed data (Slack 1980, Fig.1, p.598)

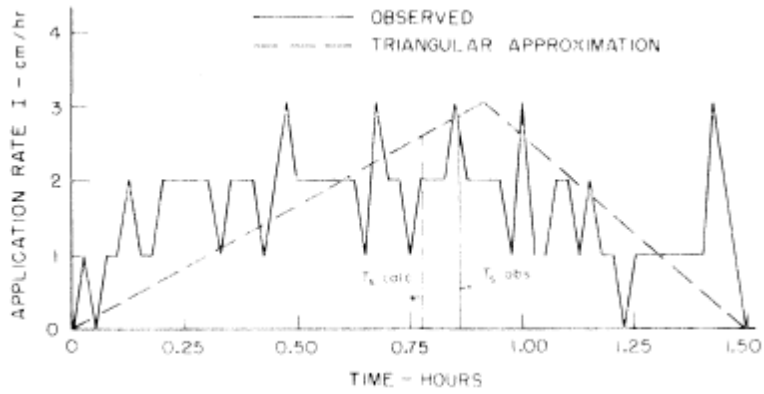


Figure 2-19: An example sprinkler application rate curve (Slack 1980, Fig.2, p.599) that demonstrates that in some cases the chosen triangular or elliptical approximation poorly reflects the observed data.

Chu (1987) noted, in his background to using the GAML model with variable rain, that the elliptical sprinkler pattern frequently encountered in the modelling of sprinkler irrigation is also being used to represent variable rain. This is exemplified by Hachum (1978) in Figure 2-20 and is in spite of the fact that a variable rainfall pattern would typically be something more like Figure 2-21 (Morel-Seytoux 1978).

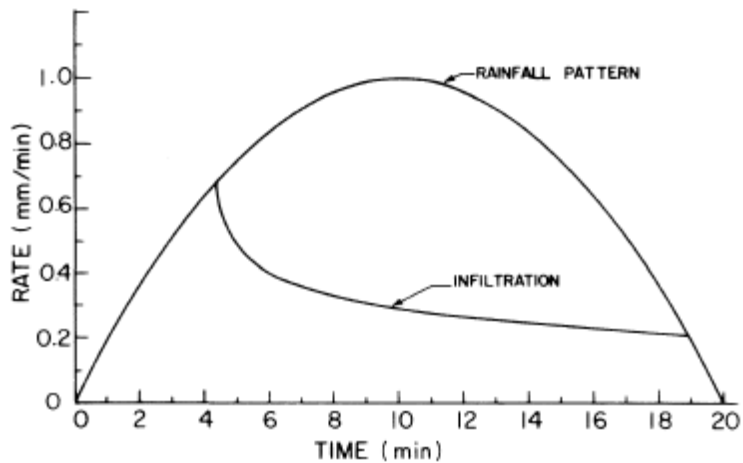


Figure 2-20: A variable rainfall pattern of an idealised elliptical form (Hachum 1978, Fig.2, p.504)

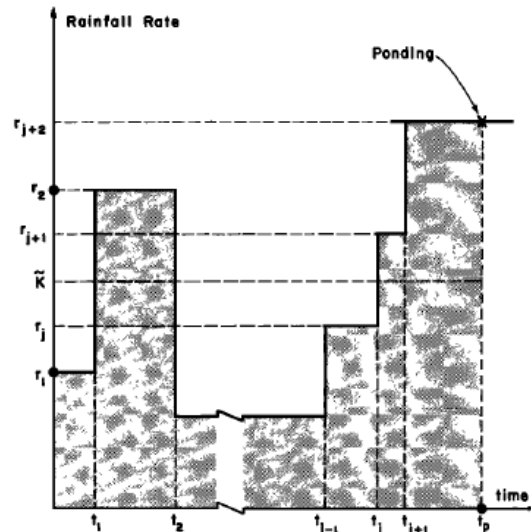


Figure 2-21: An example of a more 'typical' rainfall pattern (Morel-Seytoux 1978, Fig. 3, p.563).

DeBoer (2001, p.1217) noted that 'elliptical water application rate-time distributions have been used extensively during the past 30 years' for sprinkler irrigation simulations (Figure 2-22). However, his work identified that for three different irrigation technologies the distribution patterns tended to be more trapezoidal in shape than elliptical (DeBoer et al. 1992). He maintained that while the trapezoidal pattern had generally been a better approximation (Figure 2-23), its mathematical description required three piece-wise continuous segments which is more complex to work with than a single equation for an ellipse (DeBoer 2001).

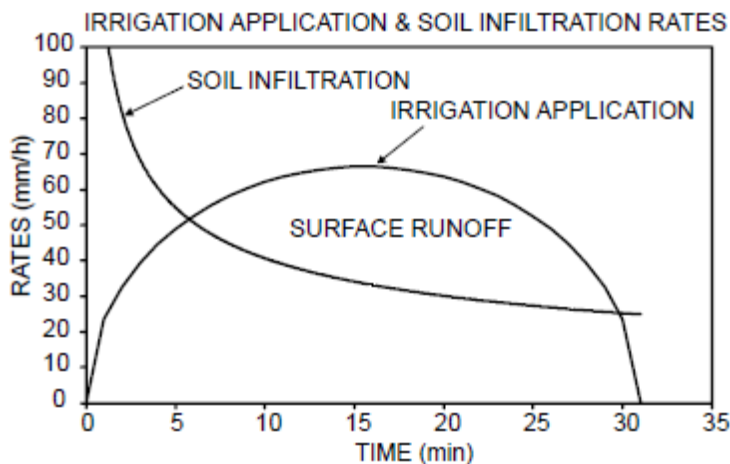


Figure 2-22: An example of the commonly assumed elliptical irrigation application pattern (DeBoer 2001, Fig. 1, p.1217).

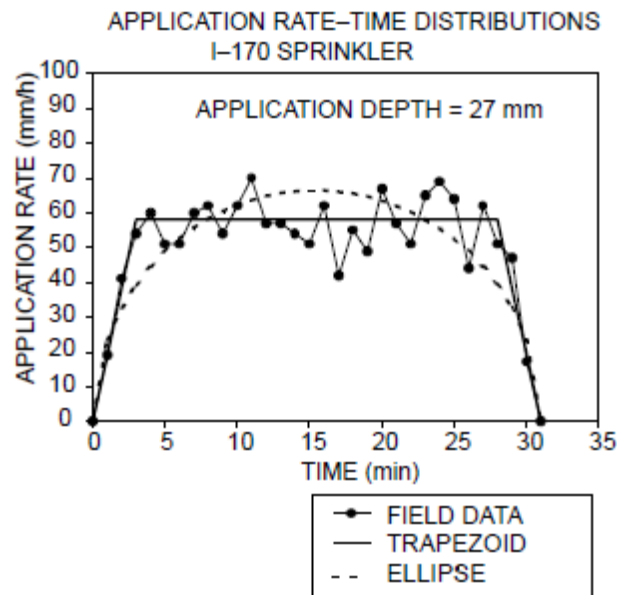


Figure 2–23: An example of trapezoidal and elliptical approximations of measured sprinkler data (DeBoer 2001, Fig.3, p.1218)

Instead of using a mathematical equation to describe the whole application profile, Luz (2011) used the sprinkler’s peak application rate and irrigation depth when modelling potential runoff under centre-pivot irrigation. Kincaid (2005, p.605) also decided to characterise application rates under traveling sprinkler laterals ‘in terms of average rate, peak rate and instantaneous rate’ for the purpose of creating an equation to predict nozzle size from system pressure and required flow.

Addink (1975, p.523) analysed the effect of different application patterns and reasoned that because the ‘intake rate of a soil is normally much higher during the first ten minutes than during the last ten minutes’ then a forward-skewed application-rate pattern would be at a definite advantage for reducing ponding and runoff. His experimental results showed forward skewed patterns to have more than 11% advantage over symmetrical patterns if the application time were equal for both, particularly for shrink-swell soils with higher percentage of clay particles (Addink 1975).

2.7 Literature Review Summary

The significance of infiltration for a wide variety of disciplines is reflected in the enormous body of literature that deals with it. Researchers and industry have resorted to a variety of techniques to model infiltration including using numerical methods involving the Richards equation; empirical curve-fitting methods; or physical/analytical models such as the Green-Ampt model. The Green-Ampt model remains pre-eminent among the physical infiltration models and many subsequent developments have emerged to deal with the significant assumptions of the original form. The Green-Ampt-Mein-Larson variant is the most significant and is the theoretical basis of this project.

Also discussed here were the issues of how the infiltration capacity function is determined and of how sprinkler patterns are represented. With regard to the former, ponded infiltrometers have been widely used but their suitability to modelling infiltration under rainfall is highly questionable; for this reason and others sprinkler infiltrometers are becoming increasingly popular. Regarding the representation of sprinkler patterns, these have tended to be modelled by idealised geometric shapes such as triangles, ellipses or trapezoids. This helps to simplify the modelling by allowing mathematical functions to describe the pattern; less work has been done with real application patterns.

Chapter 3 – Methodology

The primary objective of this project was to investigate an alternative method for estimating runoff that will be generated from a sprinkler irrigation event that has a time-varying application rate. Specifically, this required the application of two of Chu's (1986, 1987) methods to solving the GAML model to determine an infiltration characteristic for an in-situ field soil under sprinkler irrigation and thence to predict infiltration and runoff. A secondary objective that emerged during the course of the project was to explore an idea the author had for a new sprinkler infiltrometer technique.

3.1 Determining an Infiltration Characteristic and Predicting Runoff

Many of the techniques used to estimate and model the infiltration characteristic are not well suited to sprinkler irrigation which is characterised by application rates of finite magnitude that are typically smaller than the initial infiltration capacity. The work of Mein and Larson (1971) and Chu (1986, 1987) arose in response to these deficiencies. As noted in Section 2.5.5, a limitation of Mein and Larson's work was the requirement for a constant application rate, which rarely occurs in nature or under moving sprinkler systems. Chu's work sought to address this limitation but was only tested against simple, contrived data and numerical models. The primary objective in this project was to go one step further and apply Chu's methods using real sprinkler data in a field and test how well the runoff and infiltration can be predicted. For the purpose of this project this was a three-step process:

1. Use a sprinkler infiltrometer to determine the GAML parameters of a field plot and thus form an infiltration characteristic function.
2. Apply the infiltration characteristic function in a computer model to make a prediction of the runoff volume from a simple moving sprinkler system.
3. Measure the runoff from a field plot in close proximity and of similar form to that used in Step (1) and compare the results against those predicted.

3.2 STEP ONE: Determine GAML Parameters with Sprinkler Infiltrometer

Section 2.5.4.1 noted how difficult it can be to determine the K , h_f and θ_0 parameters required for Green-Ampt based equations. Chu (1986) suggested that because h_f and θ_0 always feature together in the GAML formulations, let them be lumped together as a single parameter; he labeled the lumped parameter SM (for effective soil moisture Suction at the wetting front, and the average Moisture content difference before and after wetting). That is:

$$SM \equiv h_f(\theta_s - \theta_0) \quad (3-1)$$

where the $h_f(\theta_s - \theta_0)$ term is from the Green-Ampt equation. Thus the time integrated form of the Green-Ampt equation :

$$I = K_s t - (h_f - h_s)(\theta_s - \theta_0) \log_e \left[1 - \frac{I}{(h_f - h_s)(\theta_s - \theta_0)} \right] \quad (3-2)$$

can be rewritten as:

$$\frac{I}{SM} - \log_e \left[1 + \frac{I}{SM} \right] = \frac{Kt}{SM} \quad (3-3)$$

Then it becomes necessary to only find two unknown terms K and SM . If one has an I vs t curve then solving Equation 3-3 simultaneously at two separate points will yield the two unknowns. Once K and SM are known then i vs t or i vs I infiltration characteristic curves can be generated. Chu (1986) resorted to a graphical method to overcome the difficulties of finding an analytical solution to the two simultaneous implicit logarithmic equations (detailed in Appendix B). This same method was adopted for the purposes of this project in which Chu's graphical process was encoded using Matlab (see Appendix C for the script).

The generation of an I vs t curve, necessary to this whole process, was done with a sprinkler infiltrometer. (As noted earlier, whilst ponded ring infiltrometers or other devices might also be able to generate infiltration characteristics, these rely on ponded

surface conditions and may not reflect well the physical processes happening in the sprinkler or rainfall context.)

3.2.1 The Sprinkler Infiltrometer

Section 2.4.2 noted a few of the sprinkler infiltrometer designs that are in common use. At the time of the project, none of these pieces of equipment were available to the author; furthermore, the author was keen to investigate whether an idea he had for a different approach to a sprinkler infiltrometer design might work. Thus it was decided to develop and trial a new sprinkler infiltrometer as a sub-project with the intent that it would also be used toward achieving the project’s primary objective. A second sprinkler infiltrometer design option was kept in reserve in case the first failed to perform as required; both are discussed below.

3.2.1.1 The SHCAZ Sprinkler Infiltrometer

The idea for a new approach to creating a sprinkler infiltrometer was conceived when it was noted during earlier sprinkler performance testing that a few particular sprinkler configurations produced a radial leg profile that featured a zone of constant application rate (compare Figures 3-1 and 3-2).

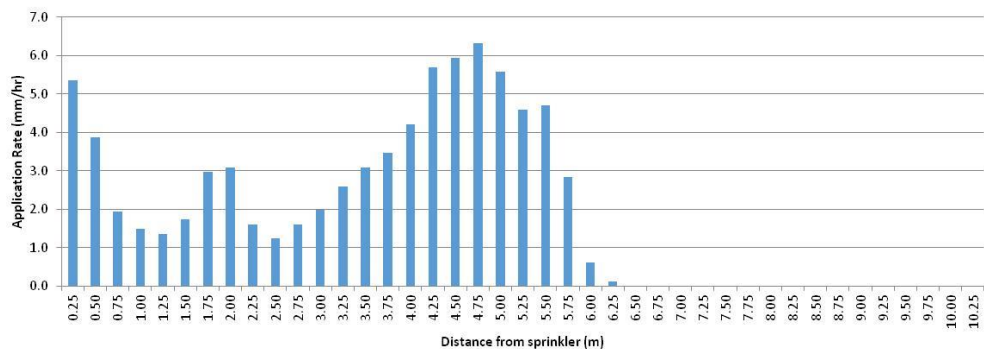


Figure 3–1: An example of a sprinkler radial leg profile. This example is of a Nelson S3000 with #21 nozzle, 10 PSI, height 2.44m, red plate. There is no zone of constant application rate in this profile.

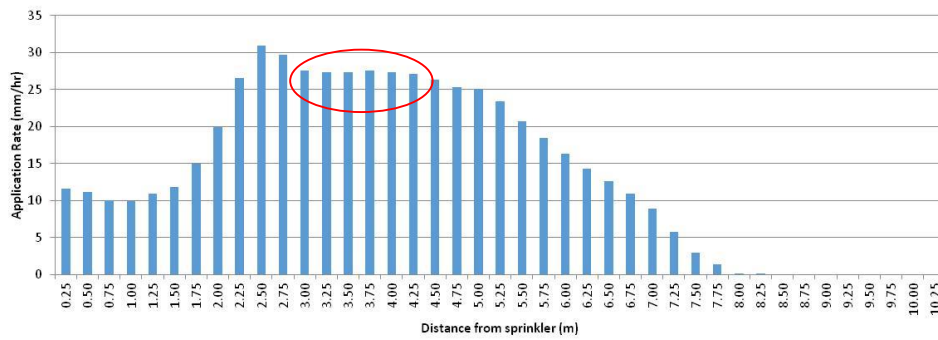


Figure 3-2: An example of a sprinkler radial leg profile that exhibits a zone of constant application rate. This example is of a Nelson S3000 #44 nozzle, 25 PSI, height 2.44m, red plate.

Thus rather than attempting to create an area of constant application rate over a soil test plot using an array of droppers, a grid of sprinkler heads, or an oscillating sprinkler head(s), it was instead proposed to locate a specifically selected sprinkler head at an appropriate distance from the soil test plot so that over the full area of the test plot there is a constant and known application rate. So, for example, if the sprinkler configuration of Figure 3-2 is used then a soil test plot that is 3.00m to 4.25m away would be expected to receive a reasonably uniform 27mm/hr of water application across its full surface (Figure 3-3). The author dubbed the concept as a Single-Head-Constant-Application-Zone (SHCAZ) Sprinkler Infiltrometer.

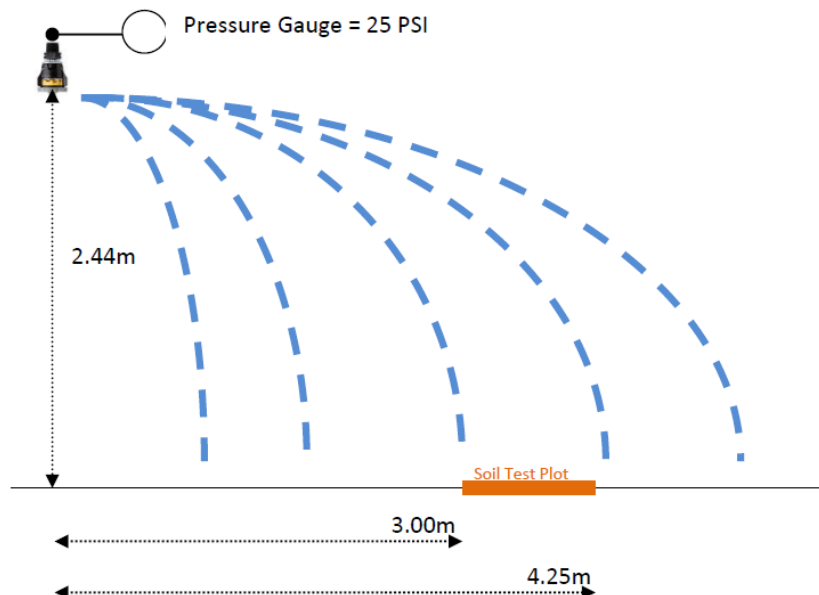


Figure 3-3: Illustration of the SHCAZ infiltrometer concept. From the data shown in Figure 3-2 this Soil Test Plot would be expected to receive a uniform 27mm/hr.

It became, then, a necessary task to first identify which combinations of nozzle size and pressure would produce suitable radial leg patterns for this purpose.

Identification of Appropriate Nozzle Size and Pressure Combinations in the Laboratory

The identification of which combinations of nozzle size and pressure would produce suitable radial leg profiles (that is, featuring a sufficiently large portion of the radial leg profile with a constant application rate) required an extensive survey of the possible combinations of nozzle sizes and operating pressures. The testing was undertaken in the hydraulics laboratory at the USQ Toowoomba campus during May and June 2015. The testing was confined to the Nelson S3000 Spinner Centre Pivot range of sprinkler products (Figure 3-4), as these were readily available at the time. The testing included only the red and yellow plates, otherwise the permutations would have become overwhelming as various nozzle size and pressure combinations were exercised.



Figure 3–4: Nelson S3000 Spinner head assembly with yellow plate and #18 nozzle (www.nelsonirrigation.com).

The hydraulics lab had a constant head delivery system that was used to supply a 415V centrifugal pump. The water was delivered by way of 20mm ($\frac{3}{4}$ inch) reinforced hose and rigid pipe to the sprinkler head that was fixed 2.54m above the ground. The catch-cans were circular plastic take-away containers that had an inner diameter at the mouth of 110mm, with a 6mm wide lip. The wide lip was removed part way through the testing process, giving a new mouth diameter of 105mm and a new lip width of 0.5mm (these new dimensions were noted in the data collected). The catch-cans were 0.10m in height, giving an effective sprinkler height of 2.44m (8ft). Water pressure was monitored by two separate gauges at 0.05m upstream of the sprinkler head (Figure 3-5) and flowrate was

monitored using a Kent mechanical flowmeter and an ABB Magmaster electromagnetic flowmeter. Pressure and flow were controlled using gate valves at the pump outlet.



Figure 3-5: Sprinkler head set-up, with the pressure line to primary pressure gauge and the secondary pressure gauge shown.

Catch-cans were spaced every 0.25m along a straight radial line, starting from immediately beneath the sprinkler head out to a distance of 9.00m (Figure 3-6). This spacing of catch-cans was much closer than generally reported in the literature and was intended to give a greater resolution in the radial leg profile.

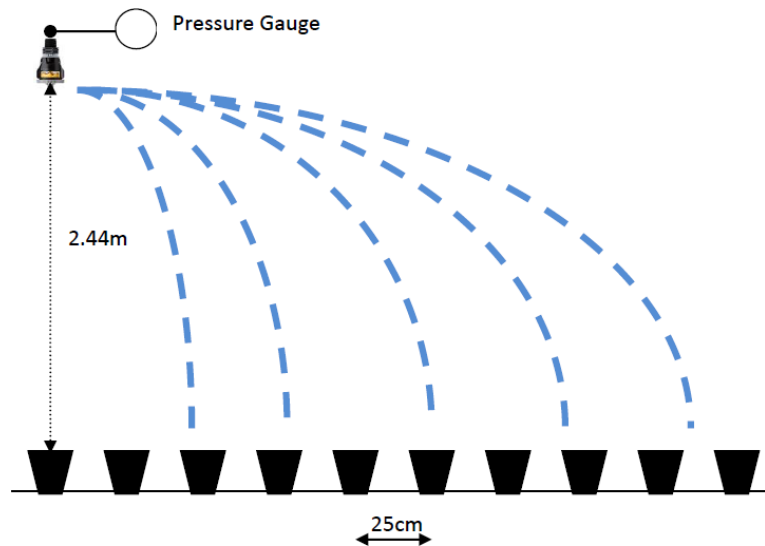


Figure 3–6: Schematic of the layout for the sprinkler radial leg data collection.

Screens were arranged around the sprinkler head so as to protect other equipment within the hydraulics laboratory. Several measures were taken in order to assure that no splash from the screens was reaching the catch-can containers: The screens were set back 1.5m from the catch-cans; the screens had soft towels draped over them where the water was travelling fastest so as to absorb some of the water’s energy; and additional catch-cans were positioned on the ground between the screens and the radial leg catch-cans in order to monitor the extent of splash (it was found that no splash came close to the radial leg catch-cans).

A wide variety of nozzle plus pressure combinations were tested, with pressures ranging between 6psi and 30psi, and nozzle sizes ranging between 14/128th inch (a #14 nozzle) through to 48/128th inch (a #48 nozzle). Each test typically ran for 30-60 minutes (longer tests were used for lower flowrate nozzles), and system pressure and flowrate were monitored during the test. The mass of water in each catch-can was measured at the end of the test and converted to an equivalent depth [mm] and application rate [mm/hour]. A plot of the sprinkler radial leg profile from each test was inspected to identify if it exhibited a zone of constant application rate, preferably of at least 1m in length. The tests that appeared suitable for the SHCAZ Sprinkler Infiltrometer were subjected to repeat testing to confirm the results.

3.2.1.2 A Reserve Sprinkler Infiltrometer: The ‘Bucket Infiltrometer’

Because the data generated from use of the sprinkler infiltrometer in the field was essential to the study, and because the proposed SHCAZ Sprinkler Infiltrometer was an untested concept, it was felt prudent to have a second sprinkler infiltrometer option in reserve. The chosen reserve infiltrometer was essentially a less sophisticated (and much less expensive) version of the Cornell Sprinkler Infiltrometer (Cornell 2003). It worked by forming droplets at a known rate above a small surface of soil and measuring the runoff (Figure 3-7), which is then compared to the water application rate to determine infiltration.



Figure 3-7: A Cornell Sprinkler Infiltrometer in use (Molacek et al. date unknown).

A 20L bucket was pierced with 21 hypodermic needles (Nipro brand, 21G - 0.8mm x 30mm) through the bottom in an equally spaced pattern; the needles used to pierce the holes in the plastic were discarded and replaced by new needles because it was found that sometimes the plastic from the bucket could partially or fully occlude the needle during the piercing process. The ‘bucket infiltrometer’ was placed on a stand at a height of 0.20m above the soil plot (Figure 3-8). A constant head of clean water was maintained by manually topping up the water level every three minutes to a pre-marked line at a depth of 0.30m. The variation in water depth was only ever about 0.01m and this delivered a

constant application rate of 178mm/hr over a soil area of 0.0638m² (a 28.5cm diameter circle).



Figure 3–8: The ‘bucket infiltrometer’ used as a reserve sprinkler infiltrometer,.

3.3 STEP TWO: A Computer Model to Predict Runoff and Infiltration

The computer model was written in Matlab r2015a Student Edition. The scripts can be found in Appendix C. A brief description of the model follows below. The computer model was created in two parts. The output of Part 1, an infiltration characteristic function based upon modified GAML parameters, became one of the inputs of Part 2.

3.3.1 Part 1 of the Computer Model: Determine the Infiltration Characteristic

Runoff versus time data was collected from a soil plot that had been subjected to a sprinkler infiltrometer. This was entered into Part 1 of the computer model and an infiltration characteristic was generated using the methods of Chu (1986). Figure 3-9 describes the process used.

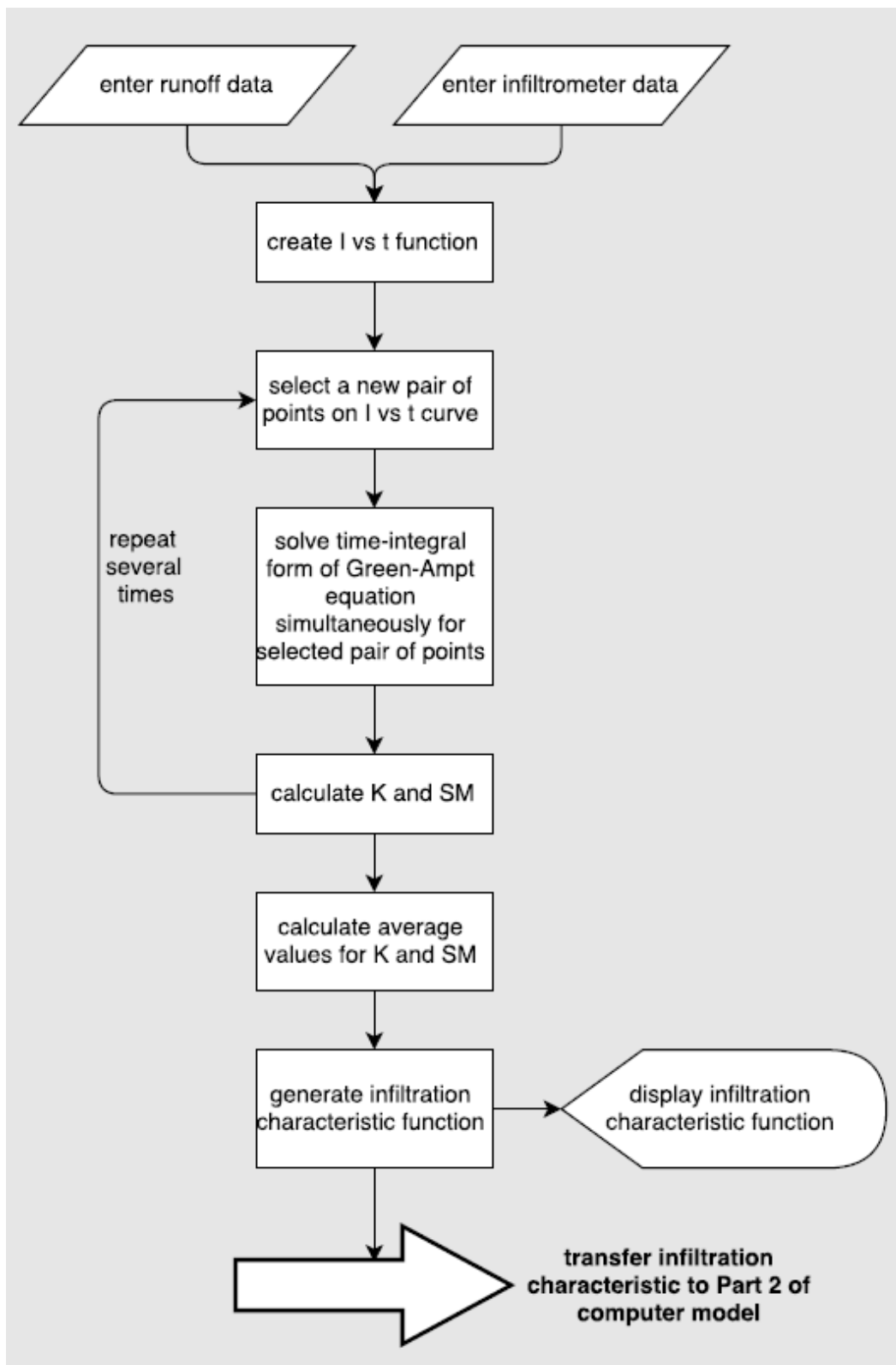


Figure 3-9: Flowchart describing the process used in Part 1 of the computer model.

3.3.2 Part 2 of the Computer Model: Estimating Runoff under Sprinklers

Laboratory radial leg catch-can data for selected individual sprinkler heads were interpolated in 2-dimensions to form a grid for each. Identical copies of the grid were superimposed, offset from the next by a distance that reflected the separation distance between adjacent sprinkler heads. This mapped the spatially varying application rates that would be expected underneath a system of sprinkler heads with overlapping areas of application. This was plotted as a 3-dimensional surface, with the x- and y- dimensions being distances along the ground, and the z- dimension being the rate of application by the system of sprinklers. A cross-sectional slice of the 3-dimensional shape, taken perpendicular to the line of sprinklers, produced a 2-dimensional curve, which was the r vs t curve (instantaneous application rate versus time).

By taking into account the travel speed of the system of sprinkler heads, an R vs t curve (cumulative application depth versus time) was yielded from the r vs t curve. The I vs t curve (cumulative infiltration depth versus time) was yielded from the i vs t curve that was generated in Part 1 of the computer model.

Using the four curves (i vs t , I vs t , r vs t , R vs t), the runoff was estimated using the methods of Chu (1987). Figure 3-10 describes the process used in Part 2 of the computer model.

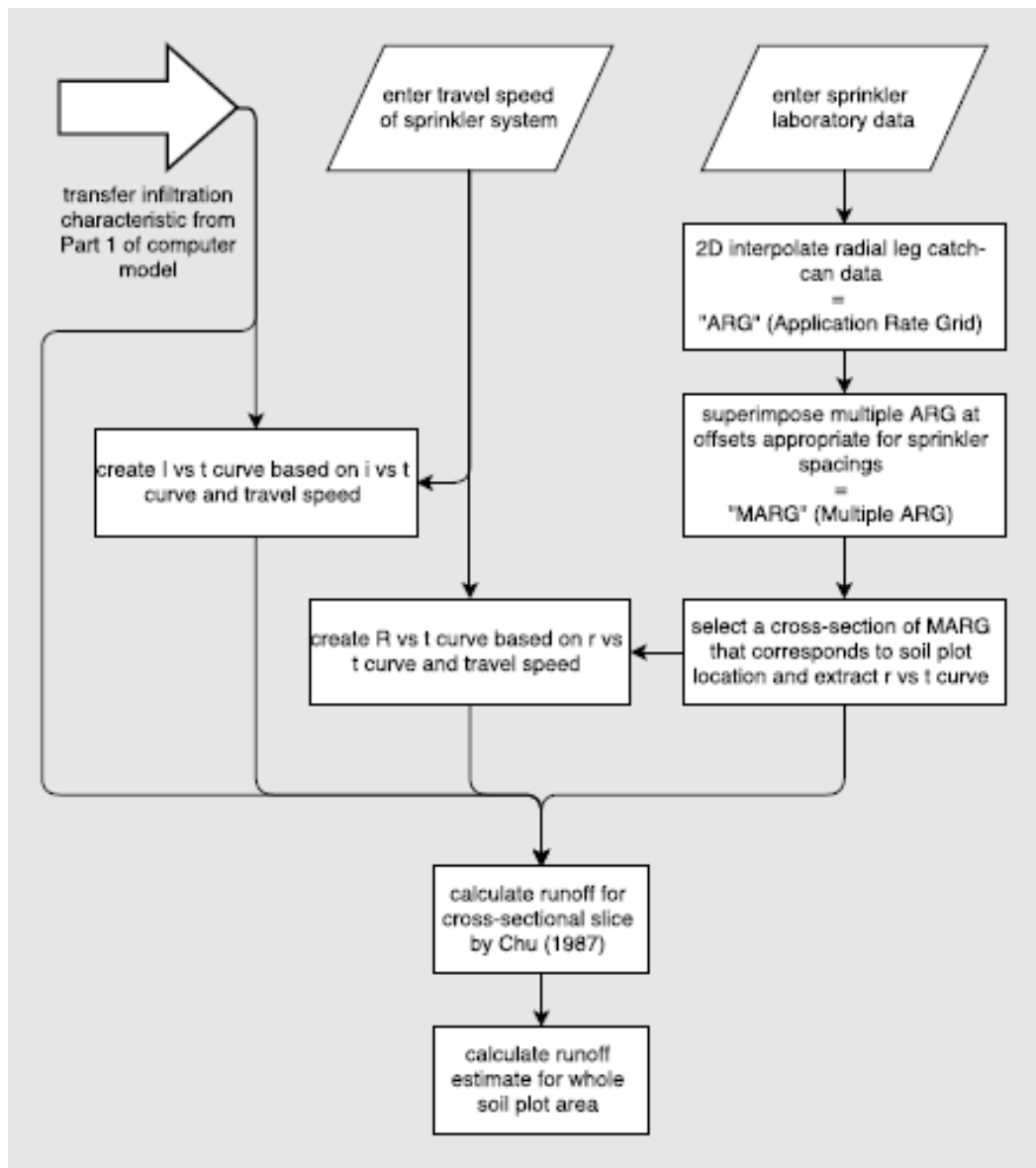


Figure 3–10: Flowchart describing the process used in Part 2 of the computer model.

Many infiltration and runoff models already existed which took into account, to varying degrees, a host of soil properties. Often there were complex data requirements that could be difficult to measure in a field environment. The appeal of this model was the simplicity of its data requirements: only cumulative infiltration vs time data was required from the field. The more difficult Step Three of the project’s research design (refer Section 3.1) was not part of the computer model per se; its purpose was just to validate the model’s predictions.

3.3.3 Desktop Testing of the Computer Model

Desktop testing of the computer model used published data from the literature to check the reliability of the model and programming. Part 1 of the computer model was fully tested. Part 2 of the computer model was only partially tested due to limited availability of suitable data.

3.4 STEP THREE: Field Measurements of Runoff

Step Three of the research design was about gathering field runoff measurements under a time-vary application rate to evaluate the accuracy of the predicted values for runoff from the computer model. It was necessary to construct a simple mobile sprinkler irrigation rig for this purpose.

3.4.1 Mobile Sprinkler Rig

A small mobile sprinkler rig was constructed during May and June 2015 (Figure 3-11).



Figure 3–11: The mobile sprinkler rig that was constructed for Step 3 of the project.

The rig was designed so that it could be dismantled easily and transported on the roof of a car. Budget constraints and a desire to re-use the materials at a later date for other purposes meant that the majority of the construction was made of timber and rope. The cantilever-type design (Figures 3-11 and 3-12) was chosen so that the rig could be more easily maneuvered around low shrubs, fences and grass embankments that were around the test area. Several passers-by likened the construction to a trebuchet! The square base was heavy for stability and sat upon four wheelbarrow wheels that proved quite suitable for rolling over the soft ground. The base also supported a battery-powered ABB AquaMaster electromagnetic flowmeter and a set of valves and pressure gauges for setting and monitoring the flow conditions in the hoses.

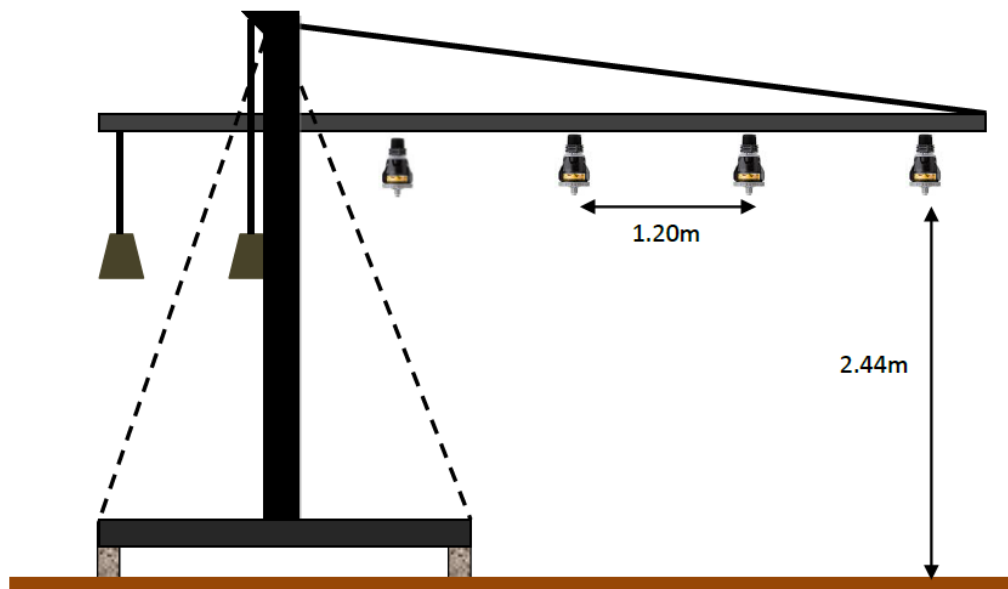


Figure 3-12: Sketch of the mobile sprinkler rig showing key dimensions. Not drawn to scale.

The horizontal beam from which the sprinklers were suspended was supported at a single pin so that its angle relative to the horizontal could be adjusted as required. This was useful, for example, when the ground under the rig's wheels was at a different slope to that of the soil test plots. The weight of horizontal beam was counterbalanced by a suspended weight; there was also a second suspended weight that tensioned a rope that was used to support the end of the beam against sagging. The vertical structure of the rig was supported by tensioned ropes connected to the base.

Four sprinkler heads were mounted on the horizontal beam at a spacing of 1.20m (4 ft) and a height of 2.44m (8 ft) above the ground. Three of the sprinkler heads were able to be removed and capped off (Figure 3-13) so that the rig could be used in a stationary mode for the SHCAZ Sprinkler Infiltrometer (refer 3.2.1), which removed the need to build a separate support structure.

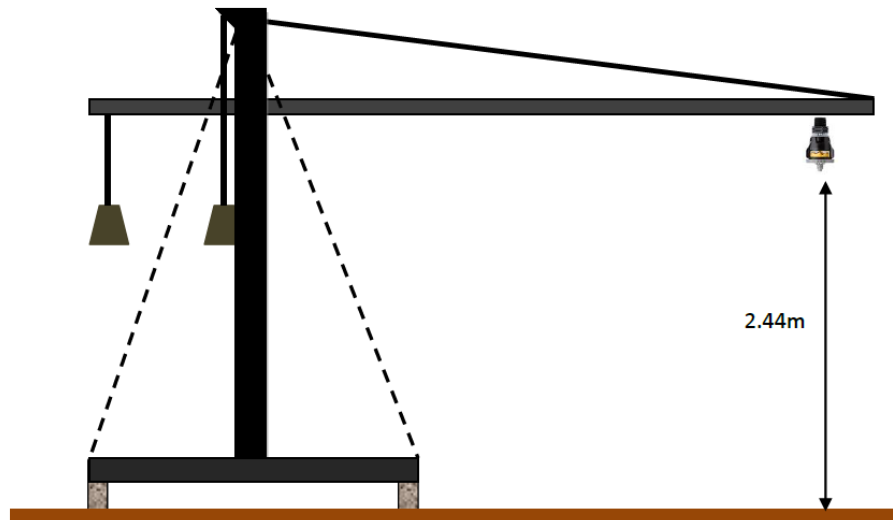


Figure 3–13: The mobile sprinkler rig as used in the static role as a sprinkler infiltrometer. The other 3 sprinkler heads have been removed and capped off.

The rig's water supply came via a 50m long 50mm lay-flat hose connected to a 50mm pressurised town water supply outlet. The pressure and flowrate were sufficient for the purposes of the testing and though an electric pump was connected to the water outlet it was not needed. The water was distributed to the four sprinkler heads by a 25mm (1") hose that was arranged in a branching configuration so that upstream of each sprinkler head was the same length of hose and the same arrangement of elbows, t-pieces and barbed connections (Figure 3-14). This was to promote an equal flow to each sprinkler head, which was an implied assumption in Part 2 of the computer model.



Figure 3–14: A schematic drawing showing how the water supply hose was repeatedly divided in an identical manner for each of the sprinklers.

The water pressure at the sprinkler heads was monitored via a pressure line that was connected immediately above one of the rigid vertical drops, with an adjustment made for the height difference between the sprinkler head and the gauge. Flowrate monitoring using the Aquamaster flowmeter helped to confirm that the correct pressures were being produced at the nozzles.

The mobile rig was pushed along manually during each test in Step Three. All of the wheels were fixed (non-swivel) and any steering required that the base of the rig be lifted and shifted sideways to set a new course, which was heavy work. Thus the soil plots from which runoff was collected were arranged in a straight line on the field so that the rig could be pushed in a straight line.

3.4.2 Collecting Runoff

Collecting the runoff was critically important to the project. It was performed when using the sprinkler infiltrometer for Step One and when using the mobile sprinkler rig for Step Three (refer Section 3.1).

3.4.2.1 Soil Plots for Runoff Generation

For the purposes of this project, ten soil plots were prepared near the USQ Agricultural Plot in Toowoomba. The soil plot sites were selected for their gently sloping ground

(gradient 5-7%) that would facilitate the collection of runoff, and their proximity to a suitable water source that would be needed for the tests.

The soil plots were prepared in pairs, located nearly adjacent to each other and of 0.75m x 0.75m size. The grass cover on each plot was reduced to approximately 50% using a line trimmer ('whipper snipper') so that the soil could be readily observed. A trench was dug along the bottom end of each plot, sloping toward a hole that was deep and wide enough to hold a collection container. A trough made from half of a 90mm PVC storm-water pipe was laid into the trench to collect the runoff water. The trench was cut so that its upslope wall angled beneath the soil plot to improve the chances of the PVC trough collecting the runoff water (Figure 3-15). Additionally, the PVC trough was pressed firmly into the soil wall by wooden chocks to improve runoff collection.

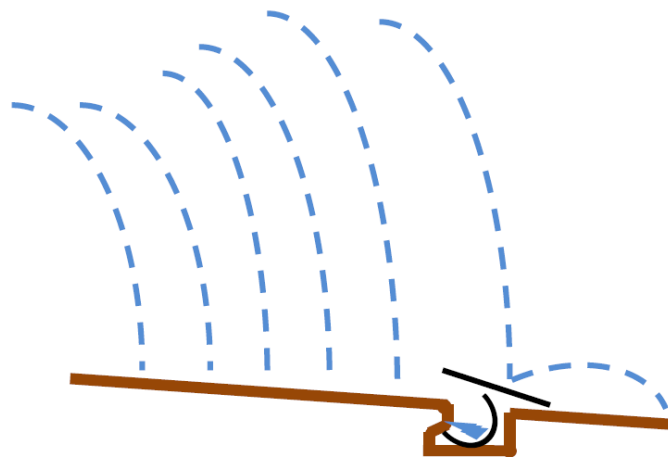


Figure 3–15: Sketch of side profile of the soil plot sloping down to the trench with an inlaid PVC half-pipe.

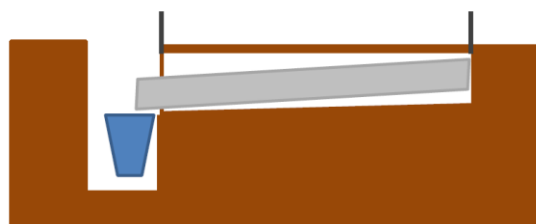


Figure 3–16: Sketch of end-view of PVC trough sitting in soil trench and sloping down to collection container.

The trench and the hole with the collection container were both covered so that there was no direct collection of sprinkler water. Thus what water was measured in the collection container was only runoff from the soil plot that came via the PVC trough.

A second trench was dug into the ground just uphill of each soil plot (not shown in Figure 3-17). Its purpose was to divert around the soil plot any runoff from further up the slope. A low border made of plywood with a sharpened edge was pressed into the ground around the top and side edges of each soil plot to encourage the runoff from the soil plot down toward the PVC trough and also to minimize runoff from outside the soil plot flowing sideways onto the soil plot (which would have been unlikely anyhow because that would require cross-slope flow).



Figure 3–17: One of the soil plots. The adjacent soil plot, the diverting trench (upslope) and protective cover have not been prepared yet and are not shown.

The soil plots were prepared in adjacent pairs. The first plot in each pair was used for the sprinkler infiltrometer testing (Step One); the second plot was used with the mobile sprinkler rig to confirm the computer model’s runoff predictions (Step Three). A tarpaulin covered the second plot during the infiltrometer testing and it was assumed that the second plot would have equivalent soil and hydraulic properties as the first plot given their close proximity and equal treatments. The mobile sprinkler rig was used on the second plot very soon after the cessation of the sprinkler infiltrometer at the first plot, usually within an hour.

3.4.2.2 Runoff from the Sprinkler Infiltrometers

Runoff was initially being measured using a tipping bucket rain gauge connected to a TinyTag data logger. A small pond pump was used to keep the water level in the hole below that of the rain gauge so that its function was not interfered with. However, technical difficulties with the equipment such as the data logger sometimes failing to make recordings or the tipping bucket rain gauge failing to signal tipping events meant that a simpler approach ended up being preferred. Runoff was simply measured using a 500mL plastic collection container in the hole that was weighed every three minutes during the test.

3.4.2.3 Runoff from the Mobile Sprinkler Rig

Only the total runoff was measured during the testing with the mobile sprinkler rig. This was because the computer model only produced a single value for the total runoff and no extra benefit would have been produced by trying to record the rate of runoff production. Also, because the mobile sprinkler rig was being pushed manually, an additional worker would have been required if frequent measurements were required. The total runoff was simply collected in a bucket and weighed at the end of the test, with the result rounded to the nearest 100ml.

Chapter 4 – Results and Analysis

The results from the preparatory work in the hydraulics laboratory and the results of the desktop testing of the computer model are presented first in Section 4.1. Then the results of the field phase of the project are presented in Section 4.2. Further discussion on the results is presented in Chapter 5.

4.1 Preparatory Work and Computer Model Testing

The preparatory work for the project was that which occurred before undertaking the field trials. It consisted of obtaining sprinkler data in the hydraulics laboratory for use by the SHCAZ Sprinkler Infiltrimeter and also for use by the computer model to predict the runoff generated by the mobile sprinkler rig. The preparatory work also included some basic desktop testing of the computer model against published data.

4.1.1 Laboratory Sprinkler Testing

Testing of sprinkler heads occurred as per Section 3.2 during May and June 2015 in the hydraulics laboratory at USQ, Toowoomba. The data from 67 sprinkler tests, each of about 30min to 60min duration, were recorded into an Excel file and the nine test results that were potentially suitable for the SHCAZ Sprinkler Infiltrimeter concept are listed in Table 4-1. The naming format used in Table 4-1 is explained in Figure 4-1. The full record of raw data and the accompanying sprinkler radial leg profiles of each of those nine tests are contained in Appendix D.

Table 4-1: Suitable sprinkler configurations for SHCAZ Sprinkler Infiltrometer concept.

Sred10_18
Sred10_21
Sred10_32
Sred15_26
Sred20_14
Sred20_38
Sred25_44
Sred30_38
Syellow20_21

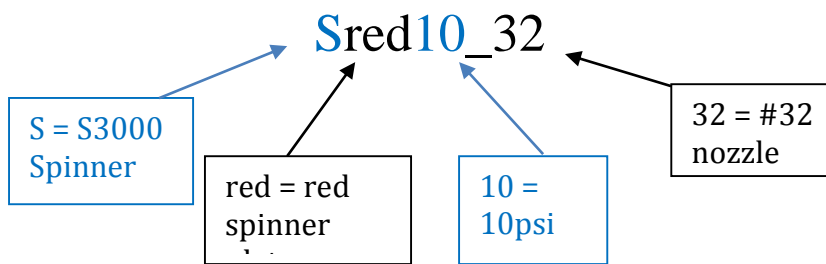


Figure 4-1: Naming format for sprinkler test results.

Of the nine test results in Table 4-1 the one that had the most potential for the SHCAZ Sprinkler Infiltrometer was the Sred25_44. Another test result that is not listed in Table 4-1 but was used heavily with the mobile sprinkler rig was the Sred6_44.

The Sred25_44 was a Nelson brand S3000 centre-pivot sprinkler head with a red spinner plate and #44 size nozzle (44/128ths of an inch), operating at 25psi from a height of 2.44m. Out of the nine sprinkler configurations that were suitable for the SHCAZ Sprinkler Infiltrometer concept this one had the highest application rate (27mm/hr). The collected data for the Sred25_44 sprinkler configuration are shown in Tables 4-2 and 4-3 and two radial leg plots are included in Figure 4-2. (Discussion on the difference between these radial leg plots can be found in Chapter 5.)

Table 4-2: Catch-can data for Sred25_44 test.

Distance (m)	Mass			Average Mass (g)	Depth (mm)	Application Rate (mm/hr)
	Can 1 (g)	Can 2 (g)	Can 3 (g)			
0.00	3743			3743	70	127
0.25	45.0	68.0	55.0	56	6	12
0.50	52.0	65.0	45.0	54.0	6.2	11
0.75	48.0	38.0	60.0	48.7	5.6	10
1.00	47.0	42.0	54.0	47.7	5.5	10
1.25	53.0			53.0	6.1	11
1.50	57.0			57.0	6.6	12
1.75	72.0			72.0	8.3	15
2.00	96.0			96.0	11.1	20
2.25	128.0			128.0	14.8	27
2.50	149.0			149.0	17.2	31
2.75	143.0			143.0	16.5	30
3.00	133.0			133.0	15.4	28
3.25	132.0			132.0	15.2	27
3.50	132.0			132.0	15.2	27
3.75	133.0			133.0	15.4	28
4.00	132.0			132.0	15.2	27
4.25	131.0			131.0	15.1	27
4.50	127.0			127.0	14.7	26
4.75	122.0			122.0	14.1	25
5.00	121.0			121.0	14.0	25
5.25	113.0			113.0	13.0	23
5.50	100.0			100.0	11.5	21
5.75	89.0			89.0	10.3	18
6.00	79.0			79.0	9.1	16
6.25	69.0			69.0	8.0	14
6.50	61.0			61.0	7.0	13
6.75	53.0			53.0	6.1	11
7.00	43.0			43.0	5.0	9
7.25	28.0			28.0	3.2	6
7.50	14.0			14.0	1.6	3
7.75	6.5			6.5	0.8	1
8.00	0.7			0.7	0.1	0
8.25	0.2			0.2	0.0	0

Table 4-3: Test conditions for the Sred25_44 test.

<u>Sprinkler Settings</u>	
Nozzle	44 1/128ths
Pressure	25 PSI
Sprinkler Type	S3000 (Grey Cap)
Plate Colour	Red
Height sprinkler	2.54 m
Height catch-cans	0.1 m
Effective Height	2.44 m
Catch-can Diameter	105 mm
Catch-can lip thickness	0.5 mm
Zero Pt Can Diameter	260 mm

<u>Date & Duration</u>	
Test Date:	2/06/2015 (hh:mm 24hr)
Time Start	<input type="text"/>
Time Finish	<input type="text"/>
Total Time	or Stopwatch Time 0:33:26 (h:mm:ss)
Total Time (digital)	0.56 hrs

<u>Flow Rates</u>	
KENT FLOWMETER	
Flow Meter @ START	<input type="text"/> 23.9887 m3
Flow Meter @ END	<input type="text"/> 26.2888 m3
Av. Flow Rate	68.8 L/min
Av. Flow Rate	18.2 US GPM
ABB MAGMASTER ELECTROMAGNETIC FLOWMETER	
Velocity	<input type="text"/> 6.5 m/s
Instantaneous Flow Rate	<input type="text"/> 1.14 L/s @ time <input type="text"/>
Instantaneous Flow Rate	<input type="text"/> 1.14 L/s @ time <input type="text"/>
Instantaneous Flow Rate	<input type="text"/> 1.13 L/s @ time <input type="text"/>
Av. Instantaneous Flow Rate	1.137 L/s
Equivalent Av. Flow Rate	68.2 L/min
Equivalent Av. Flow Rate	18.02 US GPM
NELSON SUPPLIED FLOW VALUES FOR GIVEN NOZZLE + PRESSURE	
Flow Rate per 3TN Nozzle Chart	<input type="text"/> 64.3 L/min
Flow Rate per 3TN Nozzle Chart	<input type="text"/> 17 US GPM

<u>Environment</u>	
Test Location?	Lab (Indoors)
Solar Irradiance?	No
Wind?	No
Wind Speed (kph)	0
Dry Bulb Air Temp (deg C)	14
Wet Bulb Air Temp (deg C)	n/a
Water Temp (deg C)	16
Relative Humidity	n/a
Av. Hourly Loss to Evaporation on 10.0mL sample in catch-can	0.1 ml

<u>Scales</u>	
Brand	Digitech
Measurement Increments	0.01g up to 1kg
Tolerance Checked?	Yes (May 2015)
Tolerance	<0.03%
<u>Pressures</u>	
Gauge 1 (Primary)	Wika Mechanical (-100 - 250kPa)
Gauge 2 (Secondary)	(0 PSI - 60 PSI)

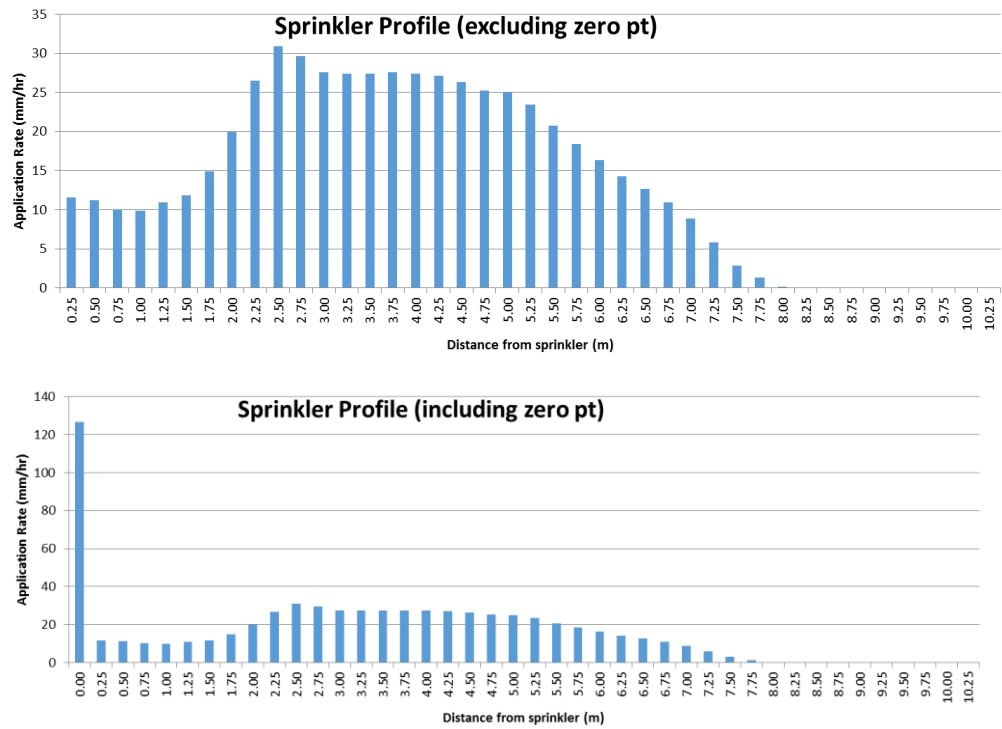


Figure 4–2: Plots of the catch-can data for the Sred25_44 sprinkler test. The second plot includes the catch-can directly beneath the sprinkler head.

The second laboratory test result that was heavily used in the field phase on the mobile sprinkler rig was the Sred6_44. This was also a Nelson brand S3000 centre-pivot sprinkler head with a red spinner and a #44 size nozzle, but operated at only 6psi from 2.44m. The tables of data and the radial leg plots are presented in Tables 4-4 and 4-5, and Figure 4-3.

Table 4-4: Catch-can data for Sred6_44 test.

Distance [m]	Mass			Average Mass [g]	Depth [mm]	Application Rate [mm/hr]
	Can 1 [g]	Can 2 [g]	Can 3 [g]			
0.00	1484			1484	28	47.9
0.25	24.4	21.7	18.5	22	2	4.3
0.50	14.1	17.9	13.6	15.2	1.8	3.0
0.75	8.7	7.5	12.7	9.6	1.1	1.9
1.00	9.2	7.6	7.8	8.2	0.9	1.6
1.25	9.4			9.4	1.1	1.9
1.50	13.6			13.6	1.6	2.7
1.75	20.2			20.2	2.3	4.0
2.00	25.9			25.9	3.0	5.1
2.25	33.7			33.7	3.9	6.7
2.50	44.8			44.8	5.2	8.9
2.75	61.4			61.4	7.1	12.2
3.00	75.7			75.7	8.7	15.0
3.25	83.5			83.5	9.6	16.5
3.50	99.4			99.4	11.5	19.7
3.75	119.3			119.3	13.8	23.6
4.00	126.2			126.2	14.6	25.0
4.25	110.4			110.4	12.7	21.8
4.50	86.4			86.4	10.0	17.1
4.75	94.6			94.6	10.9	18.7
5.00	167.9			167.9	19.4	33.2
5.25	208.7			208.7	24.1	41.3
5.50	97.2			97.2	11.2	19.2
5.75	34.0			34.0	3.9	6.7
6.00	16.5			16.5	1.9	3.3
6.25	5.3			5.3	0.6	1.0
6.50	0.7			0.7	0.1	0.1
6.75	0.0			0.0	0.0	0.0
7.00	0.0			0.0	0.0	0.0
7.25	0.0			0.0	0.0	0.0
7.50	0.0			0.0	0.0	0.0
7.75	0.0			0.0	0.0	0.0
8.00	0.0			0.0	0.0	0.0
8.25	0.0			0.0	0.0	0.0

Table 4-5: Test conditions for the Sred6_44 test.

Sprinkler Settings		
Nozzle	44	1/128ths
Pressure	6 PSI	(53kPa Big Gauge)
Sprinkler Type	S3000	(Grey Cap)
Plate Colour	Red	
Height Sprinkler	2.54 m	
Height Catch-cans	0.1 m	
Effective Height	2.44 m	
Catch-can Diameter	105 mm	
Catch-can Thickness	0.5 mm	
Zero Pot Can Diameter	260 mm	

Date & Duration		
Test Date:	24/06/15	
	(hh:mm:24hr)	
Time Start		or
Time Finish		
Total Time		
		Stopwatch Time
		0:35:01
		(h:mm:ss)
Total Time (digital)	0.58 hrs	

Flow Rates		
KENT FLOWMETER		
Flow Meter @ START	45.2857	m3
Flow Meter @ END	46.4040	m3
Av. Flow Rate	31.9	L/min
Av. Flow Rate	8.4	US GPM
ABB MAGMASTER ELECTROMAGNETIC FLOWMETER		
Velocity	3	m/s
Instantaneous Flow Rate	0.53	L/s @ Time 0:01:00
Instantaneous Flow Rate	0.53	L/s @ Time 0:16:00
Instantaneous Flow Rate	0.53	L/s @ Time
Av. Instantaneous Flow Rate	0.530	L/s
Equivalent Av. Flow Rate	31.8	L/min
Equivalent Av. Flow Rate	8.40	US GPM
NELSON SUPPLIED FLOW VALUES FOR GIVEN NOZZLE PRESSURE		
Flow Rate per BTN Nozzle Chart	31.52	L/min
Flow Rate per BTN Nozzle Chart	8.33	US GPM

Environment	
Test Location?	Lab (Indoors)
Solar Irradiance?	No
Wind?	No
Wind Speed (kph)	0
Dry Bulb Air Temp (deg C)	15
Wet Bulb Air Temp (deg C)	n/a
Water Temp (deg C)	15
Relative Humidity	n/a
Av. Hourly Loss to Evaporation on 0.0m L Sample in Catch-can	0

Scales		
	Brand	Digitech
Measurement Increments		0.01g (up to 2kg)
Tolerance Checked?		Yes (May 2015)
Tolerance		<0.03%

Pressures	
Gauge (Primary)	Wika Mechanical (-100 to 250kPa)
Gauge (Secondary)	(0 PSI to 0 PSI)

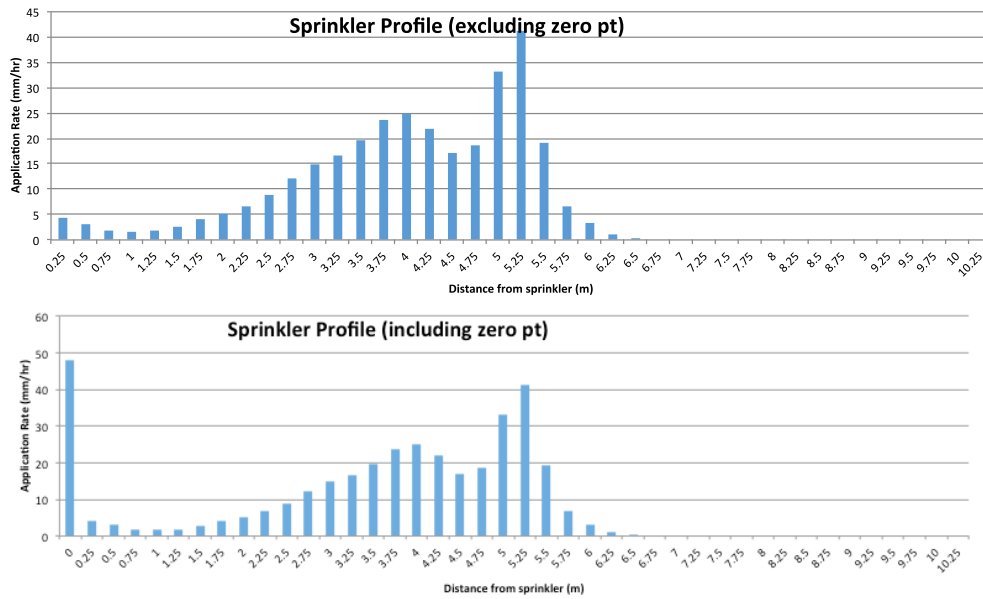


Figure 4-3: Plots of the catch-can data for Sred6_44 sprinkler test.

4.1.2 Desktop Testing of Computer Model

The results of the desktop testing of the computer model are included here. For the computer model's outputs using the sprinkler infiltrometer and mobile sprinkler rig field data see Section 4.2.

4.1.2.1 Desktop Testing of Part 1 of the Computer Model

Chu (1986) proposed a graphical method to determine the GAML parameters using a sprinkler infiltrometer with a constant application rate. The method was encoded by the author in Matlab and the scripts are included in Appendix C.

Two sets of published I vs t data (Table 4-6) were used to validate the programming. The values for K and SM that Chu determined (refer Appendix B) are included below each data set.

Table 4-6: Cumulative Infiltration (I) vs time (t) data from Chu (1986).

t (min)	I (mm)
0	0.0
6	7.6
7	8.1
8	8.1
9	9.1
10	9.7
11	10.2
12	10.7
13	11.4
14	11.9
15	12.4
16	13.0
17	13.5
18	14.0
19	14.5
20	15.2
21	15.7
22	16.3
25	17.5
30	19.8
35	22.6
39	24.4
40	24.9
45	27.2
50	30.0
55	32.3
60	34.3

K = 2.11cm/hr
SM = 0.74cm

t (min)	I (mm)
0	0.0
5	7.6
7	10.9
10	15.5
15	21.8
20	27.2
25	32.0
30	36.3
35	40.9
40	45.0
44	48.0
50	52.3
54	55.4
58	58.2
65	63.0
70	66.0
80	72.4
90	78.5

K = 7.72cm/hr
SM = 0.13cm

Figure 4-4 shows the output plots from testing Part 1 of the computer model using the first set of Chu's (1986) data in Table 4-6. The top-left plot shows the I vs t data. The bottom two plots are included only to assist with understanding the process used to solve the implicit form of the Green-Ampt equation simultaneously (see Appendix B for a mathematical description of the process). Here the computer model calculated that $K = 2.17\text{cm/hr}$ and $SM = 0.70\text{cm}$, both of which are within 5% of Chu's manually calculated values of $K = 2.11\text{cm/hr}$ and $SM = 0.74\text{cm}$. The i vs I plot that can be generated once K and SM are determined is shown at the top-right plot in Figure 4-4.

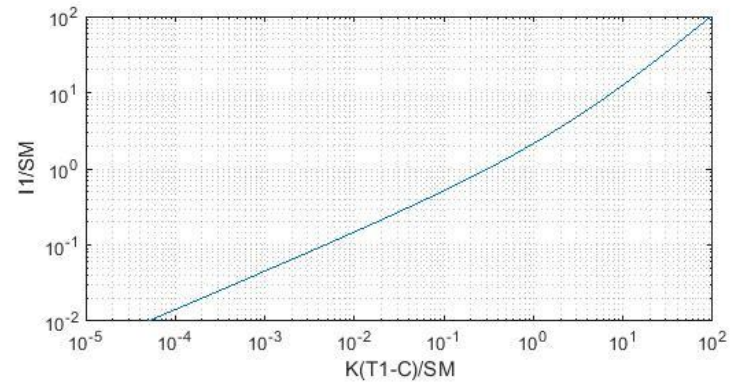
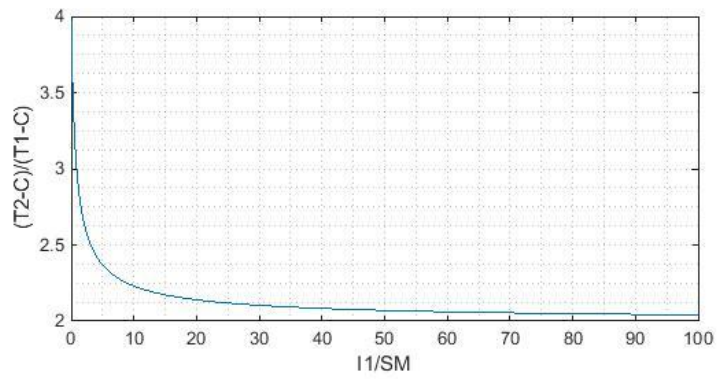
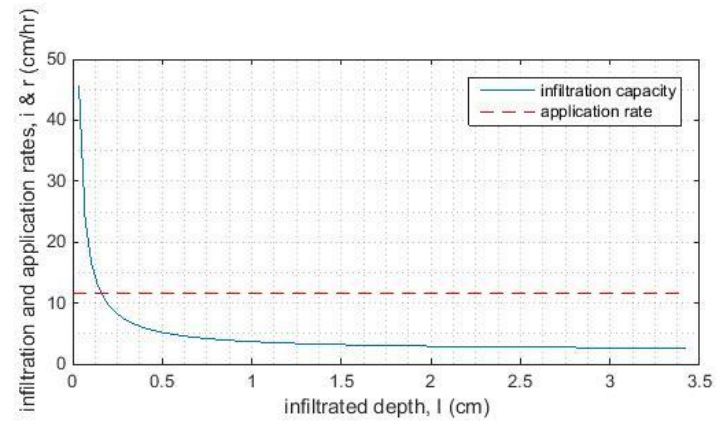
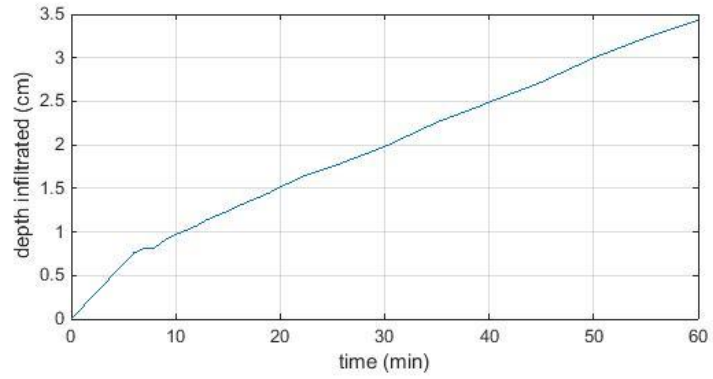


Figure 4-4: Output from desktop testing of Part 1 of computer model using the first set of Chu's (1986) infiltration data.

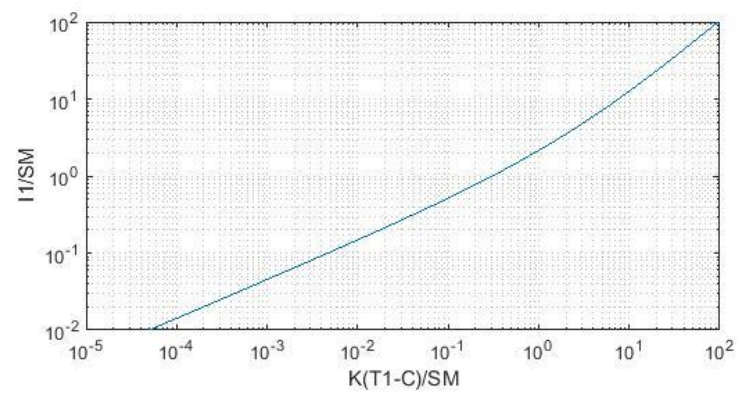
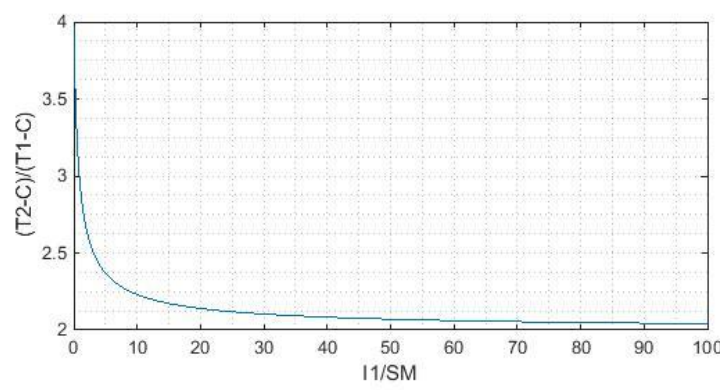
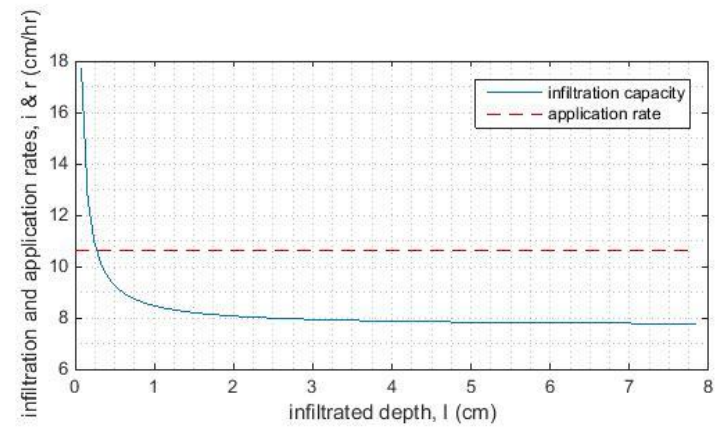
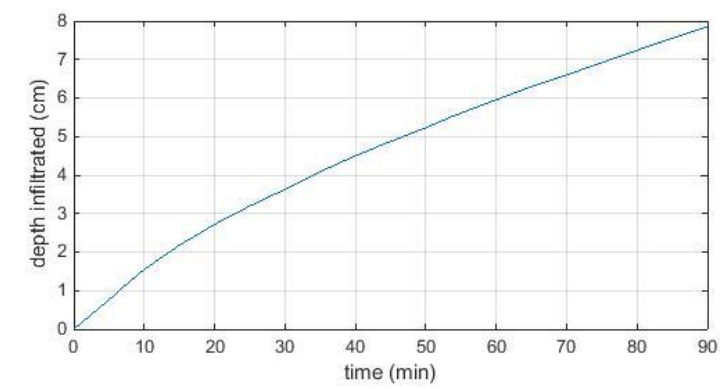


Figure 4-5: Output from desktop testing of Part 1 of computer model using second set of Chu's (1986) infiltration data.

To repeat the process, the second of Chu's data sets in Table 4-6 was used to check the computer program. The output plots are presented in Figure 4-5. The computer model determined that K and SM are 7.67cm/hr and 0.103cm respectively, which compared favourably to Chu's manually determined values of 7.72cm/hr and 0.13cm.

4.1.4.2 Desktop Testing of Part 2 of the Computer Model

Only a small part of Part 2 of the computer model could be subjected to desktop testing before implementation with real field data. This was because no suitable information sources that combined sprinkler information and cumulative infiltration/runoff data could be found.

Chu (1987) used only highly idealised functions to demonstrate the efficacy of his method. Nevertheless, his data and results were used for the desktop testing of the programming of Part 2 of the computer model. Note that whilst predicting the time-to-ponding was not an explicit objective in this project, the computer model was able to estimate the time-to-ponding in the course of estimating runoff and it was convenient to use the time-to-ponding value to compare other methods (Table 4-7 and Figure 4-6).

Table 4-7: Comparison of predicted time-to-ponding for two different soils by different approaches. The numerical solution to Richard's equation and Chu's graphical method are both per Chu (1987)

		Silt Loam	Loamy Sand
Equations of curves used for modelling		$i = 1.15t^{-0.587}$ $I = 2.79t^{0.413}$ $r = 1500t$ $R = 750t^2$	$i = 15.8t^{-0.336}$ $I = 23.8t^{0.664}$ $r = 1500t$ $R = 750t^2$
Predicted time to ponding	Numerical solution to Richards equation	0.018 days	0.043 days
	Chu's graphical method	0.018 days	0.043 days
	Part 2 of computer model	0.020 days	0.049 days

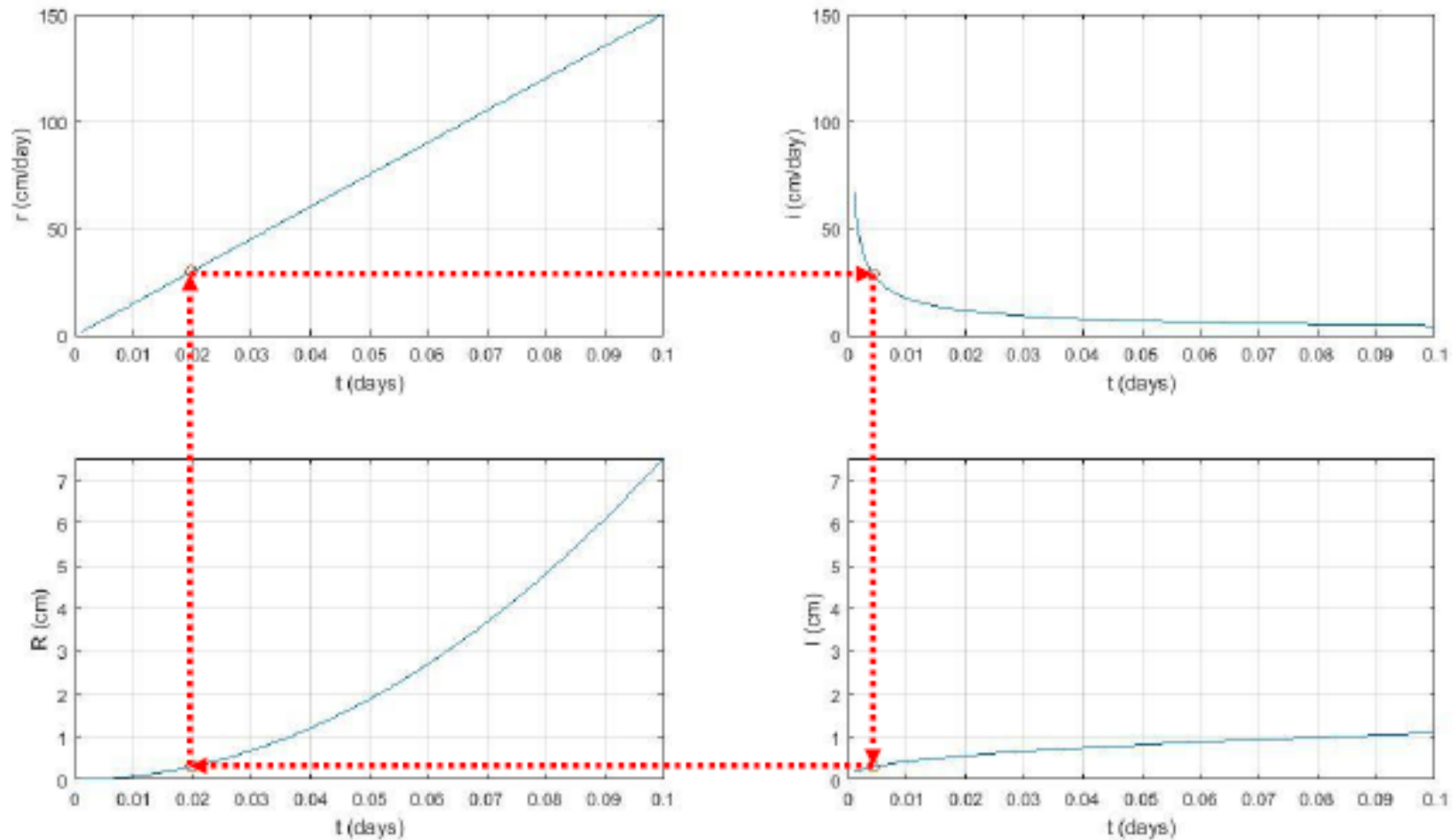


Figure 4-6: Example of the iterative process used per Chu (1987) for Part 2 of the computer model. These plots correspond to the Silt Loam of Table 4-7. The red dashed line has been added in for illustrative purposes.

For the two desktop tests performed on Part 2 of the computer model it appears that results were within 10-15% of the values produced by the other modelling methods.

In summary, then, Part 1 and Part 2 of the computer model appeared to be working reasonably to the extent that it could be tested against published data.

4.2 Field Observations and Model Predictions

The field testing phase of the project involved using the sprinkler infiltrometer to generate *I vs t* data, making runoff predictions using that same data with Part 1 and Part 2 of the computer model, and then using the mobile sprinkler rig to supply a time-varying sprinkler application pattern to test the computer model's runoff predictions. The results of these three activities are presented here.

4.2.1 The SHCAZ Sprinkler Infiltrator

The SHCAZ Sprinkler Infiltrator was implemented in the field by capping off three of the four sprinkler heads on the (stationary) mobile sprinkler rig (Figure 3-13, refer 3.4.1). The Sred25_44 sprinkler configuration (refer 4.1.1) was used as it had the highest application rate. However, disappointingly, the SHCAZ Sprinkler Infiltrator concept was eventually abandoned after repeated attempts to collect *I vs t* data due to several intractable problems. Most notable of these problems was interference by gusting and shifting winds, but long test times and high rates of water consumption were also contributory factors to abandoning the concept for this project.

No attempts at collecting *I vs t* data using the SHCAZ Sprinkler Infiltrator in the field were successful. Further discussion on this matter is presented in Chapter 5. All *I vs t* data that was measured in the field during this project was generated using the 'bucket infiltrometer' (refer 3.2.1.2 and 4.2.2).

4.2.2 The Bucket Infiltrometer

The alternative sprinkler infiltrometer for this project was the so-called ‘bucket infiltrometer’ (refer 3.2.1.2). This option had been held in reserve and was only constructed and applied in the field when it became apparent that the SHCAZ Sprinkler Infiltrometer concept was not going to perform as hoped.

The bucket had twenty-one hypodermic needles pierced through the bottom, with the hubs of the needles pointing toward the ground. The dripping rate of the needles was tested several times and the overall performance was as per Table 4-8.

Table 4-8: Bucket Infiltrometer performance parameters.

Head of water [m] over the needle tip	0.30 m
Water temperature [°C]	14
Gauge of needle (Nipro brand)	21G (0.8 mm x 30 mm long)
Diameter [m] of soil plot under bucket Area [m ²]	0.285 m 0.0638 m ²
Flowrate of a single needle	0.15 ml/sec (540 ml/hour)
Flowrate of 21 needles	11.34 L/hour
APPLICATION RATE OF 21 NEEDLES	178 mm/hour

Clean town water was used in the bucket infiltrometer but some small pieces of grass or dirt still occasionally made their way into the water and proceeded to occlude some of the needles. Thus the water was fully changed in between each test and all of the needles were flushed through using a syringe.

Runoff that was generated from each of the soil plots under the bucket infiltrometer was collected via the soil plot runoff collection system (refer 3.4.2). Every three minutes the water collection container was exchanged with an empty one, and the mass of the water collected was measured. At this point the water level in the bucket was also topped up so

that the head of 0.30m over the needles remained constant. Any reduced flow through the needles manifested itself by a reduction in the amount of water required to top up the bucket for the three minute interval, and served as a prompt to take corrective action (generally requiring the piece/s of grass to simply be removed from the needle bevel).

The field tests were undertaken in July through September 2015. The tests were arranged in pairs (e.g. Test 1A and 1B) on adjacent soil plots. The first test involved the use of the sprinkler infiltrometer (the ‘bucket infiltrometer’) on the first soil plot to generate the *I vs t* data (Step One per Section 3.1). The second test involved the use of the mobile sprinkler rig to provide a time-varying application rate over the second soil plot to generate surface runoff which was collected and measured (Step Three per Section 3.1).

18 field tests were conducted, arranged into 9 pairs (Test 1A/1B etc. where Test A was the first test with the sprinkler infiltrometer and Test B was the corresponding second test with the time-varying sprinkler application rate provided by the mobile sprinkler rig). The test conditions common to all of the 9 pairs of tests are detailed in Table 4-9. Field results are given in Sections 4.2.4 and 4.2.5.

Table 4-9: Details of test conditions common to all pairs of tests.

	Test A	Test B
Method of water application	Bucket infiltrometer	Mobile sprinkler rig 4 x Sred6_44 at 2.44m
Application rate	178mm/hr	Time-variable application rate, but the system throughput was 2.1L/s, or 7.6m ³ /hr. Peak application rate = 140mm/hr. Mean application rate = 48mm/hr.
Speed of system	Stationary	36m/hour

4.2.3 Mobile Sprinkler Rig

The mobile sprinkler rig worked remarkably well during Step Three of the project. It was easily assembled and quite stable. Figure 4-7 shows it connected to the 50mm hose and Figure 4-8 shows it parked downwind of a building that had protected it from gale force winds on the preceding day. The rig rolled easily over the ground and the height of the sprinklers could be accurately set at 2.44m.



Figure 4–7: Photo of the mobile rig with sprinklers running. Note the flowmeter and pressure gauge at the bottom right.



Figure 4–8: Photo of the rig before sunrise. Note the reflective ropes used to stabilise the structure and reduce sagging of the horizontal bar.

The rig had to be ‘driven’ by manual pushing. Every 30 seconds the rig was pushed an increment of 30cm, as measured with a ruler, giving an average speed of 0.6m/min, or 36m/hour. This was not a continuous motion, as assumed in the modelling; however, it was considered a reasonable compromise because maintaining a continuous motion by mechanical drive, electric winch or by continuous manual pushing of the rig was just too expensive or difficult to control. A short video of the sprinkler rig being pushed along (Figure 4-9 contains a screenshot) can be viewed at:

http://www.youtube.com/watch?v=8fFEglt_iJg.



Figure 4-9: Screen-shot of video of sprinkler rig www.youtube.com/watch?v=8fFEglt_iJg

Figure 4-10 contains plots generated by Part 2 of the computer model using the laboratory test data for the Sred6_44 as used on the mobile sprinkler rig. Shown in Figure 4-10 are the:

- sprinkler application rate profile, as collected in the laboratory (top left)
- 2-dimensional interpolation of the application rate profile to represent a single sprinkler head’s full circle application pattern (top right)
- application rate pattern when four of the sprinkler heads are spaced at 1.20m separations (bottom left and right plots, each showing the same information but from different 3-dimensional viewpoints).

The information presented in Figure 4-10 was applicable to Test B for every pair of tests as only the Sred6_44 sprinkler was ever used with the mobile sprinkler rig.

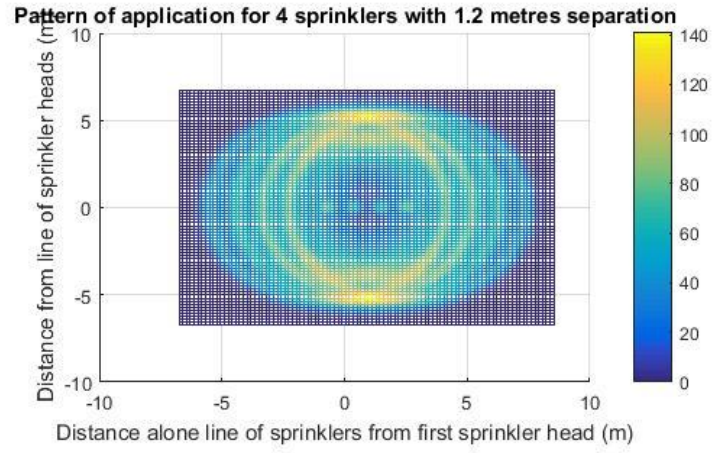
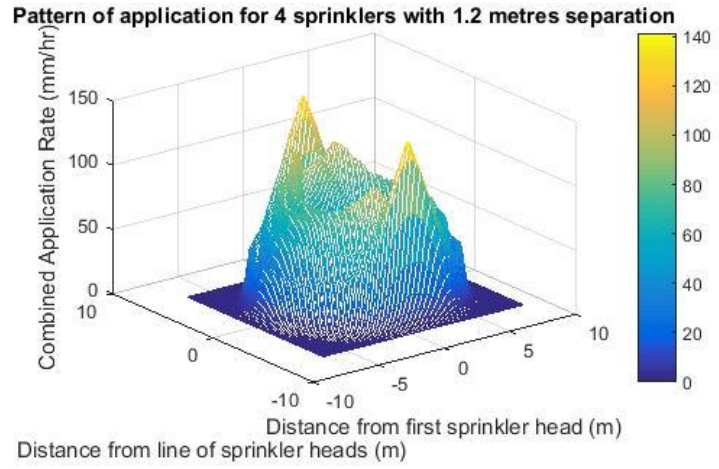
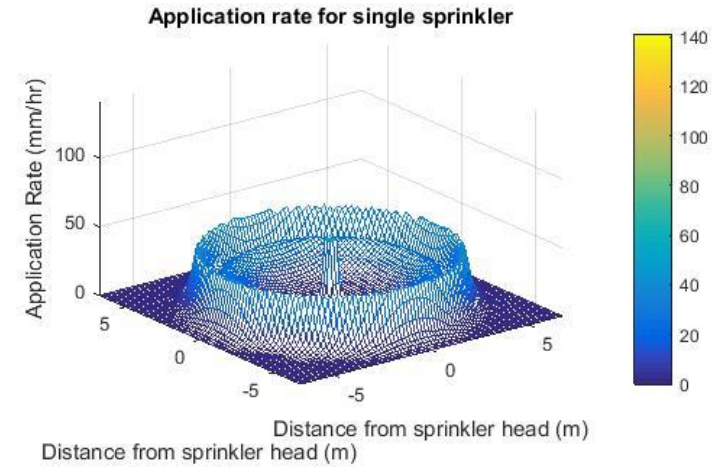
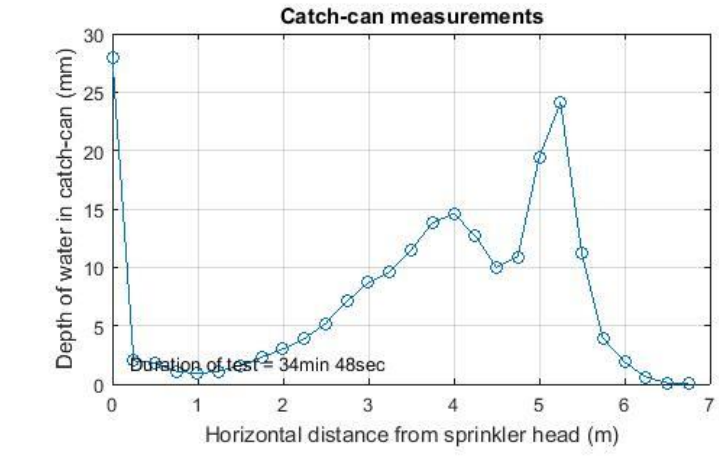


Figure 4-10: Plots produced by the computer model for the Sred6_44 sprinkler. The top two plots are for the single sprinkler, and the bottom two are for four overlapping sprinklers.

The raw data and the outputs of Part 1 and Part 2 of the computer model are given in Section 4.2.4 for just a single pair of field tests as an example of the process used to generate the results. A summary table and summary plots of the results for all of the 9 pairs of tests are given in Section 4.2.5. Complete tables of the raw field data are contained in Appendix E.

4.2.4 Detailed Results for a Single Pair of Tests

The results for Tests 6A and 6B are presented in full here to exemplify the process used in each of the nine test pairs.

4.2.4.1 Results for Test 6A – Runoff and Cumulative Infiltration

Table 4-10 contains the measured runoff values created using the sprinkler infiltrometer (bucket infiltrometer) in Step One, in the left two columns. The computed cumulative infiltration is in the far right column. A plot of the I vs t data is shown in Figure 4-11.

Table 4-10: Example data (from Test 6A) collected when using sprinkler infiltrometer.

Test 6A		Application Rate: 178 mm/hr Plot Area: 0.0638 m ²			
t (min)	runoff for period (ml)	runoff cumulative (ml)	runoff cumulative (m ³)	runoff cumulative (mm)	infiltration cumulative (mm)
0	0	0	0	0	0
3	163	163	0.00016	3	6
6	182	345	0.00035	5	12
9	198	543	0.00054	9	18
12	236	779	0.00078	12	23
15	246	1025	0.00103	16	28
18	233	1258	0.00126	20	34
21	223	1481	0.00148	23	39
24	225	1706	0.00171	27	44
27	202	1908	0.00191	30	50
30	235	2143	0.00214	34	55
33	192	2335	0.00234	37	61
36	200	2535	0.00254	40	67
39	140	2675	0.00268	42	74
42	166	2841	0.00284	45	80
45	185	3026	0.00303	47	86

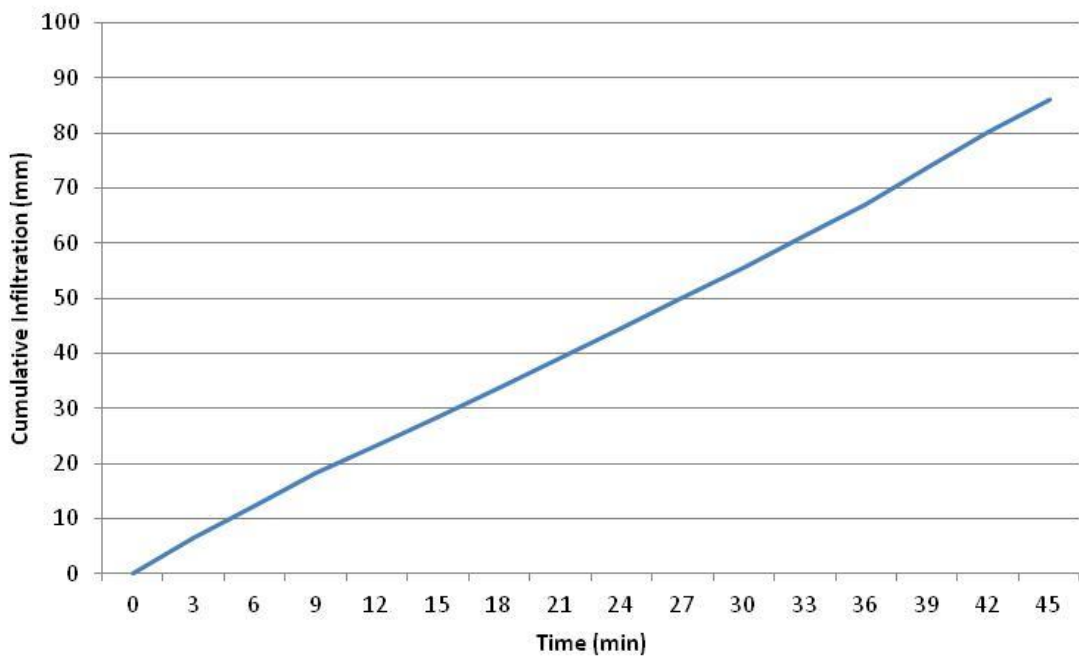


Figure 4-11: Cumulative infiltration (I) versus time (t) for Test 6A

4.2.4.2 Results for Test 6A – Output of Part 1 of Computer Model

The I vs t data was entered into Part 1 of the computer model. The top-right plot of Figure 4-12 shows several different curves for i vs I that were generated by the computer model. The reason there are several curves is because the final results for K and SM can differ slightly depending upon which pairs of points on the I vs t curve were chosen for solving the GAML equations. Each infiltration characteristic curve is based on different sets of K and SM values. It was decided to take an average value for K and SM , in this case giving $K = 10.3433\text{cm/hr}$ and $SM = 0.0673\text{cm}$.

To check if the infiltration characteristic equation (that has been created using the values for K and SM) was reasonable, the area under the infiltration characteristic curve was compared to the total accumulated infiltration. Theoretically they should be equal. The process is detailed below.

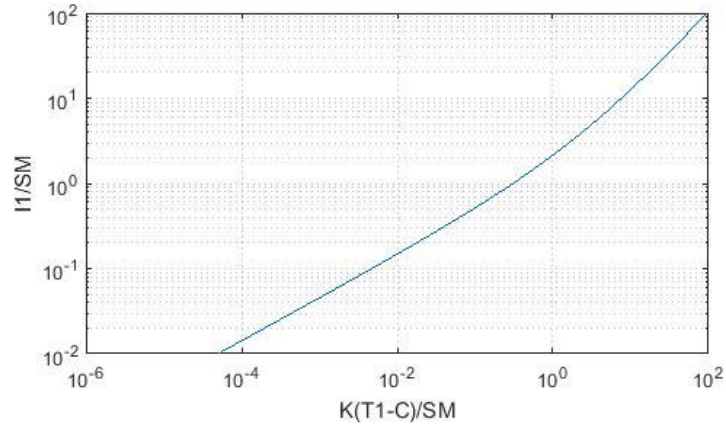
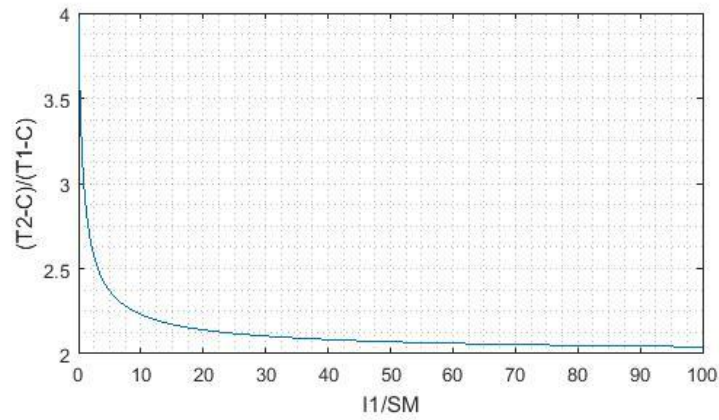
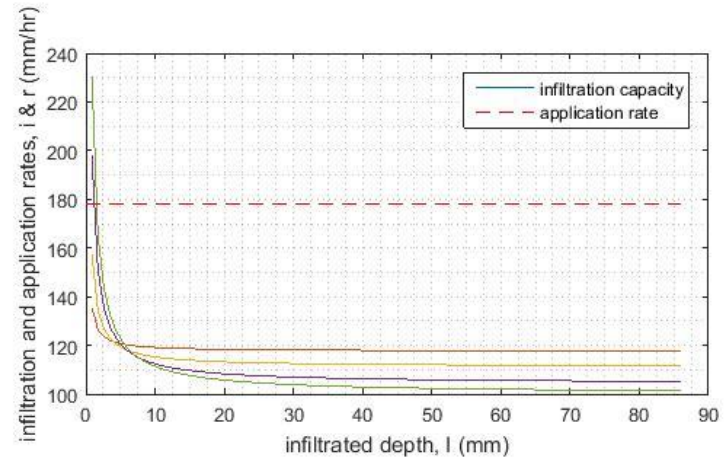
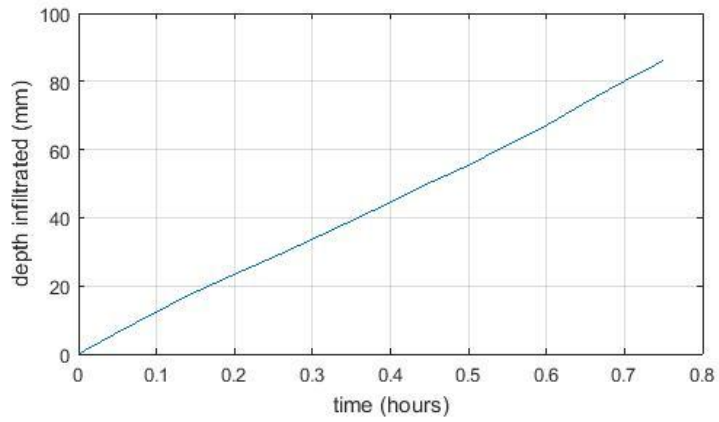


Figure 4-12: Plots from Part 1 of computer model for Test 6A.

The infiltration characteristic equation was found by substituting K and SM into

$$i = K \left(1 + \frac{SM}{I} \right) \quad (4-1)$$

where the values for I were found by interpolating the I vs t field data to match specified values for t . The i vs I curve (equation 4-1) was then able to be converted to an i vs t curve because the I vs t curve (the original field data) was known. Thus the (time-based) infiltration characteristic equation for Test 6A was found to be:

$$i = 99.3975t^{-0.061317} \quad (4-2)$$

Making the check then:

- The area under the i vs t curve (Equation 4-2) was 80mm. This was calculated using the Matlab *trapz* function in Part 1 of the computer model.
- The total cumulative infiltration was read from Table 4-10 as 86mm.

These figures are reasonably close and so the decision was made to accept the infiltration characteristic function (Equation 4-2) based on these values for K and SM . It was thus with some confidence that this infiltration characteristic function was exported to Part 2 of the computer model (refer 3.3.1 and 3.3.2).

4.2.4.3 Results for Test 6B – Observed Runoff versus Predicted Runoff

When using the infiltration characteristic function (Equation 4-2) as determined from the data of Test 6A and Part 1 of the computer model, the predicted runoff from Part 2 of the computer model was 8.11L, or a depth of 14.4mm. The measured runoff was, however, only 5.10L, or a depth of 9.1mm. This is a significant difference. Discussion on the error evident here, which was typical of most of the project's field test results, is presented in Chapter 5.

4.2.5 Summarised Results for All Tests

A summary of the results for all of the remaining tests, which were all carried out in the same manner as the example case of Section 4.2.4, is given in Table 4-11. Note that in Table 4-11 the closer the two values under the ‘Quality Check’ heading are the more confidence one would have in the infiltration characteristic function that is output from Part 1 of the computer model. The results from Test No’s 4, 6, 7 and (especially) 8 appeared promising.

Table 4-11: Summary of results for the 9 pairs of field tests.

Test No.	Results Generated By Test ‘A’ – Stationary Sprinkler Infiltrometer					Results From Test ‘B’ - Mobile Sprinkler Rig	
	Computed Values		Computed Infiltration Characteristic Function	Quality Check		Runoff Predicted (L)	Runoff Measured (L)
	K (cm/hr)	SM (cm)		Total I (mm)	Area under i vs t (mm)		
1	7.6765	0.8355	$i = 73.1264t^{-0.28362}$	111.7	99.3	7.91	2.00
2	9.6817	0.3977	$i = 90.8232t^{-0.18429}$	92.7	110.5	7.80	3.05
3	6.1446	1.5559	$i = 56.6788t^{-0.41912}$	73.1	80.0	7.90	5.20
4	2.8717	2.2363	$i = 31.1227t^{-0.50417}$	55.0	51.2	8.60	8.15
5	6.0353	0.9206	$i = 53.9393t^{-0.34549}$	76.1	66.0	8.30	6.10
6	10.3433	0.0673	$i = 99.3975t^{-0.06132}$	86.0	80.0	8.11	5.10
7	9.6468	0.1807	$i = 89.1797t^{-0.12942}$	82.4	78.4	8.10	5.85
8	10.3990	0.2398	$i = 94.6975t^{-0.15525}$	85.4	86.4	7.82	6.00
9	9.8107	0.2029	$i = 89.5046t^{-0.1452}$	71.9	80.9	8.00	4.95

Figure 4-13 shows all of the I vs t curves generated from the nine sprinkler infiltrometer (bucket infiltrometer) tests. Note that only the first two sprinkler infiltrometer tests were of 60 minutes duration; all of the rest were 45 minutes each.

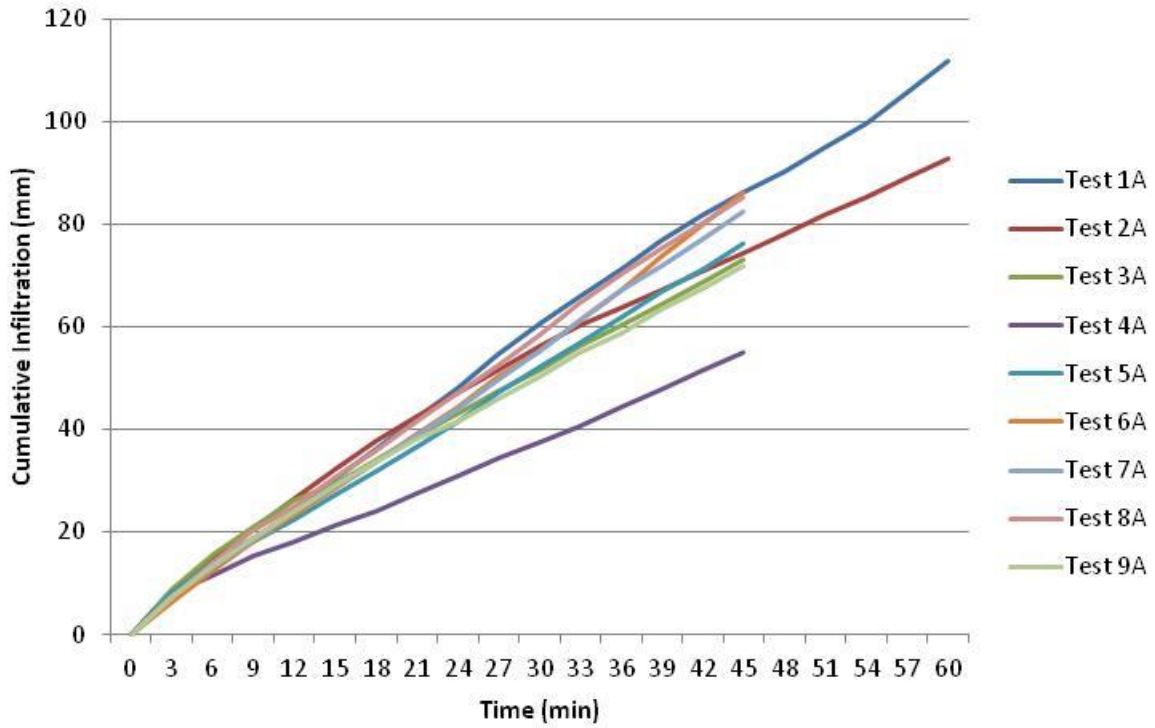


Figure 4-13: Cumulative infiltration versus time (I vs t) for all of the sprinkler infiltrometer tests.

Figure 4-14 is a summary plot of how the predicted runoff for each test compared to the measured runoff. The red square-shaped markers are where the data should have plotted if the runoff that was measured matched what was predicted by the computer model; the blue diamond-shaped markers are where the data actually plotted. Clearly there was a trend for the measured runoff values to be well below what was predicted, often markedly so.

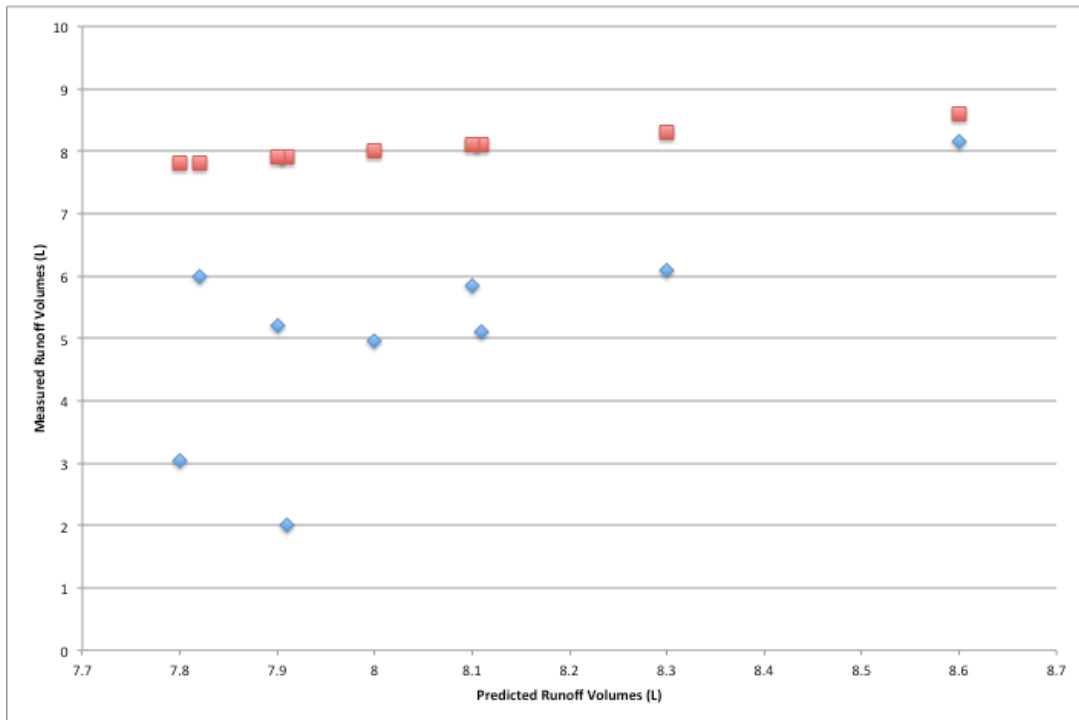


Figure 4–14: Comparison of predicted runoff volumes (red squares) from the sprinkler infiltrometer tests and the measured runoff volumes (blue diamonds) using the mobile sprinkler rig.

4.3 Summary of Results

A large amount of laboratory data was collected for two purposes. Firstly, to provide quality sprinkler performance data for use in the computer model; and secondly, to identify a sprinkler nozzle size and pressure combination that would be suitable for application in a SHCAZ Sprinkler Infiltrator application. The Sred25_44 was considered to be the option most suitable for the purpose.

However, the SHCAZ Sprinkler Infiltrator concept did not work as well in the field as hoped. Wind interference and high rates of water consumption (as there was no water recycling facility in the field) made it impractical and unreliable. An improvised drip-generating infiltrator ('bucket infiltrator'), modelled after the Cornell Sprinkler Infiltrator, was used instead to good effect.

A mobile sprinkler rig with four sprinkler heads at a height of 2.44m (8 ft) and spaced apart at 1.2m (4 ft) was constructed for the project. It performed well and enabled a time-varying application rate to be delivered. However, significant differences between the runoff values predicted by the computer model and those actually observed were almost universally present. Discussion as to the possible causes and implications of the apparent error is presented in Chapter 5.

Chapter 5 – Discussion

The discussion will focus on the preparatory sprinkler data collection work first before turning to the issues encountered in the field testing phases of this project.

5.1 Sprinkler Data Collection

Significant work went into the collection of sprinkler data in the laboratory. In the end much of this proved to be of little direct value to the project but the efforts were not all in vain. The extensive testing did eventually discover the necessary information to allow the trial of the SHCAZ Sprinkler Infiltrometer concept in the field.

There were several points of interest regarding the sprinkler data collection worth discussing here.

Firstly, Figure 4-2 (refer 4.1.1) showed two radial leg patterns, one with a ‘zero point’ and one without. The zero point refers to the catch-can (actually a 9L bucket) that was located directly beneath the sprinkler head. The practice of measuring the application rate at the zero point is not commonly performed in industry. As a result published sprinkler performance data has generally failed to report that the magnitude of the application rate at the zero point can be several times larger than the highest application rate anywhere else on the radial leg profile. It was observed during the testing that there was a constant trickle of water from the sprinkler head during operation that probably resulted from when the jets of water from the spinner plate hit the supporting vanes (refer Figure 3-4 in Section 3.2.1.1). This phenomenon was seen across all of the sprinkler tests undertaken with the Nelson brand centre-pivot sprinkler heads. The yellow spinner plates generally produced higher rates of water trickle from the sprinkler head than the red spinner plates. A possible explanation is that the supporting vanes were noted to be oriented radially whereas the exiting streams of water would have slightly tangential velocities (due to the rapidly spinning plate). This means that there is an increased cross-sectional area of the vanes in the path of the water streams and thus an increased splash occurring within the sprinkler head body, with a resultant trickle of water. It is possible that a researcher or industry tester may miss this altogether if the application rate directly below the sprinkler

head is not measured - an omission all the more significant if a sprinkler machine features large numbers of sprinkler heads spaced at close intervals.

Secondly, Table 4-2 showed that, besides at the zero point, which can only have a single catch-can beneath it, the other close-in catch-can measurements were made in triplicate. This was done because it was observed that spray from water hitting the vanes of the sprinkler head caused marked variation between catch-cans located at equal radial distance but on different radial legs. Thus several catch-cans at equal radial distances but on different radial legs were measured and an average value obtained. For catch-cans further away from the sprinkler head there was no noticeable effect as long as the vanes of the sprinkler head were consistently oriented for each test.

Thirdly, the question of the accuracy of the catch-can data should be discussed. On the one hand the catch-cans were spaced every 0.25m which is a much closer interval than used in many sprinkler tests. The significance of this is illustrated in Figures 5-1 and 5-2. The higher resolution of data in Figure 5-1 gives a more complete and accurate representation of what is really happening. All of the laboratory sprinkler tests were undertaken using 0.25m catch-can intervals.

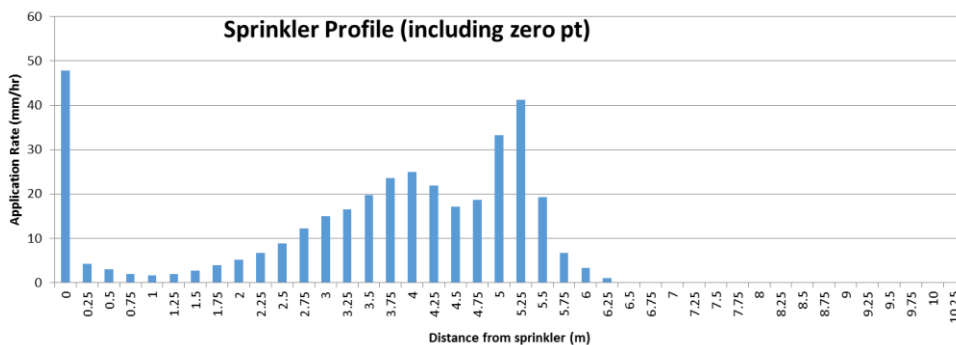


Figure 5-1: Sprinkler test data for a Nelson Sred6_44 when measured at 0.25m intervals.

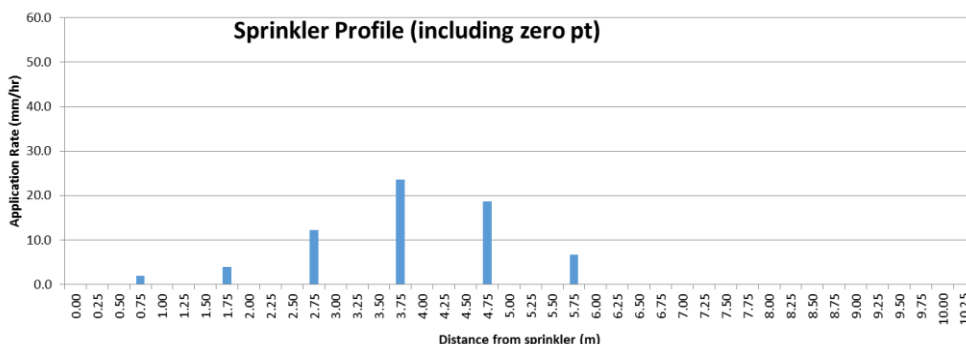


Figure 5-2: Sprinkler test data for the same Nelson Sred6_44 when measured at 1.0m intervals

However, some doubt over the accuracy of the catch-can data was created when a water balance was performed during the course of testing. When the total volume of water that was emitted from the sprinkler head during the Sred25_44 test, for example, was estimated based on the radial catch-can data using a summation of the ANNULA_AREA \times DEPTH products, the emitted volume was estimated to be about 1900L. This differed significantly from the volume estimated for the same Sred25_44 test using AVERAGE_FLOWRATE \times TIME which came to 2300L... a difference of nearly 20%. There was every reason to have confidence in the flowmeters as the two types being used agreed with each other and were close to Nelson's published data for nozzle flowrates. Thus, unless there was significant error in the process of calculating the volumes, this suggested that water had been 'lost' at some point.

Evaporation loss was initially considered as a possible explanation, but soon ruled out as a significant enough factor. The potential for evaporation losses from the catch-cans was monitored in the laboratory using 5 catch-cans (identical to those being used in the testing) containing 5ml, 10ml, 20ml, 50ml and 100ml of water. These were placed on the floor near the test area but out of the sprinkler's reach. The mass of water in each was measured at the start and end of each day to determine an average hourly evaporative loss. As it turned out, the hourly evaporative losses were very small in all cases, typically less than 0.1ml per hour, and so no adjustment to the sprinkler catch-can data was ever made. The very low evaporative losses could be attributed to several factors: cool air and water temperatures, typically about 10°C - 17°C; no solar irradiance because the tests were indoors; high relative humidity due to the abundance of water on the floor of the laboratory and being sprayed through the air; no air-conditioning or dehumidification in the laboratory; and an absence of any wind.

It is possible that some water droplets splashed out of the catch-cans on impact. This might account for the discrepancy during the volume balance. Splash-out was watched for and none was apparent but it was not always easy to identify if this was in fact occurring.

5.2 Field Testing

Points of interest discussed here are the use of the sprinkler infiltrometers, the mobile sprinkler rig, and collecting the runoff in the field. The difference between predicted and observed runoff values is also discussed at length.

5.2.1 Sprinkler Infiltrometers

Whilst not one of the original objectives of this project, the desire to trial a new idea for a sprinkler infiltrometer came to be something of a sub-project. It was born of both a need to supply a sprinkler infiltrometer for the purposes of the project, and of a simple curiosity as to whether the new sprinkler infiltrometer concept might even have some merit.

The laboratory testing was successful in identifying several appropriate nozzle-plus-pressure configurations for the SHCAZ Sprinkler Infiltrometer. However, as already noted in Chapter 4, the SHCAZ Sprinkler Infiltrometer was abandoned after repeated attempts to use it in the field.

The main problem encountered was with wind interference. The extent that wind that was gusting and varying direction could affect the application pattern of the sprinkler head had hitherto been grossly underappreciated. Catch-cans that were placed around the perimeter of the soil test plots (as a rudimentary quality check) were observed to have varying depths of water in them. Thus it was difficult to know what the application rate was across the soil plot or even if the application rate was constant over time across the soil plot. Wind-free days proved to be rare and this was problematic to the progress of the project. The need for such wind-free conditions was also problematic to the very utility of the SHCAZ Sprinkler Infiltrometer concept; unless there existed the ability to erect a wind-proof shelter of some form, or be able to work indoors, then the concept was arguably unreliable and impractical.

The use of software to model wind distortion effects on the sprinkler pattern and incorporate this into the computer model's predictions was considered. However, the

wind was typically gusting or shifting direction many times even within the timeframe of a single test and so the inclusion of such software was not pursued.

A second difficulty with implementing the SHCAZ Sprinkler Infiltrator concept was the relatively low application rate of water onto the soil plot. Even though the Sred25_44 was selected because it had the highest application rate among the nine suitable options in Table 4-1, it still only applied water at a rate of 27mm/hr. This meant that each infiltrator test had to run for an extended period of time - in the order of hours when the soil was very dry - before any runoff was seen and then for a further 45 minutes to generate the required runoff vs time data. There were two issues here: Firstly, it was taking far too long to complete each infiltrator test. This was a problem in itself, but when coupled with the very uncertainty of the quality of the data (due to the wind interference), the situation was unacceptable. And secondly, the SHCAZ Sprinkler Infiltrator was applying water at 68L/min, or 4m³/hour, over a fixed area of ground causing some difficulties with flooding and mud as well as being wasteful of water. (The 4m³/hour of water was applied over a circular area with a diameter of 13m; the soil plot being tested occupied only a small 0.75m x 0.75m area within this.) No means of collecting and recycling water had been incorporated into the SHCAZ Sprinkler Infiltrator design and the importance of being able to capture and recirculate water during the test, such as had been done in the hydraulics laboratory, quickly became apparent in the field.

Thus the SHCAZ Sprinkler Infiltrator was abandoned as a concept suitable for the purposes of this project. However, the author can envisage some scenarios where the concept might still work well. In a sheltered environment, particularly inside a laboratory or a wind-proof screen, where wind is of no concern and where the water can be drained and recycled back through the system, the SHCAZ Sprinkler Infiltrator concept could provide a method of using existing sprinkler components to provide a sprinkler infiltrator capability. It could also be a sprinkler infiltrator method that better simulates droplet impact energy than a droplet-forming sprinkler infiltrator.

An alternative form of sprinkler infiltrator, the 'bucket infiltrator' (as the author dubbed it) was constructed and implemented when it became apparent that the SHCAZ Sprinkler Infiltrator was to be abandoned. The bucket infiltrator was simple and worked rather well. However, a drawback of the bucket infiltrator was that the area of

the soil plot was only 0.0638m² (0.285m diameter circle) as opposed to the SHCAZ Sprinkler Infiltrometer's 0.5625m² (0.75m x 0.75m) plot. Thus there was more risk that the small soil plot area used would be less representative of the general area around it. An unusually large crack, macropore or micro-topographic feature, for example, might severely affect the runoff results. Another concern with the bucket infiltrometer was that there was a small amount of leaking that occurred from around the base of the bucket infiltrometer where it sat on the soil. Efforts to mitigate against this included cutting the soil so that the bucket infiltrometer could be pressed deeper into the soil, and pre-moistening the surrounding soil so as to reduce its matric pull in the lateral direction (but not adding so much moisture that it would ingress into the soil test plot area).

Despite its drawbacks there were two significant advantages of the bucket infiltrometer. Firstly, the surrounding ground did not become inundated with water and the overall rate of water consumption declined dramatically. And secondly, the application rate of the bucket infiltrometer was significantly higher than the SHCAZ Sprinkler Infiltrometer (178mm/hr versus 27mm/hr). This meant that runoff was often being generated within minutes and each sprinkler infiltrometer test was able to be entirely completed with 45 minutes.

5.2.2 Mobile Sprinkler Rig

The mobile sprinkler rig had been constructed so that field testing could be performed at a location and on a schedule that was suitable for this project. The mobile sprinkler rig's purpose was to provide a time-varying application rate of water. Four Sred6_44 sprinkler heads spaced at 1.20m intervals were exclusively used on the mobile sprinkler rig for several reasons:

- They had a sufficiently high flow rate to be able to generate runoff in the field, which was necessary to test the computer model, whilst being within the flow and pressure capacity of the 50mm town water supply outlet.
- The large nozzle size created large droplets that were less subject to wind drift.
- The low operating pressure reduced the throw distance of the sprinkler and reduced the creation of fine spray particles. This also helped to reduce wind drift.

- The low operating pressure meant that the mobile sprinkler rig could be operated using pressurised town water supply using a 50m long, 50mm diameter lay-flat pipe. This removed the requirement to increase the pressure head using a pump.

5.2.3 Measuring Runoff

Table 4-10 and Figure 4-11 showed the pattern of runoff and of accumulation of infiltration with time for Test 6A. These data were typical of the test results in this project. By contrast, a textbook case of infiltration would have the rate of runoff very small to begin with (when infiltration capacity is very large) and then steadily increasing over time until it reaches a steady rate, for a constant application rate. However, as can be seen in Table 4-10, this doesn't always occur. Several thoughts are put forward that might offer some explanation for the difference between the pattern of runoff that should have occurred (theoretically) and what actually occurred:

- On the soil surface water was frequently observed to pond behind micro-topographic features, like tiny dam walls. After a while the surface water would start to run over these tiny dam walls and erode the soil away, eventually causing a breach and a temporary (small) rush of runoff. When this effect is multiplied over the whole test area this might account for some of the non-‘textbook’ pattern of runoff.
- Another explanation is that the hydraulic conductivity of the soil was probably not constant. The dynamic processes of pores becoming occluded and having air entrapped, or having air escape to open new flow paths, can cause the infiltration capacity of the soil to increase or decrease over time.
- It was clear that not all of the runoff was even collected. The data of Table 4-10 and Figure 4-11 are thus not fully representative of what actually was occurring in the field. This is probably the strongest contributor to the non-‘textbook’ runoff/infiltration patterns (refer 5.2.4).

5.2.4 Difference between Predicted and Measured Runoff Values

As was seen in the results of Sections 4.2.1 and 4.2.2, the measured values of runoff were consistently less than what had been predicted. Several possibilities as to the cause of the error are discussed in turn.

5.2.4.1 Error due to GAML Assumptions

As discussed in Chapter 2, the Green-Ampt model made a number of strong assumptions. These included uniform soil moisture with depth; piston-flow of wetting front due to no cracks or macropores; no shrink-swell properties; no lateral dispersion of water within the soil profile; and a ponded surface. The Mein-Larson model dealt with the latter assumption. However, the other assumptions were observed as not holding true in the present project.

- Soil was not uniformly moist. The soil near the surface was observed to be drier than that below it for most tests.
- Cracks and macropores were abundant within the soil plots and proved particularly troublesome.
- Some lateral dispersion of water from the test plots was observed.

The significance of the violations of these Green-Ampt assumptions in contributing to the error in the present results was not quantified. However, some authors believed that the assumptions are, nonetheless, not unreasonable (refer 2.5.4). Relative to the other sources of error, then, the Green-Ampt assumptions were possibly only a minor source of the error observed.

5.2.4.2 Error due to the Programming of the Computer Model

The computer model written by the author may itself have been producing incorrect runoff predictions. This is a real possibility given the many points at which flaws in the modelling and programming processes could have produced errors in the final outputs. However, the outputs of the computer model had performed reasonably well during the

desktop testing phase of the project (refer 4.1.2) when tested against the same data that Chu had used.

5.2.4.3 Error due to Chu's Graphical Methods

Chu's (1987) graphical methods were shown to work well for simplistic sprinkler patterns. The methods relied on an iterative approach that eventually settled on stable values for time-to-ponding and potential runoff. It was found during the course of this project, however, that Chu's iterative process failed to arrive at stable values (even after thousands of iterations) when the sprinkler application pattern was complex, as was the case when using multiple sprinklers on the mobile sprinkler rig (Figure 5-3). Consequently the very values predicted for runoff in this project by Chu's method should be regarded with some suspicion. It is suggested here that Chu's (1987) graphical method may be unable to handle more complex-shaped real time-varying sprinkler systems.

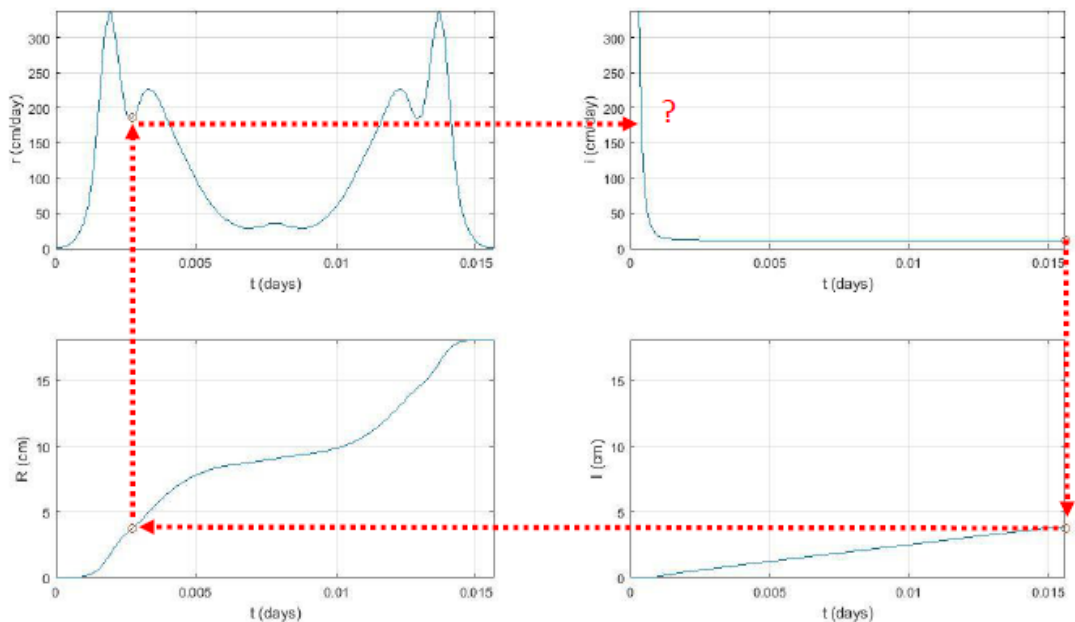


Figure 5–3: Chu's (1987) iterative graphical method failing to settle on stable values for a complex sprinkler application pattern (Compare Figures 2-17 and 4-6).

5.2.4.4 Error due to Measurements in the Field

This project attempted to apply Chu's methods to real time-varying sprinkler systems on a real field. (Chu had only tested against idealised contrived data and against the Richards equation.) As with any real-world testing scenario there are a myriad of opportunities for error to be introduced. Some of the key ones for this project are noted as below.

- Wind was generally present to varying degrees on each of the testing dates, even early in the morning or late in the evening when conditions were expected to be calmest. The Sred6_44 was used to produce large droplets with relatively small throw distances to mitigate against this. However, some wind distortion of sprinkler patterns was sometimes still apparent. Furthermore, the wind was typically not constant in its direction or intensity during any given test which precluded the retrofitting of wind-distortion modelling software into the computer model.
- The mobile sprinkler rig was not pushed continuously (as the computer model supposed) but was pushed in 30cm increments every 30 seconds. However, any error generated in this respect would likely have been small.
- Collection of runoff was highly problematic and was probably the most significant source of measurement error in the field. That there was going to be error in the runoff data collected in the field was readily apparent even during the testing; not all of the runoff was able to be captured and measured. What was not able to be quantified, or even reasonably estimated, was just how much runoff evaded capture. Soil plots had been prepared so that runoff would drain toward a collection trench inside which was located a PVC half-pipe that then drained into a collection container (refer 3.4.2). It was observed, however, that some of the runoff water instead followed preferential pathways through cracks and macropores and avoided entering the half-pipe. Also, it was very difficult to get a good seal between the side of the trench and the half-pipe, and runoff water was sometimes able to sneak between the two and avoid entering the halfpipe. This was more evident on some soil plots than others and occurred in spite of extensive efforts to promote the water's passage into the half-pipe. Without doubt this was contributory to the consistent over-prediction of runoff by the computer model versus that observed in the field.

Whether runoff measurement error should shoulder all of the blame, or whether the computer model and/or Chu's method were also contributory was not clear.

As a final point in this discussion it is perhaps worth noting that very few of the research papers encountered in the literature review had actually attempted to collect their own infiltration data in the field. Sometimes the language used was even suggestive that to obtain such data would be a straightforward and accurate process. This was not the experience of this project. Among the authors who did collect field infiltration data, as opposed to laboratory infiltration data, none cited any difficulties with its collection process or any estimates of error. This was surprising, not only because of the scope for potential problems in collecting such data, but also because so many other authors have, in turn, utilised and referenced that same data in their own work.

Chapter 6 – Conclusions

6.1 Achievement of Project Objectives

This project set out to investigate whether the Green-Ampt (1911) equation can be used to model infiltration into soils under centre-pivot and lateral-move sprinkler irrigation systems. In short, the answer is “possibly yes”, but difficulties measuring data during the field phases of this project meant that a conclusive statement was not possible.

The literature review revealed that the Green-Ampt equation in its original form was not ideal for modelling infiltration under sprinkler irrigation due to the assumption of a ponded surface. However, the Green-Ampt equation was the basis for Mein and Larson’s (1971) work where the ponded surface assumption was able to be removed. Thus the Green-Ampt equation could now be applied to a sprinkler irrigation scenario albeit in a modified form which has become known as the Green-Ampt-Mein-Larson (GAML) model. Yet, in order that there could be a neat analytical mathematical solution, Mein and Larson (1971) had made the necessary assumption that the sprinkler application rate was constant, which would not be the case under centre-pivot or lateral-move machines.

Chu (1987) was able to bypass this major constraint by not attempting to obtain an analytical solution; instead he resorted to a graphical method and was able to predict time-to-ponding and runoff volumes for time-varying application rates. Thus it appeared that the Green-Ampt equation, expressed through a GAML-plus-Chu solution, could be used to model infiltration under centre-pivot and lateral-move sprinkler systems. However, Chu (1987) only ever demonstrated the efficacy of his method for very simple scenarios or against numerical solutions of the Richards equation, neither of which reflected real conditions under moving sprinkler systems particularly well. This project, then, in order to address the original objective, had the task of going a step further than the simple idealised scenario and sought to investigate whether the GAML-plus-Chu method could work when dealing with real sprinklers out in the field.

There were two key problems that were addressed.

The first key problem was the matter of determining the GAML parameters in the field. This had long been one of the principal difficulties with applying the GAML model. Chu's (1986) method for determining a set of modified GAML parameters was applied in this project and the results appeared promising. This was very significant because Chu's (1986) method may well obviate the need to measure difficult soil hydraulic parameters in the field thus removing one of the barriers to applying the GAML-plus-Chu method.

The second key problem was to make Chu's (1987) graphical method work with real sprinkler data. However, Chu's iterative process appeared to break down when confronted by complex-shaped real world data. Also, significant practical difficulties in measuring runoff during this project meant that there was insufficient confidence in the field data to draw conclusions on the performance of the GAML-plus-Chu model (or of the computer model) for real sprinkler systems.

In summary, the usefulness of the Green-Ampt equation for modelling infiltration under centre-pivot and lateral move sprinkler machines was investigated. It was found that the GAML-plus-Chu approach had potential but had not been tested in the literature against real field data. Field testing in this project that attempted to fill this knowledge gap suffered from measurement problems and no conclusions could be reached as a result. However, the inability of Chu's (1987) iterative process, which was so critical to his graphical method, to settle on stable values when faced with data from real sprinkler systems is suggestive that the existing GAML-plus-Chu approach may struggle to handle real world moving sprinkler systems.

A New Sprinkler Infiltrometer?

A secondary objective that emerged as the project progressed, effectively becoming a sub-project, entailed assessing a new concept for a sprinkler infiltrometer design. It was found that the proposed new sprinkler infiltrometer concept (the SHCAZ Sprinkler Infiltrometer) was impractical and unreliable in an open field setting exposed to the wind, especially when facilities for water recycling were not present.

6.2 Further Work and Recommendations

The investigation of Chu's (1987) methods for modelling infiltration under sprinkler systems was hampered particularly by difficulties with measuring the water runoff from the soil plots. The technique for collecting runoff in this project was inspired by the literature review; interestingly no other authors reported having the same difficulties as was experienced during the present project. An opportunity for further work exists, then, for finding better methods for runoff measurement in the field so that more reliable field testing may be undertaken.

The methods of Chu (1986) as an alternative method for determining a soil's infiltration characteristic function under sprinkler irrigation (or rainfall) appeared promising in this project. The author believes that this is worthy of further investigation.

The proposed new concept for a sprinkler infiltrometer did not work well in this project. However, the concept may be made to work when wind-interference can be eliminated and a water recycling system can be implemented. Further work here may develop a useful system that has the ability to not only evenly apply a constant rate of random water droplets over a surface area but also has the ability to deliver the sorts of droplet impact energy as might be expected in a real sprinkler system.

List of References

- ABS 2015, Water use on Australian farms, Table 1, 46180DO001_201314, Australian Bureau of Statistics, Australian Government, released 29 May 2015, online at <http://www.abs.gov.au/ausstats/abs@.nsf/mf/4618.0>
- Addink J.W., Miles D.L. & Skogerboe G.V. 1975, 'Water intake under centre-pivots from time-varying application rates', *Transactions of the ASAE*, Vol. 10 No. 3 pp.523-525, online at <http://elibrary.asabe.org/azdez.asp?JID=3&AID=36624&CID=t1975&v=18&i=3&T=2&redirType=>
- Ahuja L.R., Nofziger D.L., Swartzendruber D. & Ross J.D. 1989, 'Relationship between Green and Ampt parameters based on scaling concepts and field-measured hydraulic data', *Water Resources Research*, Vol. 25, No. 7, pp. 1766-1770, online at <http://onlinelibrary.wiley.com/doi/10.1029/WR025i007p01766/pdf>
- API 1996, 'Review of methods to estimate moisture infiltration, recharge, and contaminant migration rates in the vadose zone for site risk assessment', API Publication No. 4643, American Petroleum Institute, Washington DC, cited in Ravi V. & Williams J.R. 1998, 'Estimation of infiltration rate in the vadose zone: Compilation of simple mathematical models, Volume 1', US EPA, online at <http://nepis.epa.gov/Adobe/PDF/30003L26.pdf>
- Assouline S. 2013, 'Infiltration into soils: Conceptual approaches and solutions', *Water Resources Research*, Vol. 49, pp.1755-1772.
- ASTM 2009, 'Standard test method for infiltration rate of soils in field using double-ring infiltrometer', standard designation D3385-09, ASTM International, Pennsylvania.
- Bard, Y. 1974, *Nonlinear Parameter Estimation*, Academic Press, New York, p. 11.
- Beven K. & Germann P. 1982, 'Macropore and water flows in soils', *Water Resources Research*, Vol. 18, pp.1311-1325.
- Bodman G.B. & Coleman E.A. 1943, 'Moisture and energy conditions during downward entry of water into soils', *Soil Science Society American Proceedings*, Vol. 8, pp.116-122, cited in Morel-Seytoux H.J. & Khanji J. 1974, 'Derivation of an equation of infiltration', *Water Resources Research*, Vol. 10, No. 4, pp. 795-800, online at <http://onlinelibrary.wiley.com/doi/10.1029/WR010i004p00795/pdf>
- Brakensiek D.L. 1977, 'Estimating the effective capillary pressure in the Green and Ampt infiltration equation', *Water Resources Research*, Vol. 13, No. 3, pp. 680-682, online at <http://onlinelibrary.wiley.com/doi/10.1029/WR013i003p00680/pdf>
- Brackensiek D.L. & Onstad C.A. 1977, 'Parameter estimation of the Green and Ampt infiltration equation', *Water Resources Research*, Vol. 13, No. 6, pp. 1009-1012.

- Brakensiek D.L., Rawls W.J. & Hamon W.R. 1979, 'Application of an infiltrometer system for describing infiltration into soils', *Transactions of the ASABE*, Vol. 22, No. 2, pp. 320-325, online at <http://elibrary.asabe.org/azdez.asp?search=1&JID=3&AID=35013&v=22&i=2&CID=t1979&T=2&urlRedirect=>
- Brakensiek D.L., Engleman R.L. & Rawls W.J. 1981, 'Variation within texture classes of soil water parameters', *Transactions of the ASABE*, Vol. 24, No. 2, pp. 335-339, online at <http://elibrary.asabe.org/azdez.asp?search=1&JID=3&AID=34253&v=24&i=2&CID=t1981&T=2&urlRedirect=>
- Brakensiek D.L. & Rawls W.J. 1983, 'Agricultural management effects on soil water processes, Part 2: Green and Ampt parameters for crusting soils', *Transactions of the ASABE*, Vol. 26, No. 6, pp. 1753-1757, online at <http://elibrary.asabe.org/azdez.asp?search=1&JID=3&AID=33838&v=26&i=6&CID=t1983&T=2&urlRedirect=>
- Broadbridge P. & White I. 1987, 'Time to ponding: Comparison of analytic, quasi-analytic, and approximate predictions', *Water Resources Research*, Vol. 23, No. 12, pp. 2302-2310, online at <http://onlinelibrary.wiley.com/doi/10.1029/WR023i012p02302/pdf>
- Bouwer H. 1964, 'Unsaturated flow in ground-water hydraulics', *Journal of the Hydraulics Division of the ASCE*, Vol. 90, pp.121-144, cited in Smith R.E. 1975, 'Comments on 'Derivation of an equation of infiltration' by H.J. Morel-Seytoux and J. Khanji', *Water Resources Research*, Vol. 11, No. 5, p. 762, online at <http://onlinelibrary.wiley.com/doi/10.1029/WR011i005p00762/pdf>
- Bouwer H. 1969, 'Infiltration of water into nonuniform soil', *Proceedings of the ASCE Journal, Irrigation and Drainage Division*, Vol. 95, pp.451-462, cited in Brakensiek D.L., Rawls W.J. & Hamon W.R. 1979, 'Application of an infiltrometer system for describing infiltration into soils', *Transactions of the ASABE*, Vol. 22, No. 2, pp. 320-325, online at <http://elibrary.asabe.org/azdez.asp?search=1&JID=3&AID=35013&v=22&i=2&CID=t1979&T=2&urlRedirect=>
- Carsel R.F. & Parrish R.S. 1988, 'Developing joint probability distributions of soil water retention characteristics', *Water Resources Research*, Vol. 24, pp. 755-769, cited in Williams J.R., Ouyang Y. & Chen J. 1998, 'Estimation of infiltration rate in the vadose zone: Application of selected mathematical models, Volume 2', US EPA, online at <http://nepis.epa.gov/Adobe/PDF/30003L4K.pdf>
- Childs E.C. & Bybordi M. 1969, 'The vertical movement of water in a stratified porous material, 1: Infiltration', *Water Resources Research*, Vol. 5, No. 2, p.446, cited in Neuman S.P. 1976, 'Wetting front pressure head in the infiltration model of Green and Ampt', *Water Resources Research*, Vol. 12, No. 3, pp. 564-566, online at <http://onlinelibrary.wiley.com/doi/10.1029/WR012i003p00564/pdf>

- Cook H.L. 1946, 'The infiltration approach to the calculation of surface runoff', *Transactions of the American Geophysical Union*, Vol. 27, pp.726-747, cited in Kincaid D.C., Heerman D.F. & Kruse F.G. 1969, 'Application rates and runoff in centre-pivot sprinkler irrigation', *Transactions of the ASAE*, Vol.
- Cornell 2003, 'Field procedures and data analysis for the Cornell Sprinkler Infiltrometer', Department of Crop and Soil Sciences Research Series R03-01, College of Agriculture and Life Sciences, Cornell University, online at http://soilhealth.cals.cornell.edu/research/infiltrometer/infil_manual.pdf
- Chu S.T. 1978, 'Infiltration during an unsteady rain', *Water Resources Research*, Vol. 14, No. 3, online at <http://onlinelibrary.wiley.com/doi/10.1029/WR014i003p00461/pdf>
- Chu S. 1986, 'Determination of Green-Ampt parameters using a sprinkler infiltrometer', *Transactions of the ASAE*, Vol. 29, No. 2, pp. 501-4.
- Chu S.T. 1987, 'Generalized Mein-Larson infiltration model', *Journal of Irrigation and Drainage Engineering*, Vol. 113, No. 2, online at [http://ascelibrary.org/doi/pdf/10.1061/\(ASCE\)0733-9437\(1987\)113%3A2\(155\)](http://ascelibrary.org/doi/pdf/10.1061/(ASCE)0733-9437(1987)113%3A2(155))
- Chu S.T. 1995, 'Effect of initial water content on Green-Ampt parameters', *Transactions of the ASABE*, Vol. 38, No. 3, pp. 839-841. <http://elibrary.asabe.org/azdez.asp?search=1&JID=3&AID=27898&v=38&i=3&CID=t1995&T=2&urlRedirect=>
- Craig J.R., Liu G. & Soulis E.D. 2010, 'Runoff-infiltration partitioning using an upscaled Green-Ampt solution', *Hydrological Processes*, DOI 10.1002/hyp.7601, online at <http://www.usask.ca/ip3/download/publications/upscaledgreenamptcraigsoulis.pdf>
- Crescimanno G., De Santis A. & Provenzano G. 2007, 'Soil structure and bypass flow processes in a Vertisol under sprinkler and drip irrigation', *Geoderma*, Vol. 138, pp. 110-118.
- DeBoer D.W. 2001, 'Sprinkler application pattern shape and surface runoff', *Transactions of the ASAE*, Vol. 44, No. 5, pp. 1217-1220, online at <http://elibrary.asabe.org/azdez.asp?search=1&JID=3&AID=6447&v=44&i=5&CID=t2001&T=2&urlRedirect=>
- DeBoer D.W., Beck D.L. & Bender A.R. 1992, 'A field evaluation of low, medium and high pressure sprinklers', *Transactions of the ASAE*, Vol. 35, No. 4, pp. 1185-9, cited in DeBoer D.W. 2001, 'Sprinkler application pattern shape and surface runoff', *Transactions of the ASAE*, Vol. 44, No. 5, pp. 1217-1220, online at <http://elibrary.asabe.org/azdez.asp?search=1&JID=3&AID=6447&v=44&i=5&CID=t2001&T=2&urlRedirect=>
- Foley J. 2015, National Centre for Engineering in Agriculture, USQ, Toowoomba, personal communication, March 2015.

- Gencoglan C., Gencoglan S., Merdun H. & Ucan K. 2005, 'Determination of ponding time and number of on-off cycles for sprinkler irrigation applications', *Agricultural Water Management*, Vol. 72, pp. 47-58.
- Green W.H. & Ampt G.A. 1911, 'Study on soil physics', *Journal of Agricultural Science*, Vol. 4, pp. 1-24, online at <http://journals.cambridge.org/action/displayAbstract?fromPage=online&aid=1953116&fulltextType=RA&fileId=S0021859600001441>
- Hachum A.Y. & Alfaro J.F. 1978, 'A physically based model to predict runoff under variable rain intensity', *Transactions of the ASAE*, Vol. 21, No. 3, online at <http://elibrary.asabe.org/azdez.asp?search=1&JID=3&AID=35333&v=21&i=3&CID=t1978&T=2&urlRedirect=>
- Hall M.J. 1970, 'A critique of methods of simulating rainfall', *Water Resources Research*, Vol. 6, No. 4, pp. 1104-1114.
- Hillel D. 1982, *Introduction to Soil Physics*, Academic Press, New York.
- Hillel D. & Garner W.R. 1970, 'Transient infiltration into crust-topped profiles', *Soil Science*, Vol. 109, No. 2, p.69, cited in Neuman S.P. 1976, 'Wetting front pressure head in the infiltration model of Green and Ampt', *Water Resources Research*, Vol. 12, No. 3, pp. 564-566, online at <http://onlinelibrary.wiley.com/doi/10.1029/WR012i003p00564/pdf>
- Humphrey J.B., Daniel T.C., Edwards D.R. & Sharpley A.N. 2002, 'A portable rainfall simulator for plot-scale runoff studies', *Applied Engineering in Agriculture*, Vol. 18, No. 2, pp. 199-204.
- Jarret A.R. & Fritton D.D. 1978, 'Effect of entrapped soil air on infiltration', *Transactions of the ASABE*, Vol. 21, No. 5, pp. 901-906, online at <http://elibrary.asabe.org/azdez.asp?search=1&JID=3&AID=35411&v=21&i=5&CID=t1978&T=2&urlRedirect=>
- Kale R. & Sahoo B. 2011, 'Green-Ampt infiltration models for varied field conditions: a revisit', *Water Resources Management*, Vol. 25, No. 14, pp.3505-3536.
- Kincaid D.C., Heerman D.F. & Kruse E.G. 1969, 'Application rates and runoff in centre-pivot sprinkler irrigation', *Transactions of the ASABE* Vol. 12, No. 6, pp. 790-794, online at <http://elibrary.asabe.org/azdez.asp?search=1&JID=3&AID=38955&v=12&i=6&CID=t1969&T=2&urlRedirect=>
- Kincaid D.C. 2005, 'Application rates from centre-pivot irrigation with current sprinkler types', *Applied Engineering in Agriculture*, Vol. 21 No. 4 pp. 605-610, online at <http://lq6tx6lb4h.scholar.serialssolutions.com/?sid=google&aunit=DC&aulast=Kincaid&atitle=Application+rates+from+center+pivot+irrigation+with+current+sprinkler+types&title=Applied+engineering+in+agriculture&volume=21&issue=4&date=2005&spage=605&issn=0883-8542>

- Kincaid D. 2002, 'The WEPP model for runoff and erosion prediction under sprinkler irrigation', *Transactions of the ASAE*, Vol. 45, pp.67-72, cited in Luz P.B. 2011, 'A graphical solution to estimate potential runoff in centre pivot irrigation', *Transactions of the ASABE* Vol. 54, No. 1, pp. 81-92, online at <http://elibrary.asabe.org/azdez.asp?search=1&JID=3&AID=36262&v=54&i=1&CID=t2011&T=2&urlRedirect=>
- King B.A. & Bjorneberg D.L. 2011, 'Evaluation of potential runoff and erosion of four centre pivot irrigation sprinklers', *Applied Engineering in Agriculture*, Vol. 27, No. 1, pp. 75-85, online at <http://naldc.nal.usda.gov/download/49743/PDF>
- Kunze R.J. & Shayya W.H. 1993, 'Assessing the constancy of the potential term in the Green and Ampt infiltration equation', *Transactions of the ASABE*, Vol. 36, No. 4, pp. 1093-1098, online at <http://elibrary.asabe.org/azdez.asp?search=1&JID=3&AID=28439&v=36&i=4&CID=t1993&T=2&urlRedirect=>
- Lewis M.R. 1937, 'The rate of infiltration of water in irrigation practice', *Transactions of the American Geophysical Union*, Vol. 18, pp. 361-368, cited in Swartzendruber D. 1993, 'Revised attribution of the power form infiltration equation', *Water Resources Research*, Vol. 29, No. 7, pp. 2455-2456, online at <http://onlinelibrary.wiley.com/doi/10.1029/93WR00612/pdf>
- Luz P.B. 2011, 'A graphical solution to estimate potential runoff in centre pivot irrigation', *Transactions of the ASABE* Vol. 54, No. 1, pp. 81-92, online at <http://elibrary.asabe.org/azdez.asp?search=1&JID=3&AID=36262&v=54&i=1&CID=t2011&T=2&urlRedirect=>
- McQueen I.S. 1963, 'Development of a hand portable rainfall-simulator infiltrometer', United States Department of the Interior, Geological Survey Circular 482, Washington.
- Mein R.G. & Farrell D.A. 1974, 'Determination of wetting-front suction in the Green-Ampt equation', *Soil Science Society American Proceedings*, Vol. 38, pp.872-876, cited in Brakensiek D.L. 1977, 'Estimating the effective capillary pressure in the Green and Ampt infiltration equation', *Water Resources Research*, Vol. 13, No. 3, pp. 680-682, online at <http://onlinelibrary.wiley.com/doi/10.1029/WR013i003p00680/pdf>
- Mein R.G. & Larson C.L. 1971, 'Modelling the infiltration component of the rainfall-runoff process', Water Resources Research Center, University of Minnesota, Bulletin 43, online at <http://conservancy.umn.edu/bitstream/handle/11299/92134/ModellingInfiltrationComponentRainfallRunoffProcess.pdf?sequence=1>
- Mein R.G. & Larson C.L. 1973, 'Modelling infiltration during a steady rain', *Water Resources Research*, Vol. 9, No. 2, pp. 384-394, online at <http://onlinelibrary.wiley.com/doi/10.1029/WR009i002p00384/pdf>

- Mein R.G. & Larson C.L. 1973, 'Reply to "Comments on 'Modelling infiltration during a steady rain' by Russell G. Mein and Curtis L. Larson" [Swartzendruber 1974]', *Water Resources Research*, Vol. 9, No. 5, p. 1478, online at <http://onlinelibrary.wiley.com/doi/10.1029/WR009i005p01478/pdf>
- Morel-Seytoux H.J. & Khanji J. 1974, 'Derivation of an equation of infiltration', *Water Resources Research*, Vol. 10, No. 4, pp. 795-800, online at <http://onlinelibrary.wiley.com/doi/10.1029/WR010i004p00795/pdf>
- Morel-Seytoux H.J. 1975, 'Reply to "Comments on 'Derivation of an equation of infiltration' by H.J. Morel-Seytoux and J. Khanji" [Smith 1975]', *Water Resources Research*, Vol. 11, No. 5, pp. 763-765, online at <http://onlinelibrary.wiley.com/doi/10.1029/WR011i005p00763/pdf>
- Morel-Seytoux H.J. 1978, 'Derivation of equations for variable rainfall infiltration', *Water Resources Research*, Vol. 14, No. 4, pp. 561-568, online at <http://onlinelibrary.wiley.com/doi/10.1029/WR014i004p00561/pdf>
- Morel-Seytoux H.J. & Nimmo J.R. 1999, 'Soil water retention and maximum capillary drive from saturation to oven dryness', *Water Resources Research*, Vol. 35, No. 7, pp. 2031-2041, online at <http://onlinelibrary.wiley.com/doi/10.1029/1999WR900121/pdf>
- Narasimhan T.N. 2005, 'Buckingham, 1907: an appreciation', *Vadose Zone Journal*, Vol. 4, pp.434-441, cited in Raats P.A.C. & van Genuchten M.T. 2006, 'Milestones in soil physics', *Soil Science*, Vol. 171, Suppl. 1, pp.S21-S28.
- Neuman S.P. 1976, 'Wetting front pressure head in the infiltration model of Green and Ampt', *Water Resources Research*, Vol. 12, No. 3, pp. 564-566, online at <http://onlinelibrary.wiley.com/doi/10.1029/WR012i003p00564/pdf>
- Nielsen D.R., Biggar J.W. & Erh K.T. 1973, 'Spatial variability of field-measured soil-water properties', *Hilgardia*, Vol. 42, No. 7, pp.215-259, cited in Brackensiek D.L. & Onstad C.A. 1977, 'Parameter estimation of the Green and Ampt infiltration equation', *Water Resources Research*, Vol. 13, No. 6, pp. 1009-1012.
- Oxford 2015, Oxford English Dictionary, online at <http://www.oxforddictionaries.com/definition/english/model>.
- Pajjan T.F. 1987, 'Unsaturated flow properties data catalog, Volume II, Publication #45061, Water Resources Centre, Desert Research Institute, DOE/NV/10384-20, cited in Williams J.R., Ouyang Y. & Chen J. 1998, 'Estimation of infiltration rate in the vadose zone: Application of selected mathematical models, Volume 2', US EPA, online at <http://nepis.epa.gov/Adobe/PDF/30003L4K.pdf>
- Philip J.R. 1957, 'The theory of infiltration 4. Sorptivity and algebraic infiltration equations', *Soil Science*, Vol. 84, pp.257-264.
- Philip J.R. 1998, 'Infiltration into crusted soils', *Water Resources Research*, Vol. 34, pp. 1919-1927, cited in Assouline S. 2013, 'Infiltration into soils: Conceptual approaches and solutions', *Water Resources Research*, Vol. 49, pp.1755-1772.

- Postel S. 1999, *Pillar of Sand: Can the Irrigation Miracle Last?*, W.W. Norton & Co.
- Rawls W.J., Brakensiek D.L., Simanton J.R. & Kohl K.D. 1990, 'Development of a crust factor for a Green-Ampt model', *Transactions of the ASAE*, Vol. 33, No. 4, pp.1224-1228, cited in Van den Putte A., Govers G., Leys A., Langhans C., Clymans W. & Diels J. 2013, 'Estimating the parameters of the Green-Ampt infiltration equation from rainfall simulation data: Why simpler is better', *Journal of Hydrology*, Vol. 476, pp. 332-344.
- Raats P.A.C. & van Genuchten M.T. 2006, 'Milestones in soil physics', *Soil Science*, Vol. 171, Suppl. 1, pp.S21-S28.
- Rawls W.J., Brakensiek D.L. & Soni B. 1983, 'Agricultural management effects on soil water processes, Part 1: Soil water retention and Green and Ampt infiltration parameters', *Transactions of the ASABE*, Vol. 26, No. 6, pp. 1747-1752, online at <http://elibrary.asabe.org/azdez.asp?search=1&JID=3&AID=33837&v=26&i=6&CID=t1983&T=2&urlRedirect=>
- Ravi V. & Williams J.R. 1998, 'Estimation of infiltration rate in the vadose zone: Compilation of simple mathematical models, Volume 1', US EPA, online at <http://nepis.epa.gov/Adobe/PDF/30003L26.pdf>
- Richards L.A. 1931, 'Capillary conduction of liquids through porous medium', *Physics*, Vol. 1, pp. 318-333, cited in Ravi V. & Williams J.R. 1998, 'Estimation of infiltration rate in the vadose zone: Compilation of simple mathematical models, Volume 1', US EPA, online at <http://nepis.epa.gov/Adobe/PDF/30003L26.pdf>
- Rossi M.J. & Ares J.O. 2015, 'Efficiency improvements in linear-move sprinkler systems through moderate runoff-runon control', *Irrigation Science*, DOI 10.1007/s00271-015-0460-x, online at <http://lq6tx6lb4h.scholar.serialssolutions.com/?sid=google&auinit=MJ&auplast=Rossi&atitle=Efficiency+improvement+in+linear-move+sprinkler+systems+through+moderate+runoff-runon+control&id=doi:10.1007/s00271-015-0460-x>
- Slack D.C. 1980, 'Modelling infiltration under moving sprinkler systems', *Transactions of the ASAE*, 0001-2351/80/2303-0596\$02.00, online at <https://elibrary.asabe.org/azdez.asp?AID=34631&T=2>
- Slack D.C., Killen M.A., Berglund E.R. & Onstad C.A. 1988, 'Application of the Green-Ampt-Mein-Larson model to taconite tailings', *Transactions of the ASAE*, Vol. 31, No. 5, online at <https://elibrary.asabe.org/azdez.asp?JID=3&AID=30885&CID=t1988&v=31&i=5&T=2>
- Skaggs R.W., Miller D.E. & Brooks R.H. 1983, Soil Water: Part I. Properties, in *Design and Operation of Farm Irrigation Systems*, pp.77-123, ASAE Monograph 3, Jenson M.E. (Ed.), St Joseph Michigan, cited in Luz P.B. 2011, 'A graphical solution to estimate potential runoff in centre pivot irrigation', *Transactions of the ASABE* Vol. 54, No. 1, pp. 81-92, online at <http://elibrary.asabe.org/azdez.asp?search=1&JID=3&AID=36262&v=54&i=1&CID=t2011&T=2&urlRedirect=>

- Smith R.E. 1975, 'Comments on 'Derivation of an equation of infiltration' by H.J. Morel-Seytoux and J. Khanji', *Water Resources Research*, Vol. 11, No. 5, p. 762, online at <http://onlinelibrary.wiley.com/doi/10.1029/WR011i005p00762/pdf>
- Smith R.E. 1976, 'Approximations for vertical infiltration rate patterns', *Transactions of the ASABE*, Vol. 19, No. 3 pp. 505-509, online at <http://elibrary.asabe.org/azdez.asp?search=1&JID=3&AID=36058&v=19&i=3&CID=t1976&T=2&urlRedirect=>
- Smith R.E. & Parlange J.-Y 1978, 'A parameter-efficient hydrologic infiltration model', *Water Resources Research*, Vol. 14, No. 3, pp. 533-538, online at <http://onlinelibrary.wiley.com/doi/10.1029/WR014i003p00533/pdf>
- Srivastava P., Costello T.A. & Edwards D.R. 1996, 'A direct, approximate solution to the modified Green-Ampt infiltration equation', *Transactions of the ASAE*, Vol. 39, No. 4, pp. 1411-1413, online at <https://elibrary.asabe.org/azdez.asp?AID=27633&T=2>
- Stewart R.D., Rupp D.E., Abou Najm M.R. & Selker J.S. 2013, 'Modelling effect of initial soil moisture on sorptivity and infiltration', *Water Resources Research*, Vol. 49, No. 10, pp. 7037-7047, online at <http://onlinelibrary.wiley.com/doi/10.1002/wrcr.20508/pdf>
- Swartzendruber D. & Huberty M.R. 1958, 'Use of infiltration equation parameters to evaluate infiltration differences in the field', *Transactions American Geophysical Union*, Vol. 39, No. 1, pp. 84-93, online at <http://onlinelibrary.wiley.com/doi/10.1029/TR039i001p00084/pdf>
- Swartzendruber D. 1974, 'Comments on 'Modelling infiltration during a steady rain' by Russell G. Mein and Curtis L. Larson', *Water Resources Research*, Vol. 10, No. 4, p.888, online at <http://onlinelibrary.wiley.com/doi/10.1029/WR010i004p00888/pdf>
- Swartzendruber D. & Hillel D. 1975, 'Infiltration and runoff for small field plots under constant intensity rainfall', *Water Resources Research*, Vol. 11, No. 3, pp. 445-451, online at <http://onlinelibrary.wiley.com/doi/10.1029/WR011i003p00445/pdf>
- Swartzendruber D. & Clague F.R. 1989, 'An inclusive infiltration equation for downward entry into soil', *Water Resources Research*, Vol. 25, No. 4, pp. 619-626, online at <http://onlinelibrary.wiley.com/doi/10.1029/WR025i004p00619/pdf>
- Swartzendruber D. 1993, 'Revised attribution of the power form infiltration equation', *Water Resources Research*, Vol. 29, No. 7, pp. 2455-2456, online at <http://onlinelibrary.wiley.com/doi/10.1029/93WR00612/pdf>
- Swartzendruber D. 1997, 'Exact mathematical derivation of a two-term infiltration equation', *Water Resources Research*, Vol. 33, No. 3, pp. 491-496, online at <http://onlinelibrary.wiley.com/doi/10.1029/96WR03906/pdf>

- Tovey R. & Pair C.H. 1966, 'Measurement of intake rate for sprinkler irrigation design', *Transactions of the ASAE*, Vol. 9, No. 3, pp.359-363.
- Uddin J., Smith R., Hancock N. & Foley J. (2014), 'Are evaporation losses in sprinkler irrigation high?', conference paper, 17th Australian Cotton Conference.
- Van den Putte A., Govers G., Leys A., Langhans C., Clymans W. & Diels J. 2013, 'Estimating the parameters of the Green-Ampt infiltration equation from rainfall simulation data: Why simpler is better', *Journal of Hydrology*, Vol. 476, pp. 332-344.
- van Duin R.H.A. 1955, 'Tillage in relation to rainfall intensity and infiltration capacity of soils', *Netherlands Journal of Agricultural Science*, Vol. 3, p.182, cited in Neuman S.P. 1976, 'Wetting front pressure head in the infiltration model of Green and Ampt', *Water Resources Research*, Vol. 12, No. 3, pp. 564-566, online at <http://onlinelibrary.wiley.com/doi/10.1029/WR012i003p00564/pdf>
- Whisler F.C. & Bouwer H. 1970, 'Comparison of methods for calculating vertical drainage and infiltration for soils', *Journal of Hydrology*, Vol. 10, pp. 1-19, cited in Smith R.E. 1976, 'Approximations for vertical infiltration rate patterns', *Transactions of the ASABE*, Vol. 19, No. 3 pp. 505-509, online at <http://elibrary.asabe.org/azdez.asp?search=1&JID=3&AID=36058&v=19&i=3&CID=t1976&T=2&urlRedirect=>
- Wigginton D., Foley J., Schultz J. & Van Niekerk R. 2011, *Review of Centre Pivot and Lateral Move Installations in the Queensland Murray Darling Basin*, National Centre for Engineering in Agriculture, publication 1004167/1, USQ, Toowoomba.
- Williams J.R., Ouyang Y. & Chen J. 1998, 'Estimation of infiltration rate in the vadose zone: Application of selected mathematical models, Volume 2', US EPA, online at <http://nepis.epa.gov/Adobe/PDF/30003L4K.pdf>
- Wilson B.N., Slack D.C. & Young R.A. 1982, 'A comparison of three infiltration models', *Transactions of the ASABE*, Vol. 25, No. 2 pp. 349-356, online at <http://elibrary.asabe.org/azdez.asp?search=1&JID=3&AID=33534&v=25&i=2&CID=t1982&T=2&urlRedirect=>
- Wilson B.N., Slack D.C. & Larson C.L. 1981, 'An infiltration model: Development and evaluation of its parameters', *Transactions of the ASABE*, Vol. 24, No. 3, pp. 670-677, online at <http://elibrary.asabe.org/azdez.asp?search=1&JID=3&AID=34319&v=24&i=3&CID=t1981&T=2&urlRedirect=>

Appendices

Appendix A – Project Specification

University of Southern Queensland

FACULTY OF HEALTH, ENGINEERING AND SCIENCES

ENG4111/4112 Research Project **PROJECT SPECIFICATION**

FOR: **Simon Mark KELDERMAN** (0011120971)

TOPIC: INVESTIGATION INTO THE USE OF GREEN & AMPT'S EQUATION WITH MOVING SPRINKLER IRRIGATION

SUPERVISOR: Dr. Joseph Foley

SPONSORSHIP: Cotton Research and Development Corporation

PROJECT AIM: To investigate whether Green & Ampt's (1911) equation can be used to model infiltration into soils under CP & LM sprinkler irrigation systems.

PROGRAMME: (Issue A, 16 March 2015)

- i. Research the original derivation, subsequent modifications, and historical use of the Green & Ampt (1911) equation.
 - ii. Survey and evaluate current methods of modelling infiltration under sprinkler irrigation.
 - iii. Develop a computer based model for modelling infiltration under moving sprinkler systems that uses Green & Ampt's equation (or some modification thereof).
 - iv. Design and implement a process of field validation of the model for non-cracking soils.
 - v. Submit an academic dissertation on the research.
- If the model's validation proves satisfactory, and as time permits:
- vi. Use the model to investigate a range of what-if scenarios.
 - vii. Investigate whether other non-time based infiltration models exist and compare to the Green & Ampt model.
 - viii. Conduct field trials of the model on cracking clay

AGREED: _____ (student) _____ (supervisor)
Date: / / 2015 Date: / / 2015

Examiner / Co-examiner: _____

Appendix B - Chu's Method for Determining GAML Parameters

Chu (1986) developed a graphical process that avoided the need to measure the GAML parameters, if data for I vs t was available. This was very useful because the GAML parameters can be difficult to measure in the field. The development of his graphical process is explained below. This material has been summarised from Chu (1986).

The Green-Ampt (1911) equation was of the form

$$I = Kt - (h_f - h_s)(\theta_s - \theta_0) \log_e \left[1 - \frac{I}{(h_f - h_s)(\theta_s - \theta_0)} \right] \quad (\text{C-1})$$

Recognising that the suction and moisture parameters always featured together, they were replaced by a single lumped parameter called SM (for Suction & Moisture).

$$I = Kt - SM \log_e \left[1 - \frac{I}{SM} \right] \quad (\text{C-2})$$

Rearranging into a convenient form,

$$\frac{I}{SM} - \log_e \left[1 + \frac{I}{SM} \right] = K \frac{t}{SM} \quad (\text{C-3})$$

If one has an I vs t curve, then select two points (t_1, I_1) and (t_2, I_2) so that $I_2 = 2I_1$. Substituting into equation C-3,

$$\frac{I_1}{SM} - \log_e \left[1 + \frac{I_1}{SM} \right] = K \frac{t_1}{SM} \quad (\text{C-4})$$

$$\frac{I_2}{SM} - \log_e \left[1 + \frac{I_2}{SM} \right] = K \frac{t_2}{SM} \quad (\text{C-5})$$

Dividing C-5 by C-4,

$$\frac{\frac{I_2}{SM} - \log_e \left[1 + \frac{I_2}{SM} \right]}{\frac{I_1}{SM} - \log_e \left[1 + \frac{I_1}{SM} \right]} = \frac{t_2}{t_1} \quad (C-6)$$

Using the fact that $I_2 = 2I_1$,

$$\frac{2 \frac{I_1}{SM} - \log_e \left[1 + 2 \frac{I_1}{SM} \right]}{\frac{I_1}{SM} - \log_e \left[1 + \frac{I_1}{SM} \right]} = \frac{t_2}{t_1} \quad (C-7)$$

Equation C-7 is consistent only when $2 < \frac{t_2}{t_1} < 4$. The left-hand side of C-7 is an equation in the variable $\frac{I_1}{SM}$ and it is plotted in Figure B-1.

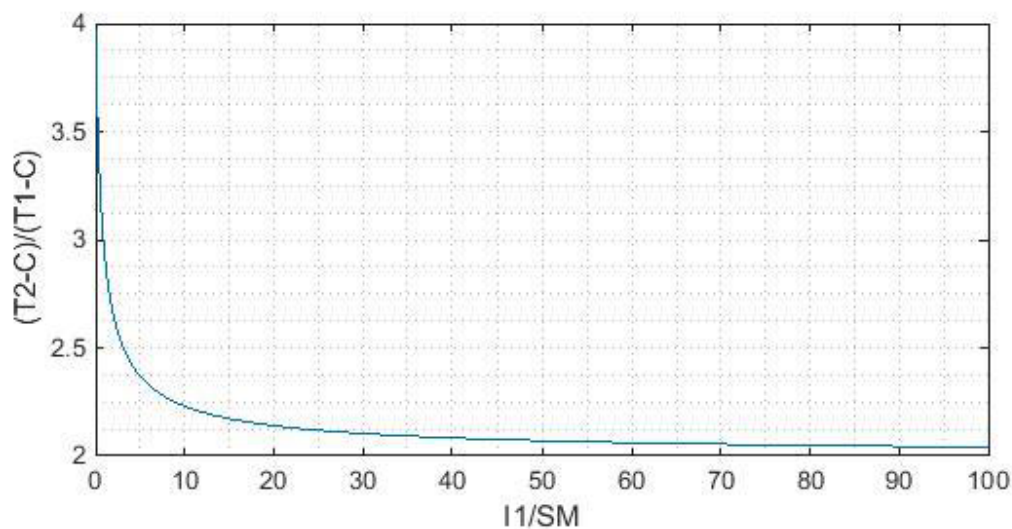


Figure B-1: A plot of equation C-7, where C is a constant used in the iterative procedure.

Equation C-4 when plotted is as per Figure B-2.

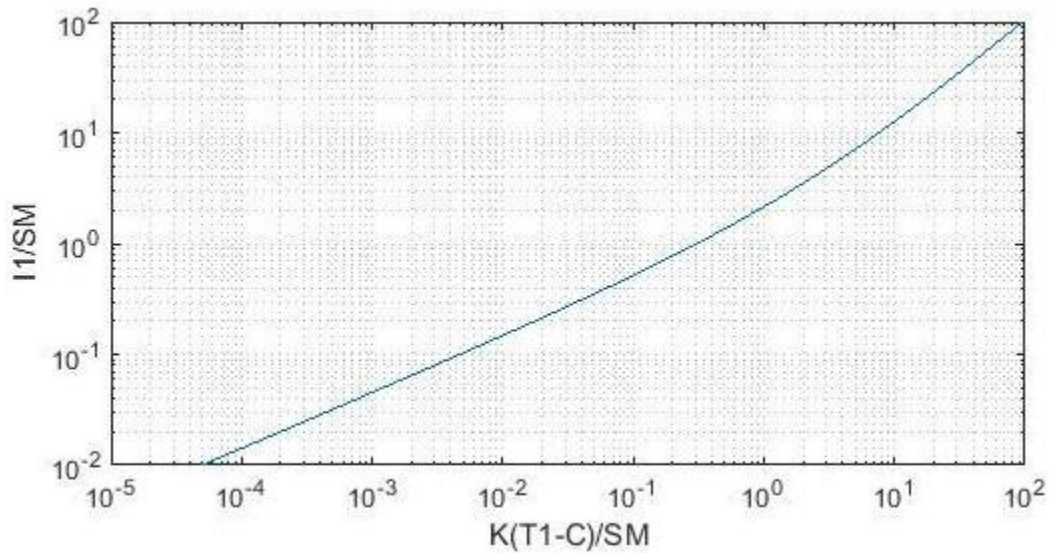


Figure B-2: A plot of equation C-4, where C is a constant used in the iterative procedure.

Chu then extended the Green-Ampt equation to accommodate the constant rainfall (or sprinkler) application rate, r , used by Mein and Larson (1971). He introduced three new terms, TP (ponding time) and TS (initial abstraction time), defined by

$$TP = \frac{K * SM}{r * (r - K)} \quad (C-8)$$

$$TS = \frac{SM}{K} * \left[\frac{K}{r - K} + \log_e \left(1 - \frac{K}{r} \right) \right] \quad (C-9)$$

$$C = TP - TS \quad (C-10)$$

So for conditions of a constant application rate, C-7 can be rewritten as

$$\frac{2 \frac{I_1}{SM} - \log_e \left[1 + 2 \frac{I_1}{SM} \right]}{\frac{I_1}{SM} - \log_e \left[1 + \frac{I_1}{SM} \right]} = \frac{t_2 - C}{t_1 - C} \quad (C-11)$$

The following iterative procedure is then followed.

1. Select two data points (t_1, I_1) and (t_2, I_2) so that $I_2 = 2I_1$.
2. Let $C = 0$.
3. Calculate the time ratio

$$\frac{t_2 - C}{t_1 - C}$$

- .
4. Enter the time ratio into Figure B-1 to find a quantity

$$QA = \frac{I_1}{SM}$$

- .
5. Rearrange to get

$$SM = \frac{I_1}{QA}$$

- .
6. Enter $QA = \frac{I_1}{SM}$ into Figure B-2 to get a quantity

$$QB = \frac{K(t_1 - C)}{SM}$$

- .
7. Rearrange to get

$$K = \frac{QB * SM}{(t_1 - C)}$$

- .
8. Calculate a new value for C using equations C-8 and C-9.
9. Repeat steps 3 – 8 until the values for K and SM become steady.

Appendix C - Matlab Code Used in Part 1 and Part 2 of Computer Model

C1. Code for Part 2 of Computer Model

```
% GAML_Chū_Part2.m

% calls user-defined function GAML_Chū_Part1.m if it is required to
% determine an infiltration characteristic from runoff data.

clc, clear all, close all

%% get infiltration characteristic equation
k = menu('Is the infiltration characteristic known?',...
    'Yes... The coefficients for the power function are known',...
    'No... It needs to be determined from cumulative infiltration vs time data');

if k == 2
    [A,B] = GAML_Chū_Part1( ); % coefficients are for infiltration characteristic, i is mm/hr
end

if k == 1
    disp('For a power function of the form i = A*t^B, enter A and B')
    disp('(units: i(mm/hr), t(hr)')
    A = input('Enter A: ');
    B = input('Enter B: ');
    disp(['The infiltration characteristic equation is'])
    disp([' i = ' num2str(A) '*t^' num2str(B)])
end

%% get application profile

q = menu('Were 4 Nelson S3000 #44 @ 6psi sprinklers from height of 2.44m, red plate, used at 1.20m
spacings?',...
    'Yes',...
    'No');

if q == 1
    can_distances = 0:0.25:6.75; % metres
    can_depths = [28,2,1.8,1.1,0.9,1.1,1.6,2.3,3.0,3.9,5.2,7.1,8.7,9.6,...
        11.5,13.8,14.6,12.7,10.0,10.9,19.4,24.1,11.2,3.9,1.9,0.6,0.1,0.0];%mm
    duration = 0.58; %digital hours
    plots_wanted = 2; % 2 means 'Yes' (see CU_TRUNK_April20.m)
    num_sprinklers = 4; % number of sprinkler heads
    sprinkler_separation = 1.20; % metres
    v = 36; % metres/hr... equivalent to 30cm/30sec
elseif q == 2
    % add ability to custom enter material here.
end

[ARG,xmax,x] =
catchcan_grid_NO_WIND_vProject2015(can_distances,can_depths,duration,plots_wanted);
[ARG_rows,ARG_cols] = size(ARG);

[ARG2,Xcoarse,num] = multiple_sprinklers_vProject2015(ARG,num_sprinklers,sprinkler_separation,
xmax, plots_wanted,can_distances,can_depths,duration);

%%
[sizeROW,sizeCOL] = size(ARG2);
```

```

midCOL = round(sizeCOL/2);
application_profile = ARG2(:,midCOL); % y-axis in mm/hr, x-axis values to be determined

%%
r = application_profile; % mm/hr
r_cm_day = r*24./10; % convert to cm/day

dx = (2*xmax)/(length(r)-1); % distance of each increment on application profile, metres
dt = dx/v; % at travel speed v (m/hr) this is the time (hours) to travel increment dx

t = 0:dt:(dt*(length(r)-1)); % hours
t(1) = 0.00001; % remove t = 0 to avoid Inf value for i

i = A*t.^B; % infiltration characteristic mm/hr
i = i*24; % convert mm/hr to mm/day
i = i./10 % convert mm/day to cm/day

t = t./24; %convert hours to days

I = zeros(size(i));
for n = 2:length(i)
    I(n) = I(n-1)+i(n-1)*dt;
end

R = zeros(size(r));
for n = 2:length(r)
    R(n)=R(n-1)+r_cm_day(n-1)*dt;
end

figure
plot(t,r_cm_day)
    grid minor
    xlabel('time (days)')
    ylabel('application rate (cm/day)')

start_value = (t(1)+t(end))/12;
tmp = abs(t-start_value);
[val idx] = min(tmp);

A1 = [t(idx),R(idx)];
A2 = [t(idx),r_cm_day(idx)];

h=1;
err = 999;
while err>0.001
    h=h+1;
    clear tmp
    tmp = abs(i-r(idx));
    clear idx idy
    [val, idx]=min(tmp);
    A3 = [t(idx),i(idx)];
    A4 = [t(idx),I(idx)];
    clear tmp
    tmp = abs(R-I(idx));
    [val, idx]=min(tmp);
    A1_2 = [t(idx),R(idx)];
    err = abs(A1(1)-A1_2(1));
    A1 = A1_2;
    A2 = [t(idx),r_cm_day(idx)];
    if h>20000

```

```

        break
    end
end
disp(['A1 = ' num2str(A1)])
disp(['A2 = ' num2str(A2)])
disp(['A3 = ' num2str(A3)])
disp(['A4 = ' num2str(A4)])
disp(' ')
disp(['Time to ponding = ' num2str(A1(1)) 'days' ])
disp(' ')
%%
figure
subplot(2,2,1)
    plot(t,r_cm_day,A2(1),A2(2),'o')
    axis([0 max(t) 0 max([max(r_cm_day),max(i(2:end))])]);
    xlabel('t (days)', ylabel('r (cm/day)')
    grid
subplot(2,2,2)
    plot(t,i,A3(1),A3(2),'o')
    axis([0 max(t) 0 max([max(r_cm_day),max(i(2:end))])]);
    xlabel('t (days)', ylabel('i (cm/day)')
    grid
subplot(2,2,3)
    plot(t,R,A1(1),A1(2),'o')
    axis([0 max(t) 0 max([max(R),max(I)])]);
    xlabel('t (days)', ylabel('R (cm)')
    grid
subplot(2,2,4)
    plot(t,I,A4(1),A4(2),'o')
    axis([0 max(t) 0 max([max(R),max(I)])]);
    xlabel('t (days)');
    ylabel('I (cm)');
    grid

%%
u_p = A3(1); % time of imbibement on i and I curves
t_p = A1(1); % time to ponding on r and R curves
offset=find(t==t_p)-find(t==u_p);

N = zeros(3*length(t),1);
N(length(t)+1+offset:2*length(t)+offset) = i;
N(find(N==0)) = 99999;
N = N(length(t)+1:2*length(t));

figure
plot(t,r_cm_day,'k-')
    axis([0 max(t) 0 max(r_cm_day)]);
    xlabel('t (days)', ylabel('r and i (cm/day)')
    grid
    hold on
plot(t,N,'r--')
    axis([0 max(t) 0 max(r_cm_day)]);
legend('application rate, r','infiltration capacity, i')

clear val idx
tmp = abs(r_cm_day-N);
[val idx]= min(tmp);
B2 = [t(idx),r_cm_day(idx)];
B1 = [t(idx),R(idx)];
clear tmp
tmp = abs(i-r_cm_day(idx));

```

```

[val idx]= min(tmp);
B3 = [t(idx),i(idx)];
B4 = [t(idx),I(idx)];

disp(['B1 = ' num2str(B1) ])
disp(['B2 = ' num2str(B2) ])
disp(['B3 = ' num2str(B3) ])
disp(['B4 = ' num2str(B4) ])
disp(' ')
disp(['Runoff = ' num2str(B1(2)-B4(2)) 'cm' ])
disp(' ')
disp('-----')

```

C2. Code for Part 1 of Computer Model

```

function [A,B] = GAML_Ch Part1()

q = menu('Test mode?','Yes','No');
if q == 1
    I = [0
        7.1
        12.1
        16.6
        21.0
        25.2
        29.4
        32.8
        36.1
        38.9
        42.4
        44.8
        47.0
        49.1
        51.3
        53.4
        55.6
        57.9
        60.1
        62.5
        64.7]; % mm depth of cumulative infiltration
    t = 0:3:(length(I)*3-3); % time, minutes
    r = 150; % mm/hr
else
    I = input('Enter cumulative infiltration (mm) values: ');
    t = input('Enter time values (mins). Leave blank if increments are in 3mins: ');
    r = input('Enter application rate (mm/hr): ');
end
I = I/10; % convert to cm depth
r = r/10; % convert to cm/hr
if isempty(t)
    t = 0:3:(length(I)*3 - 3);
end

if length(t)~=length(I)
    error('the vectors for I and t must be equal')
end

for n = 2:length(t)
    if t(n)<=t(n-1)
        error('vector for t must be monotonically increasing')
    end
end

```

```

end
if I(n)<I(n-1)
    error('vector for I must never be decreasing')
end
end

figure
subplot(2,2,1)
plot(t./60,I*10)
grid
xlabel('time (hours)')
ylabel('depth infiltrated (mm)')

I1_SM = 0.01:0.01:100;
T2mC_T1mC = (2*I1_SM - log(1+2*I1_SM))./(I1_SM - log(1+I1_SM) );

subplot(2,2,3)
plot(I1_SM,T2mC_T1mC)
grid minor
xlabel('I1/SM')
ylabel('(T2-C)/(T1-C)')

KT1mC_SM = I1_SM - log(1+I1_SM);

subplot(2,2,4)
loglog(KT1mC_SM,I1_SM)
grid minor
xlabel('K(T1-C)/SM')
ylabel('I1/SM')

K_2 = 0;
SM_2 = 0;
for count = 1:5
    C = 0;
    T1 = 3 + (count-1);
    I1 = interp1(t,I,T1);
    I2 = I1*2;
    T2 = interp1(I,t,I2);
    K = 1;
    Knew = 2;
    while abs(K - Knew) > 0.001
        Knew = K;
        timeratio = (T2-C)/(T1-C);
        if or(timeratio > 4,timeratio < 2)
            disp('Time ratio is not between 2 and 4');
        end

        QA = interp1(T2mC_T1mC,I1_SM,timeratio);
        SM = I1/QA;
        QB = interp1(I1_SM,KT1mC_SM,QA);
        K = QB*SM/(T1-C);%cm/min
        K = K*60; %cm/hr
        TP = K*SM/(r*(r-K));
        TP = TP*60;
        TS = SM/K*(K/(r-K) + log(1-K/r) );
        TS = TS*60;
        C = TP-TS;
    end
    K_2(count) = K; % cm/hr
    SM_2(count) = SM;
end

```

```

Iplot = linspace(min(I),max(I),100); %cm
i = K*(1+SM./Iplot); %cm/hr

subplot(2,2,2)
plot(Iplot*10,i*10)
grid minor
xlabel('infiltrated depth, I (mm)')
ylabel('infiltration and application rates, i & r (mm/hr)')
hold on
plot(Iplot*10,r*10*ones(1,length(Iplot)),'r--')
legend('infiltration capacity','application rate')
end

% remove any NAN
J = find(isnan(K_2));
K_2(J) = [];
SM_2(J) = [];

K = mean(K_2) %cm/hr
SM = mean(SM_2)
Iplot = linspace(min(I),max(I),100); %cm
i = K*(1+SM./Iplot); %cm/hr

figure
subplot(1,2,1)
plot(Iplot*10,i*10)
grid minor
xlabel('infiltrated depth, I (mm)')
ylabel('infiltration capacity, i (mm/hr)')

tplot = interp1(I,t,Iplot); % mins
subplot(1,2,2)
plot(tplot./60,i*10)
grid minor
xlabel('time (hour)')
ylabel('infiltration capacity, i (mm/hr)')

% find the infiltration characteristic by fitting a curve
if tplot(1) == 0
    tplot = tplot(2:end); %mins
    i = i(2:end); %cm/hr
end

i = i*10; %convert to mm/hr
tplot = tplot/60; %convert to hrs

p = polyfit(log(tplot),log(i),1);
A = exp(p(2));
B = p(1);
disp(['The infiltration characteristic equation is'])
disp([' i = ' num2str(A) '*t^' num2str(B)])

x = tplot(1):0.01:tplot(end); %hrs
y = A*x.^B; % mm/hr

figure
plot(x,y,tplot,i,'k')
grid minor

check = trapz(tplot,i);

```

```

disp('')
disp(['Total cumulative infiltration = ' num2str(I(end)*10) 'mm' ])
disp(['Total area under i vs t curve = ' num2str(check) 'mm' ])

end %end of function

```

C3. Further Code for User Written Functions

```

function [application_rate_grid, xmax,x] =
catchcan_grid_NO_WIND_vProject2015(can_distances,can_depths,duration,plots_wanted)
%catchcan_grid_v1.m converts sprinkler catch-can data into 2D grid, Version 1
%
% Uses radial spoke sprinkler catch-can data from single spoke, non-windy
% conditions (later versions will incorporate wind).
%
% Input variables:
%
% can_distances ==> vector, contains the distances along radial
% spoke from the sprinkler at which catch-cans
% are placed (units: metres);
%
% can_depths ==> vector, contains the depth measurements in each can,
% corresponding to the distance along the radial
% spoke (units: mm).
%
% duration ==> scalar, duration of catch-can trial (units: digital hours)
%
% plots_wanted ==> scalar, value must be 1 (for NO, plots are not
% wanted) or 2 (for YES, plots are wanted)
%
% Output variables:
%
% application_rate_grid ==> 2D rectangular array that shows the rate of
% application of water at points all around the
% sprinkler (units: mm/hour).
%
% xmax ==>
%
% x ==>

if can_depths(1) <= 0
    can_depths(1) = can_depths(2); % deal with problem of no catch-can measure beneath sprinkler head
end

% create grid of zeros to receive the interpolated catch-can data
resolution = 40; % this is used to set the resolution of the final grid
if min(can_distances) == 0
    first = 0;
else
    first = 0.01;
end
x = linspace(first,max(can_distances),resolution);
x = unique(x);
xmax = x(end);
L = 2*length(x)-1;
M = zeros(L);
% interpolate catch-can depths along radial spoke
for row_index = 1:L
    for col_index = 1:L
        if and(row_index < ceil(L/2),col_index < ceil(L/2))
            xi = x(ceil(L/2)-col_index);

```

```

        yi = x(ceil(L/2)-row_index);
        distance = sqrt(xi^2+yi^2);
        M(row_index,col_index) = interp1(can_distances, can_depths,distance);
    elseif and(row_index < ceil(L/2),col_index > ceil(L/2))
        xi = x(col_index-ceil(L/2));
        yi = x(ceil(L/2)-row_index);
        distance = sqrt(xi^2+yi^2);
        M(row_index,col_index) = interp1(can_distances, can_depths,distance);
    elseif and(row_index > ceil(L/2),col_index < ceil(L/2))
        xi = x(ceil(L/2)-col_index);
        yi = x(row_index-ceil(L/2));
        distance = sqrt(xi^2+yi^2);
        M(row_index,col_index) = interp1(can_distances, can_depths,distance);
    elseif and(row_index > ceil(L/2),col_index > ceil(L/2))
        xi = x(col_index-ceil(L/2));
        yi = x(row_index-ceil(L/2));
        distance = sqrt(xi^2+yi^2);
        M(row_index,col_index) = interp1(can_distances, can_depths,distance);
    elseif and(row_index == ceil(L/2),col_index == ceil(L/2))
        distance = 0;
        M(row_index,col_index) = can_depths(1);
    elseif and(row_index == ceil(L/2),col_index < ceil(L/2))
        distance = x(ceil(L/2)-col_index);
        M(row_index,col_index) = interp1(can_distances, can_depths,distance);
    elseif and(row_index == ceil(L/2),col_index > ceil(L/2))
        distance = x(col_index-ceil(L/2));
        M(row_index,col_index) = interp1(can_distances, can_depths,distance);
    elseif and(row_index < ceil(L/2),col_index == ceil(L/2))
        distance = x(ceil(L/2)-row_index);
        M(row_index,col_index) = interp1(can_distances, can_depths,distance);
    elseif and(row_index > ceil(L/2),col_index == ceil(L/2))
        distance = x(row_index - ceil(L/2));
        M(row_index,col_index) = interp1(can_distances, can_depths,distance);
    end

    if M(row_index,col_index) < 0
        M(row_index,col_index) = 0;
    end
end
end

```

```

M(isnan(M)) = 0; % replace NaN's with zeros
M = M/duration;
application_rate_grid = M;

end

```

```

.....

function [ ARG2,Xcoarse,num ] = multiple_sprinklers_vProject2015(
ARG,num_sprinklers,sprinkler_separation, xmax, plots_wanted, can_distances,can_depths,duration )
% User-defined function that overlaps multiple identical sprinklers and
% produces a new ARG (Application Rate Grid).
%
% number of sprinklers must be greater than 1 for this function
% Inputs  ARG          ==> 2D array, 'Application Rate Grid', of
%          sprinkler application rates (mm/hr)
%          num_sprinklers ==> scalar value, number of sprinklers
%          being modelled. Must be integer >= 2
%          sprinkler_separation ==> scalar value, distance between
%          sprinklers, metres (model assumes

```

```

%           sprinklers are equally spaced)
%           xmax           ==> scalar value, the maximum catch-can
%           distance (metres) from the
%           sprinkler head.
%           plots_wanted   ==> scalar value, must be either 1
%           (plots not wanted) or 2 (plots are
%           wanted)
%
% Outputs  ARG2           ==> 2D array, a new Application Rate
%           Grid of sprinkler application rates
%           (mm/hr) after the effect of
%           sprinkler overlap is accounted for

if num_sprinklers < 2
    error('num_sprinklers must be greater than one for the multiple_sprinklers_vApril_7th.m function');
end

if sprinkler_separation <= 0
    error('sprinkler_separation must be greater than zero');
end

% if too many sprinklers involved then it causes problems with memory
n1 = ceil(2*xmax/sprinkler_separation);
n2 = num_sprinklers;
n = min(n1,n2);
num = n;
[ARGrows,ARGcols] = size(ARG);

X = linspace(-1*xmax, xmax, ARGcols);
Y = linspace(-1*xmax, xmax, ARGrows);
[XX,YY] = meshgrid(X,Y);

step = 0.1; % metres (ie. to nearest 10cm)
Xfine = -1*xmax:step:xmax;
Yfine = -1*xmax:step:xmax;
d = 1/step;
sprinkler_sep_fine = round(sprinkler_separation*d)/d;
shift = ceil(sprinkler_sep_fine/step);

[XXfine,YYfine] = meshgrid(Xfine,Yfine);
ARGfine = interp2(XX,YY,ARG,XXfine,YYfine);

clear XX, clear YY
clear Xfine, clear Yfine
clear XXfine, clear YYfine
clear step, clear d, clear sprinkler_sep_fine

[ARGfine_rows,ARGfine_cols] = size(ARGfine);
% ARGfine_cols2 = ARGfine_cols + shift*(n-1);
ARGfine_cols2 = ARGfine_cols + shift*(num_sprinklers-1);
ARGfine_rows2 = ARGfine_rows;

M = zeros(ARGfine_rows2,ARGfine_cols2);
M(:,1:ARGfine_cols) = M(:,1:ARGfine_cols) + ARGfine;

for c = 1:(num_sprinklers-1)
    M(:,(c*shift+1):(ARGfine_cols+c*shift)) = M(:,(c*shift+1):(ARGfine_cols+c*shift)) + ARGfine;
end

% convert M back to more reasonable size ARG2

```

```

ratio_cols_to_rows = ARGfine_cols2/ARGfine_rows2;
ARGcols_coarse = round(ratio_cols_to_rows * ARGcols);
Xcoarse = linspace(-1*xmax,ratio_cols_to_rows*xmax,ARGcols_coarse);
Ycoarse = linspace(-1*xmax,xmax,ARGrows);
[XXcoarse,YYcoarse] = meshgrid(Xcoarse,Ycoarse);

W = linspace(-1*xmax,ratio_cols_to_rows*xmax,ARGfine_cols2);
R = linspace(-1*xmax,xmax,ARGfine_rows2);
[XX,YY] = meshgrid(W,R);

ARG2 = interp2(XX,YY,M,XXcoarse,YYcoarse);
size(ARG2);
ARG2max = max(max(ARG2));

if plots_wanted == 2
    figure('units','normalized','outerposition',[0 0 1 1]);

    subplot(2,2,1)
        plot(can_distances,can_depths,'o-')
        title('Catch-can measurements')
        xlabel('Horizontal distance from sprinkler head (m)')
        ylabel('Depth of water in catch-can (mm)')
        grid
        %xloc = max(can_distances)* 1/3;
        yloc = max(can_depths)*1/15;
        xloc = 0.2;
        test_mins = fix(duration*60);
        test_sec = (duration*60 - test_mins)*60;
        text(xloc,yloc,['Duration of test = ' num2str(test_mins) 'min ' num2str(test_sec) 'sec']);
    subplot(2,2,2)
        mesh(X,Y,ARG);
        axis([-xmax, xmax, -xmax, xmax, 0, ARG2max]);
        caxis([0, ARG2max]);
        title('Application rate for single sprinkler');
        ylabel('Distance from sprinkler head (m)');
        xlabel('Distance from sprinkler head (m)');
        zlabel('Application Rate (mm/hr)');
        colorbar

    subplot(2,2,3)
        mesh(Xcoarse,Ycoarse,ARG2);
        caxis([0, ARG2max]);
        title(['Pattern of application for ' num2str(n) ' sprinklers with ' num2str(sprinkler_separation) ' metres
separation']);
        ylabel('Distance from line of sprinkler heads (m)');
        xlabel('Distance from first sprinkler head (m)');
        zlabel('Combined Application Rate (mm/hr)');
        colorbar
    subplot(2,2,4)
        mesh(Xcoarse,Ycoarse,ARG2);
        caxis([0, ARG2max]);
        title(['Pattern of application for ' num2str(n) ' sprinklers with ' num2str(sprinkler_separation) ' metres
separation']);
        ylabel('Distance from line of sprinkler heads (m)');
        xlabel('Distance alone line of sprinklers from first sprinkler head (m)');
        zlabel('Combined Application Rate (mm/hr)');
        view(0,90);
        colorbar
end
end

```

Appendix D - Selected Laboratory Sprinkler Data

67 laboratory sprinkler tests were undertaken and recorded in an Excel file. This Excel file can be obtained by contacting the author.

Appendix D only contains the data from 10 of the sprinkler tests whose results were of particular relevance to the project. The particular tests are (after the naming convention of Section 4.1.1)

1. Sred6_44
2. Sred10_18
3. Sred10_32
4. Sred15_26
5. Sred20_14
6. Sred20_38
7. Sred25_44
8. Sred30_38
9. Syellow20_21

The raw catch-can data is presented as well as radial leg profiles. Note that for each test a catch-can was located directly beneath the sprinkler head itself (the 'zero point'). Separate radial leg profiles were plotted to include the zero point and exclude the zero point. Also, for each sprinkler test a plot of Christiansen's Uniformity (CU) versus sprinkler head spacing was produced and has been included here too.

Nelson S3000 #44 @ 6psi (red plate)

Sprinkler Settings

Nozzle	44	1/128ths
Pressure	6 PSI	(53kPa @ Big Gauge)
Sprinkler Type	S3000	(Grey Cap)
Plate Colour	Red	
Height Sprinkler	2.54 m	
Height Catch-cans	0.1 m	
Effective Height	2.44 m	
Catch-can Diameter	105 mm	
Catch-can Lip Thickness	0.5 mm	
Zero Pot Can Diameter	260 mm	

Date & Duration

Test Date:	24/06/15	
	(hh:mm@24hr)	
Time Start		or
Time Finish		
Total Time		
		Stopwatch Time
		0:35:01
		(h:mm:ss)
Total Time (digital)	0.58 hrs	

Flow Rates

KENT FLOWMETER

Flow Meter @ START	45.2857	m3
Flow Meter @ END	46.4040	m3
Av. Flow Rate	31.9	L/min
Av. Flow Rate	8.4	US GPM

ABB MAGMASTER ELECTROMAGNETIC FLOWMETER

Velocity	3	m/s	
Instantaneous Flow Rate	0.53	L/s	@ Time 0:01:00
Instantaneous Flow Rate	0.53	L/s	@ Time 0:16:00
Instantaneous Flow Rate	0.53	L/s	@ Time
Av. Instantaneous Flow Rate	0.530	L/s	
Equivalent Av. Flow Rate	31.8	L/min	
Equivalent Av. Flow Rate	8.40	US GPM	

NELSON SUPPLIED FLOW VALUES FOR GIVEN NOZZLE @ PRESSURE

Flow Rate per TN Nozzle Chart	31.52	L/min
Flow Rate per TN Nozzle Chart	8.33	US GPM

Environment

Test Location?	Lab (Indoors)
Solar Irradiance?	No
Wind?	No
Wind Speed (kph)	0
Dry Bulb Air Temp (deg C)	15
Wet Bulb Air Temp (deg C)	n/a
Water Temp (deg C)	15
Relative Humidity	n/a
Av. Hourly Loss to Evaporation on 1.0m L Sample in Catch-can	0

Scales

Brand	Digitech
Measurement Increments	0.01g (up to 1kg)
Tolerance Checked?	Yes (May 2015)
Tolerance	<0.03%

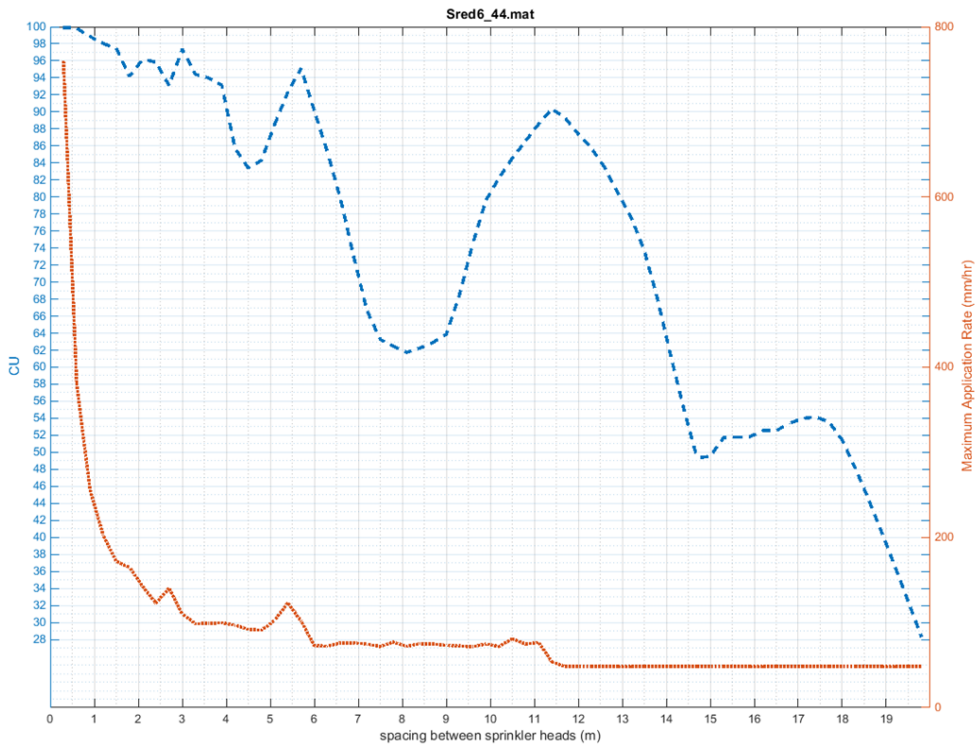
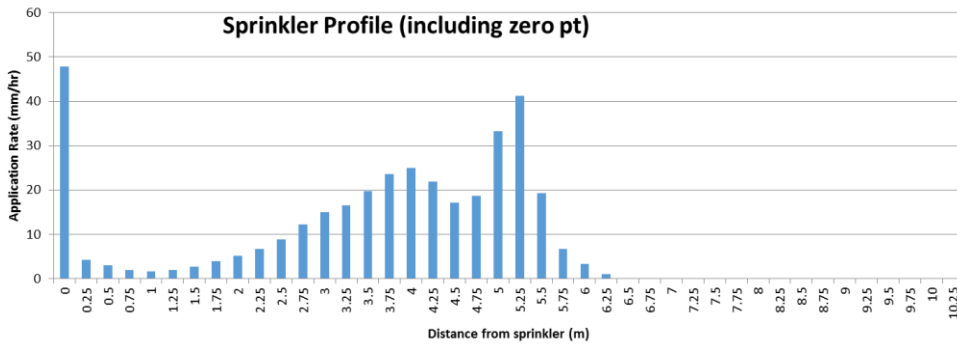
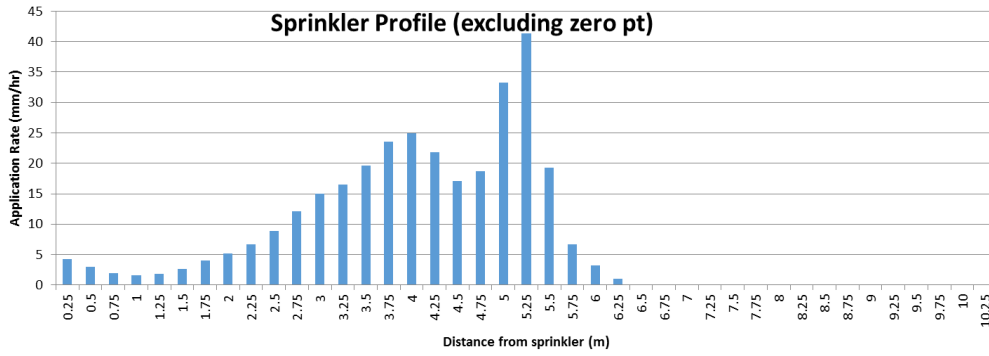
Pressures

Gauge 1 (Primary)	Wika Mechanical -100 to 250kPa
Gauge 2 (Secondary)	(0 PSI to 50 PSI)

Nelson S3000 #44 @ 6psi (red plate)

Distance (m)	Mass			Average Mass (g)	Depth (mm)	Application Rate (mm/hr)
	Can 1 (g)	Can 2 (g)	Can 3 (g)			
0.00	1484			1484	28	47.9
0.25	24.4	21.7	18.5	22	2	4.3
0.50	14.1	17.9	13.6	15.2	1.8	3.0
0.75	8.7	7.5	12.7	9.6	1.1	1.9
1.00	9.2	7.6	7.8	8.2	0.9	1.6
1.25	9.4			9.4	1.1	1.9
1.50	13.6			13.6	1.6	2.7
1.75	20.2			20.2	2.3	4.0
2.00	25.9			25.9	3.0	5.1
2.25	33.7			33.7	3.9	6.7
2.50	44.8			44.8	5.2	8.9
2.75	61.4			61.4	7.1	12.2
3.00	75.7			75.7	8.7	15.0
3.25	83.5			83.5	9.6	16.5
3.50	99.4			99.4	11.5	19.7
3.75	119.3			119.3	13.8	23.6
4.00	126.2			126.2	14.6	25.0
4.25	110.4			110.4	12.7	21.8
4.50	86.4			86.4	10.0	17.1
4.75	94.6			94.6	10.9	18.7
5.00	167.9			167.9	19.4	33.2
5.25	208.7			208.7	24.1	41.3
5.50	97.2			97.2	11.2	19.2
5.75	34.0			34.0	3.9	6.7
6.00	16.5			16.5	1.9	3.3
6.25	5.3			5.3	0.6	1.0
6.50	0.7			0.7	0.1	0.1
6.75	0.0			0.0	0.0	0.0
7.00	0.0			0.0	0.0	0.0
7.25	0.0			0.0	0.0	0.0
7.50	0.0			0.0	0.0	0.0
7.75	0.0			0.0	0.0	0.0
8.00	0.0			0.0	0.0	0.0
8.25	0.0			0.0	0.0	0.0
8.50	0.0			0.0	0.0	0.0
8.75	0.0			0.0	0.0	0.0
9.00	0.0			0.0	0.0	0.0

Nelson S3000 #44 @ 6psi (red plate)



Nelson S3000 #18 @ 10psi (red plate)

Sprinkler Settings

Nozzle	18	1/128ths
Pressure	10	PSI
Sprinkler Type	S3000	(Grey Cap)
Plate Colour	Red	
Height sprinkler	2.54	m
Height catch-cans	0.1	m
Effective Height	2.44	m
Catch-can Diameter	110	mm
Catch-can Lip Thickness	6	mm
Zero Pot Can Diameter	260	mm

Date & Duration

Test Date:	25/05/15	
	(hh:mm@24hr)	
Time Start		or Stopwatch Time
Time Finish		0:46:44
Total Time		(h:mm:ss)
Total Time (digital)	0.78	hrs

Flow Rates

KENT FLOWMETER

Flow Meter @ START	18.8834	m ³
Flow Meter @ END	19.2001	m ³
Av. Flow Rate	6.8	L/min
Av. Flow Rate	1.8	US GPM

ABB MAGMASTER ELECTROMAGNETIC FLOWMETER

Velocity		m/s	
Instantaneous Flow Rate	0.114	L/s	@ Time 0:03:13
Instantaneous Flow Rate	0.113	L/s	@ Time 0:23:10
Instantaneous Flow Rate	0.112	L/s	@ Time 0:38:00
Av. Instantaneous Flow Rate	0.113	L/s	
Equivalent Av. Flow Rate	6.8	L/min	
Equivalent Av. Flow Rate	1.79	US GPM	

NELSON SUPPLIED FLOW VALUES FOR GIVEN NOZZLE @ PRESSURE

Flow Rate per BTN Nozzle Chart	6.6	L/min
Flow Rate per BTN Nozzle Chart	1.75	US GPM

Environment

Test Location?	Lab (Indoors)
Solar Irradiance?	No
Wind?	No
Wind Speed (kph)	0
Dry Bulb Air Temp (deg C)	20
Wet Bulb Air Temp (deg C)	n/a
Water Temp (deg C)	19
Relative Humidity	n/a
Av. Hourly Loss to Evaporation on 10.0mL Sample in Catch-can	0

Scales

Brand	Digitech
Measurement Increments	0.01g (up to 1kg)
Tolerance Checked?	Yes (May 2015)
Tolerance	<0.03%

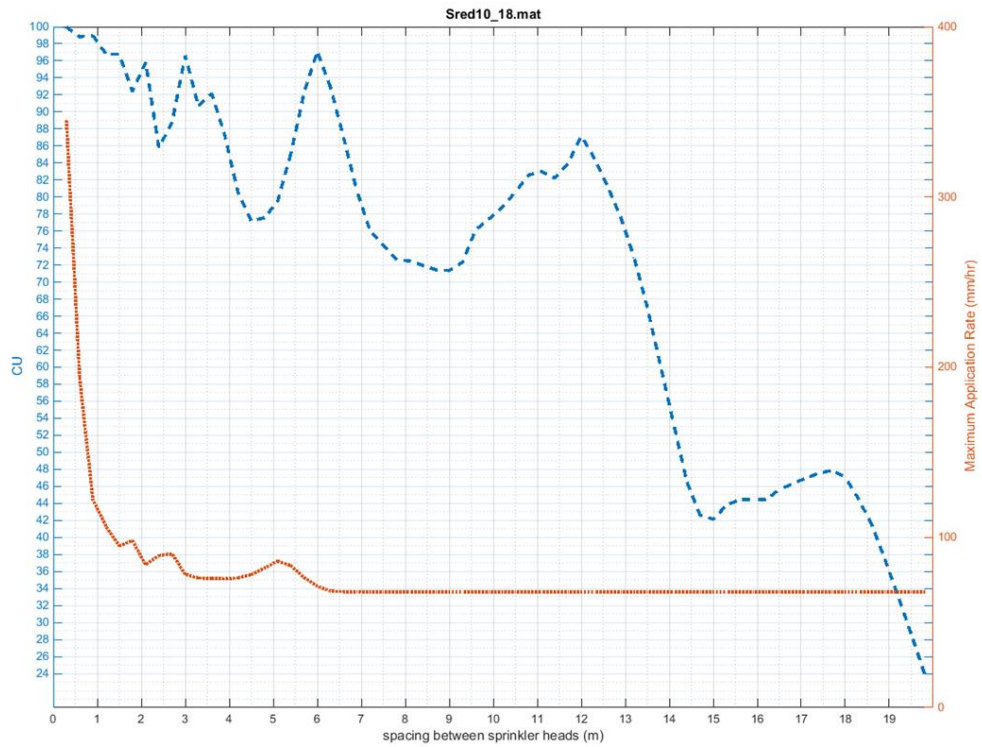
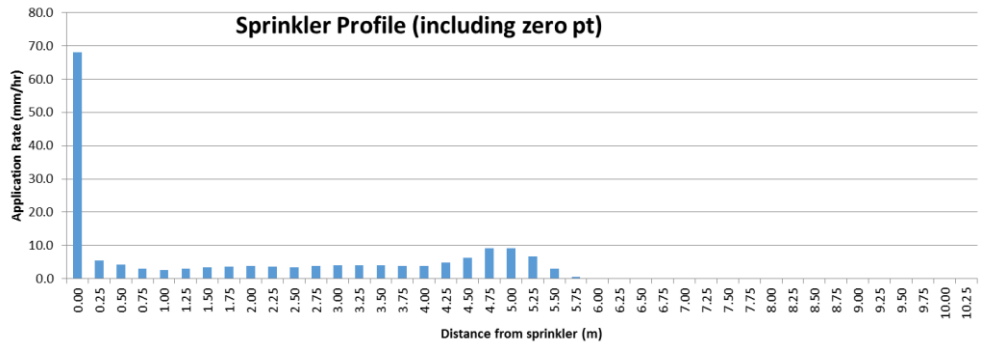
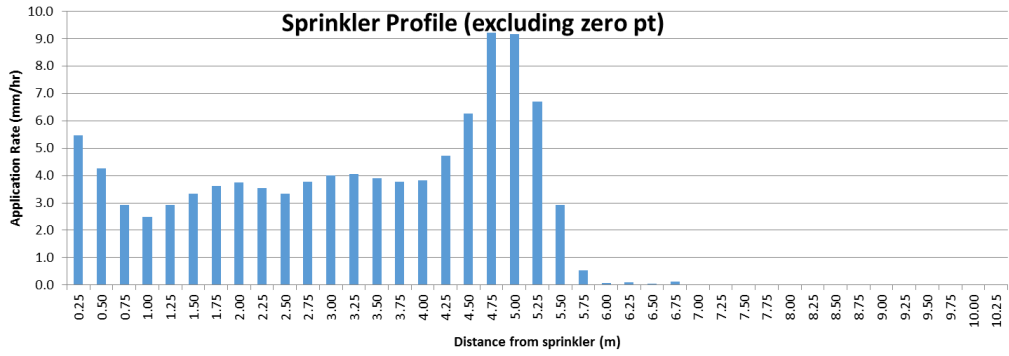
Pressures

Gauge 1 (Primary)	Wika Mechanical -100 @ 250kPa
Gauge 2 (Secondary)	(0 PSI @ 60 PSI)

Nelson S3000 #18 @ 10psi (red plate)

Distance (m)	Mass			Average Mass (g)	Depth (mm)	Application Rate (mm/hr)
	Can 1 (g)	Can 2 (g)	Can 3 (g)			
0.00	2812			2812	53	68.0
0.25	40	39	43	41	4	5.5
0.50	27	37	30	31.6	3.3	4.3
0.75	26	18	21	21.7	2.3	2.9
1.00	18	17	21	18.5	1.9	2.5
1.25	21.6			21.6	2.3	2.9
1.50	24.7			24.7	2.6	3.3
1.75	26.7			26.7	2.8	3.6
2.00	27.7			27.7	2.9	3.7
2.25	26.2			26.2	2.8	3.5
2.50	24.6			24.6	2.6	3.3
2.75	27.9			27.9	2.9	3.8
3.00	29.7			29.7	3.1	4.0
3.25	30.0			30.0	3.2	4.1
3.50	28.9			28.9	3.0	3.9
3.75	28.0			28.0	2.9	3.8
4.00	28.3			28.3	3.0	3.8
4.25	35.0			35.0	3.7	4.7
4.50	46.4			46.4	4.9	6.3
4.75	68.2			68.2	7.2	9.2
5.00	67.9			67.9	7.1	9.2
5.25	49.5			49.5	5.2	6.7
5.50	21.6			21.6	2.3	2.9
5.75	3.9			3.9	0.4	0.5
6.00	0.6			0.6	0.1	0.1
6.25	0.7			0.7	0.1	0.1
6.50	0.3			0.3	0.0	0.0
6.75	0.9			0.9	0.1	0.1
7.00	0.2			0.2	0.0	0.0
7.25	0.0			0.0	0.0	0.0
7.50	0.0			0.0	0.0	0.0
7.75	0.0			0.0	0.0	0.0
8.00	0.0			0.0	0.0	0.0
8.25	0.0			0.0	0.0	0.0
8.50	0.0			0.0	0.0	0.0
8.75	0.0			0.0	0.0	0.0
9.00	0.0			0.0	0.0	0.0

Nelson S3000 #18 @ 10psi (red plate)



Nelson S3000 #21 @ 10psi (red plate)

Sprinkler Settings

Nozzle	21	1/128ths
Pressure	10	PSI
Sprinkler Type	S3000	(Grey Cap)
Plate Colour	Red	
Height Sprinkler	2.4	m
Height Catch-cans	0.1	m
Effective Height	2.3	m
Catch-can Diameter	110	mm
Catch-can Lip Thickness	6	mm
Zero Pot Can Diameter	260	mm

Date & Duration

Test Date:	4/05/15	
	(hh:mm:24hr)	
Time Start	13:47	or
Time Finish	14:36	
Total Time	0:49	
		Stopwatch Time
		(h:mm:ss)
Total Time (digital)	0.82	hrs

Flow Rates

KENT FLOWMETER

Flow Meter @ START		m3
Flow Meter @ END		m3
Av. Flow Rate	0.0	L/min
Av. Flow Rate	0.0	US GPM

ABB MAGMASTER ELECTROMAGNETIC FLOWMETER

Velocity		m/s	
Instantaneous Flow Rate		L/s	@ Time
Instantaneous Flow Rate		L/s	@ Time
Instantaneous Flow Rate		L/s	@ Time
Av. Instantaneous Flow Rate	#DIV/0!	L/s	
Equivalent Av. Flow Rate	#DIV/0!	L/min	
Equivalent Av. Flow Rate	#DIV/0!	US GPM	

NELSON SUPPLIED FLOW VALUES FOR GIVEN NOZZLE & PRESSURE

Flow Rate per TN Nozzle Chart	9	L/min
Flow Rate per TN Nozzle Chart	1.06	US GPM

Environment

Test Location?	Lab (Indoors)
Solar Irradiance?	No
Wind?	No
Wind Speed (kph)	0
Dry Bulb Air Temp (deg C)	15
Wet Bulb Air Temp (deg C)	n/a
Water Temp (deg C)	15
Relative Humidity	n/a
Av. Hourly Loss to Evaporation on 0.0mL Sample in Catch-can	0

Scales

Brand	Digitech
Measurement Increments	0.01g (up to 1kg)
Tolerance Checked?	Yes (May 2015)
Tolerance	<0.03%

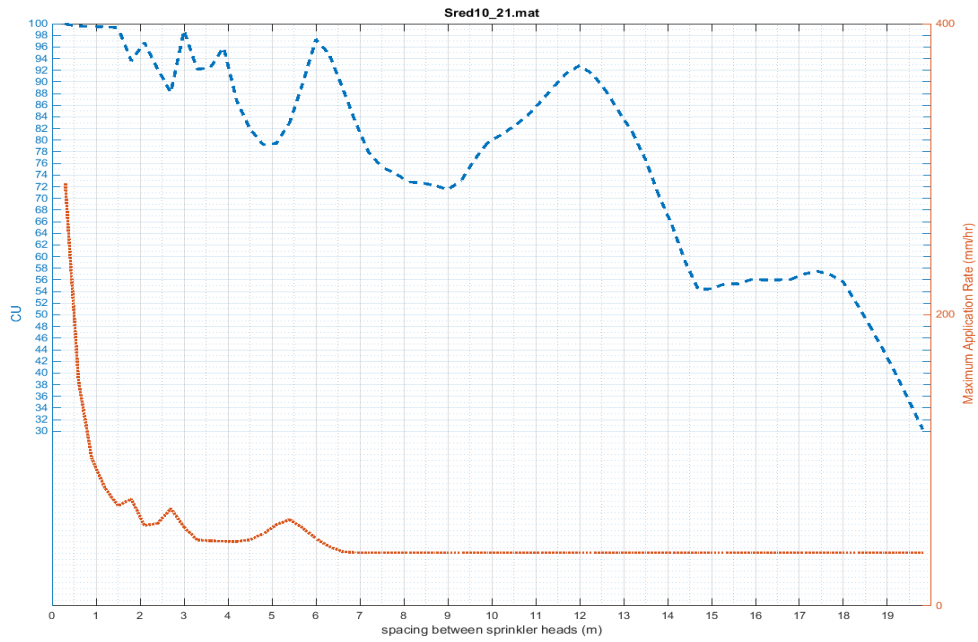
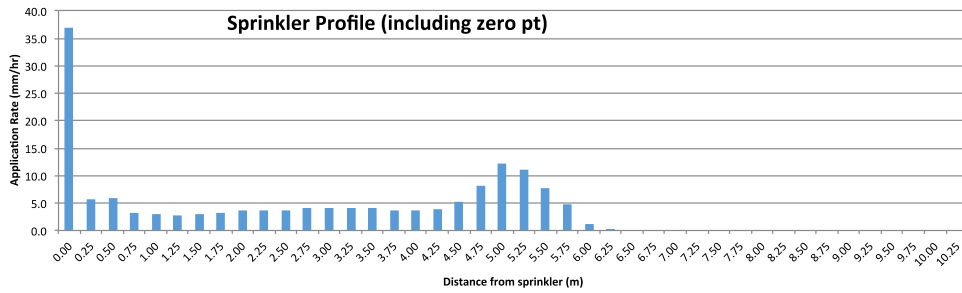
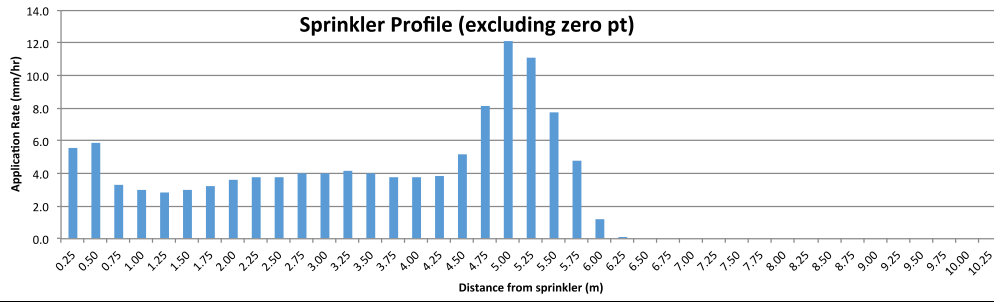
Pressures

Gauge 1 (Primary)	Wika Mechanical -100 to 250kPa
Gauge 2 (Secondary)	(0 PSI to 50 PSI)

Nelson S3000 #21 @ 10psi (red plate)

Distance (m)	Mass			Average Mass (g)	Depth (mm)	Application Rate (mm/hr)
	Can 1 (g)	Can 2 (g)	Can 3 (g)			
0.00	1597			1597	30	36.8
0.25	39	50	41	43	5	5.6
0.50	45	47	45	45.7	4.8	5.9
0.75	24	24	28	25.3	2.7	3.3
1.00	27	19	23	23.0	2.4	3.0
1.25	22			22.0	2.3	2.8
1.50	23			23.0	2.4	3.0
1.75	25			25.0	2.6	3.2
2.00	28			28.0	2.9	3.6
2.25	29			29.0	3.1	3.7
2.50	29			29.0	3.1	3.7
2.75	31			31.0	3.3	4.0
3.00	31			31.0	3.3	4.0
3.25	32			32.0	3.4	4.1
3.50	31			31.0	3.3	4.0
3.75	29			29.0	3.1	3.7
4.00	29			29.0	3.1	3.7
4.25	30			30.0	3.2	3.9
4.50	40			40.0	4.2	5.2
4.75	63			63.0	6.6	8.1
5.00	94			94.0	9.9	12.1
5.25	86			86.0	9.0	11.1
5.50	60			60.0	6.3	7.7
5.75	37			37.0	3.9	4.8
6.00	9			9.0	0.9	1.2
6.25	1			1.0	0.1	0.1
6.50	0			0.0	0.0	0.0
6.75	0			0.0	0.0	0.0
7.00	0			0.0	0.0	0.0
7.25	0			0.0	0.0	0.0
7.50	0			0.0	0.0	0.0
7.75	0			0.0	0.0	0.0
8.00	0			0.0	0.0	0.0
8.25	0			0.0	0.0	0.0
8.50	0			0.0	0.0	0.0
8.75	0			0.0	0.0	0.0
9.00	0			0.0	0.0	0.0
9.25	0			0.0	0.0	0.0
9.50	0			0.0	0.0	0.0
9.75	0			0.0	0.0	0.0
10.00	0			0.0	0.0	0.0
10.25	0			0.0	0.0	0.0

Nelson S3000 #21 @ 10psi (red plate)



Nelson S3000 #32 @ 10psi (red plate)

<u>Sprinkler Settings</u>			
Nozzle	32	1/128ths	REPEAT
Pressure	10 PSI	(82kPa)	Big Gauge
Sprinkler Type	S3000	(Grey Cap)	
Plate Colour	Red		
Height sprinkler	2.54 m		
Height catch-cans	0.1 m		
Effective Height	2.44 m		
Catch-can Diameter	105 mm		
Catch-can Lip Thickness	0.5 mm		
Zero Pot Can Diameter	260 mm		

<u>Date & Duration</u>			
Test Date:	18/06/15	REPEAT TEST	
	(hh:mm@24hr)		
Time Start		or	Stopwatch Time
Time Finish			0:48:43
Total Time			(h:mm:ss)
	Total Time (digital)		0.81 hrs

<u>Flow Rates</u>			
KENT FLOWMETER			
Flow Meter @ START	39.6234	m3	
Flow Meter @ END	40.6777	m3	
Av. Flow Rate	21.6	L/min	
Av. Flow Rate	5.7	US GPM	
ABB MAGMASTER ELECTROMAGNETIC FLOWMETER			
Velocity	2.03	m/s	
Instantaneous Flow Rate	0.36	L/s	@ Time 0:01:00
Instantaneous Flow Rate	0.36	L/s	@ Time 0:06:00
Instantaneous Flow Rate	0.36	L/s	@ Time 0:42:00
Av. Instantaneous Flow Rate	0.360	L/s	
Equivalent Av. Flow Rate	21.6	L/min	
Equivalent Av. Flow Rate	5.71	US GPM	
NELSON SUPPLIED FLOW VALUES FOR GIVEN NOZZLE @ PRESSURE			
Flow Rate per BTN Nozzle Chart	21.5	L/min	
Flow Rate per BTN Nozzle Chart	5.63	US GPM	

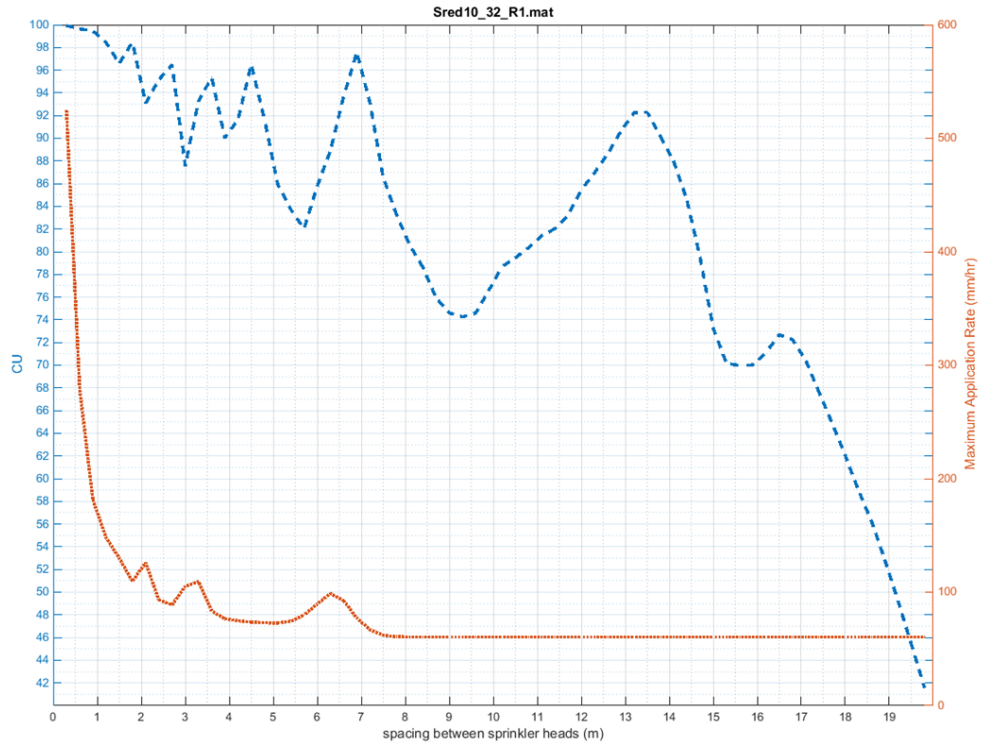
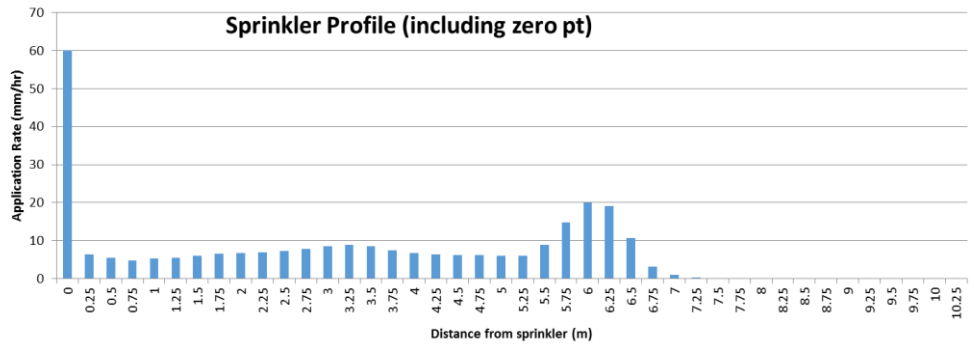
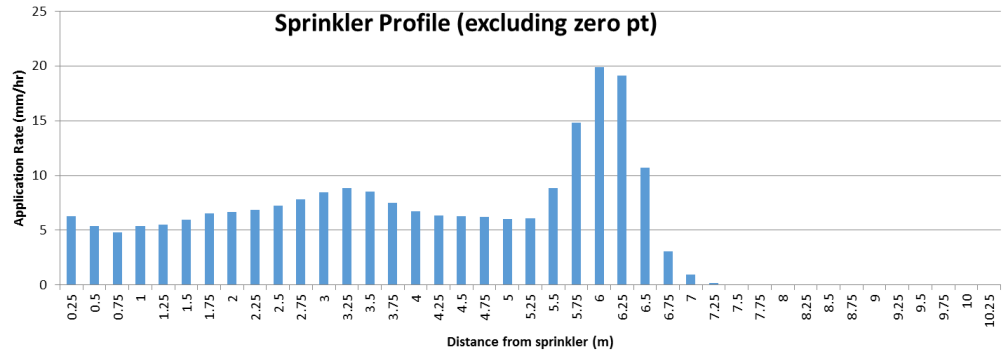
<u>Environment</u>	
Test Location?	Lab (Indoors)
Solar Irradiance?	No
Wind?	No
Wind Speed (kph)	0
Dry Bulb Air Temp (deg C)	16
Wet Bulb Air Temp (deg C)	n/a
Water Temp (deg C)	16
Relative Humidity	n/a
Av. Hourly Loss to Evaporation on 10.0mL Sample in Catch-can	0

<u>Scales</u>	
Brand	Digitech
Measurement Increments	0.01g (up to 1kg)
Tolerance Checked?	Yes May 2015
Tolerance	<0.03%
<u>Pressures</u>	
Gauge 1 (Primary)	Wika Mechanical - 100 @ 250kPa
Gauge 2 (Secondary)	(0 PSI @ 60 PSI)

Nelson S3000 #32 @ 10psi (red plate)

Distance (m)	Mass			Average Mass (g)	Depth (mm)	Application Rate (mm/hr)
	Can 1 (g)	Can 2 (g)	Can 3 (g)			
0.00	2594			2594	49	60
0.25	55.0	44.0	34.0	44	5	6
0.50	36.5	37.6	40.1	38.1	4.4	5.4
0.75	32.6	41.4	27.5	33.8	3.9	4.8
1.00	36.3	47.5	29.4	37.7	4.4	5.4
1.25	38.9	32.5	44.4	38.6	4.5	5.5
1.50	42.6	44.1	39.2	42.0	4.8	6.0
1.75	46.9	45.4	45.9	46.1	5.3	6.6
2.00	46.9	45.9	47.6	46.8	5.4	6.7
2.25	48.2	48.6	48.3	48.4	5.6	6.9
2.50	50.9	50.6	50.9	50.8	5.9	7.2
2.75	55.0	54.1	55.3	54.8	6.3	7.8
3.00	59.3			59.3	6.8	8.4
3.25	62.1			62.1	7.2	8.8
3.50	59.8			59.8	6.9	8.5
3.75	52.8	53.6	51.6	52.7	6.1	7.5
4.00	46.9	48.0	47.1	47.3	5.5	6.7
4.25	44.5	44.6	44.3	44.5	5.1	6.3
4.50	43.8	44.8	43.8	44.1	5.1	6.3
4.75	43.5	43.6	43.6	43.6	5.0	6.2
5.00	42.4	42.5	41.8	42.2	4.9	6.0
5.25	42.5	42.5	43.3	42.8	4.9	6.1
5.50	62.0			62.0	7.2	8.8
5.75	104.4			104.4	12.1	14.8
6.00	140.0			140.0	16.2	19.9
6.25	134.4			134.4	15.5	19.1
6.50	75.4			75.4	8.7	10.7
6.75	21.5			21.5	2.5	3.1
7.00	6.7			6.7	0.8	1.0
7.25	1.4			1.4	0.2	0.2
7.50	0.0			0.0	0.0	0.0
7.75	0.0			0.0	0.0	0.0
8.00	0.0			0.0	0.0	0.0
8.25	0.0			0.0	0.0	0.0
8.50	0.0			0.0	0.0	0.0
8.75	0.0			0.0	0.0	0.0
9.00	0.0			0.0	0.0	0.0

Nelson S3000 #32 @ 10psi (red plate)



Nelson S3000 #26 @ 15psi (red plate)

Sprinkler Settings	
Nozzle	26 1/128ths
Pressure	15 PSI
Sprinkler Type	S3000 (Grey Cap)
Plate Colour	Red
Height Sprinkler	2.4 m
Height Catch-cans	0.1 m
Effective Height	2.3 m
Catch-can Diameter	110 mm
Catch-can Lip Thickness	6 mm
Zero Pot Can Diameter	260 mm

Date & Duration	
Test Date:	14/05/15 (hh:mm:24hr)
Time Start	14:28
Time Finish	15:12
Total Time	0:44
or	
Stopwatch Time	
(h:mm:ss)	
Total Time (digital)	0.73 hrs

Flow Rates	
KENT FLOWMETER	
Flow Meter @ START	
Flow Meter @ END	
Average Flow Rate	0.0 L/min
Average Flow Rate	0.0 US GPM
ABB MAGMASTER ELECTROMAGNETIC FLOWMETER	
Velocity	
Instantaneous Flow Rate	
Instantaneous Flow Rate	
Instantaneous Flow Rate	
Average Instantaneous Flow Rate	#DIV/0! L/s
Equivalent Average Flow Rate	#DIV/0! L/min
Equivalent Average Flow Rate	#DIV/0! US GPM
NELSON SUPPLIED FLOW VALUES FOR GIVEN NOZZLE & PRESSURE	
Flow Rate per TN Nozzle Chart	17.1 L/min
Flow Rate per TN Nozzle Chart	US GPM

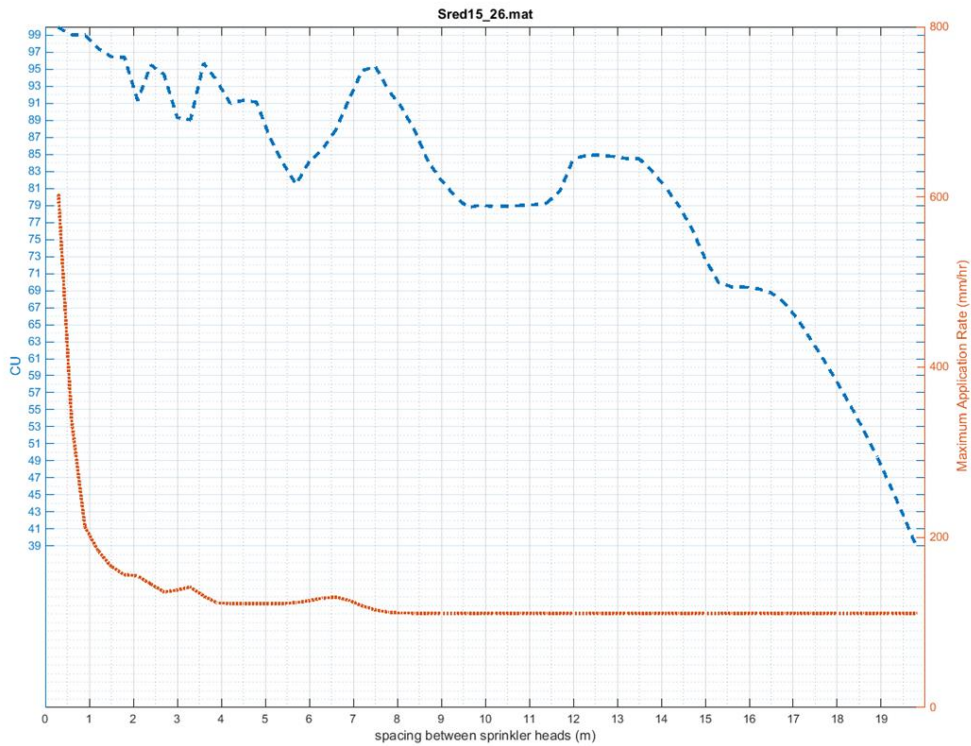
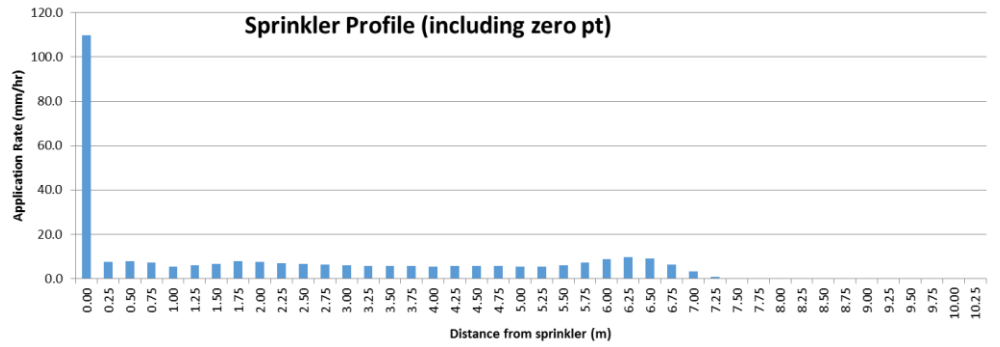
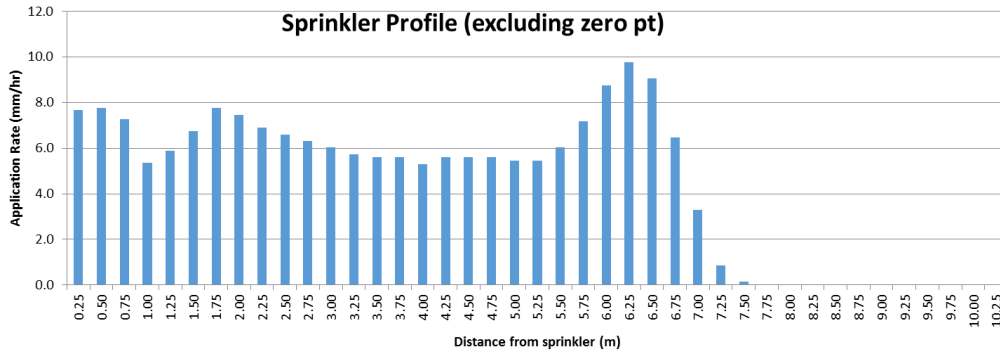
Environment	
Test Location?	Lab (Indoors)
Solar Irradiance?	No
Wind?	No
Wind Speed (kph)	0
Dry Bulb Air Temp (deg C)	14
Wet Bulb Air Temp (deg C)	n/a
Water Temp (deg C)	13
Relative Humidity	n/a
Average Hourly Loss to Evaporation on 0.0mL Sample in Catch-can	0

Scales	
Brand	Digitech
Measurement Increments	0.01g (up to 1kg)
Tolerance Checked?	Yes (May 2015)
Tolerance	<0.03%
Pressures	
Gauge 1 (Primary)	Wika Mechanical -100 to 250kPa
Gauge 2 (Secondary)	(0 PSI to 30 PSI)

Nelson S3000 #26 @ 15psi (red plate)

Distance (m)	Mass			Average Mass (g)	Depth (mm)	Application Rate (mm/hr)
	Can 1 (g)	Can 2 (g)	Can 3 (g)			
0.00	4280			4280	81	109.9
0.25	52	55	53	53	6	7.7
0.50	51	61	50	54.0	5.7	7.7
0.75	50	51	51	50.7	5.3	7.3
1.00	39	34	39	37.3	3.9	5.4
1.25	41			41.0	4.3	5.9
1.50	47			47.0	4.9	6.7
1.75	54			54.0	5.7	7.7
2.00	52			52.0	5.5	7.5
2.25	48			48.0	5.1	6.9
2.50	46			46.0	4.8	6.6
2.75	44			44.0	4.6	6.3
3.00	42			42.0	4.4	6.0
3.25	40			40.0	4.2	5.7
3.50	39			39.0	4.1	5.6
3.75	39			39.0	4.1	5.6
4.00	37			37.0	3.9	5.3
4.25	39			39.0	4.1	5.6
4.50	39			39.0	4.1	5.6
4.75	39			39.0	4.1	5.6
5.00	38			38.0	4.0	5.5
5.25	38			38.0	4.0	5.5
5.50	42			42.0	4.4	6.0
5.75	50			50.0	5.3	7.2
6.00	61			61.0	6.4	8.8
6.25	68			68.0	7.2	9.8
6.50	63			63.0	6.6	9.0
6.75	45			45.0	4.7	6.5
7.00	23			23.0	2.4	3.3
7.25	6			6.0	0.6	0.9
7.50	1			1.0	0.1	0.1
7.75	0			0.0	0.0	0.0
8.00	0			0.0	0.0	0.0
8.25	0			0.0	0.0	0.0
8.50	0			0.0	0.0	0.0
8.75	0			0.0	0.0	0.0
9.00	0			0.0	0.0	0.0

Nelson S3000 #26 @ 15psi (red plate)



Nelson S3000 #14 @ 20psi (red plate)

<u>Sprinkler Settings</u>		REPEAT
Nozzle	14	1/128ths
Pressure	20 PSI	(143kPa Big Gauge)
Sprinkler Type	S3000	(Grey Cap)
Plate Colour	Red	
Height Sprinkler	2.54 m	
Height Catch-cans	0.1 m	
Effective Height	2.44 m	
Catch-can Diameter	105 mm	
Catch-can Lip Thickness	0.5 mm	
Zero Pot Can Diameter	260 mm	

<u>Date & Duration</u>		REPEAT TEST
Test Date:	12/06/15	
	(hh:mm@24hr)	
Time Start		or Stopwatch Time
Time Finish		0:34:46
Total Time		(h:mm:ss)
Total Time (digital)	0.58 hrs	

<u>Flow Rates</u>			
KENT FLOWMETER			
Flow Meter @ START	35.6827	m3	
Flow Meter @ END	35.8805	m3	
Av. Flow Rate	5.7	L/min	
Av. Flow Rate	1.5	US GPM	
ABB MAGMASTER ELECTROMAGNETIC FLOWMETER			
Velocity	0.53	m/s	
Instantaneous Flow Rate	0.094	L/s	@ Time 0:01:00
Instantaneous Flow Rate	0.093	L/s	@ Time 0:17:00
Instantaneous Flow Rate	0.094	L/s	@ Time 0:28:00
Av. Instantaneous Flow Rate	0.094	L/s	
Equivalent Av. Flow Rate	5.6	L/min	
Equivalent Av. Flow Rate	1.48	US GPM	
NELSON SUPPLIED FLOW VALUES FOR GIVEN NOZZLE & PRESSURE			
Flow Rate per BTN Nozzle Chart	5.63	L/min	
Flow Rate per BTN Nozzle Chart	1.49	US GPM	

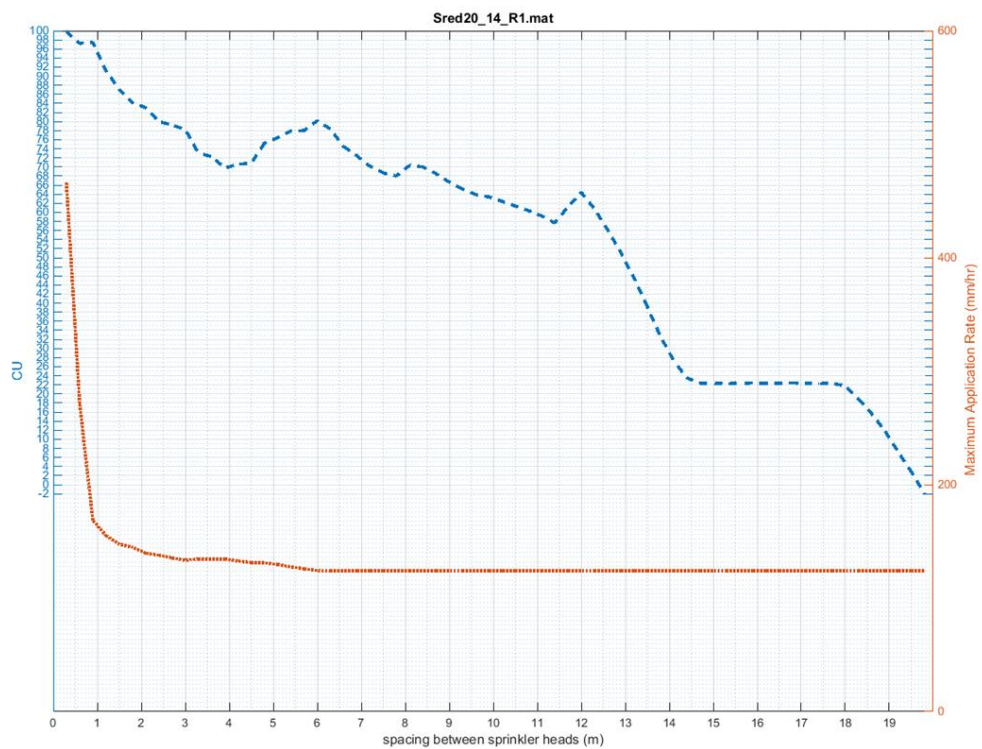
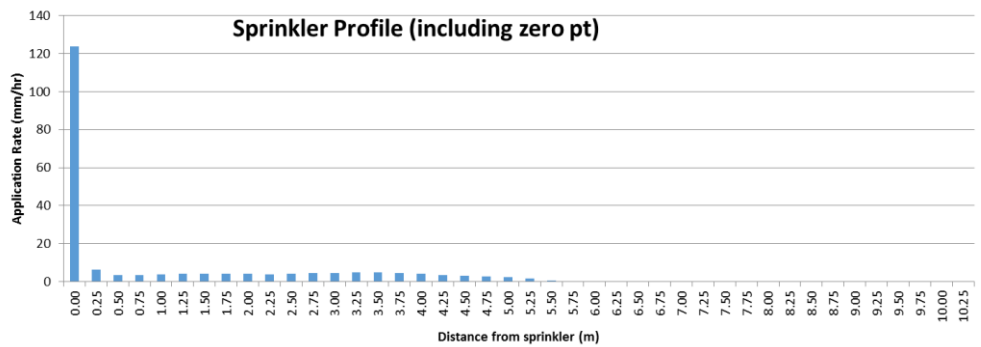
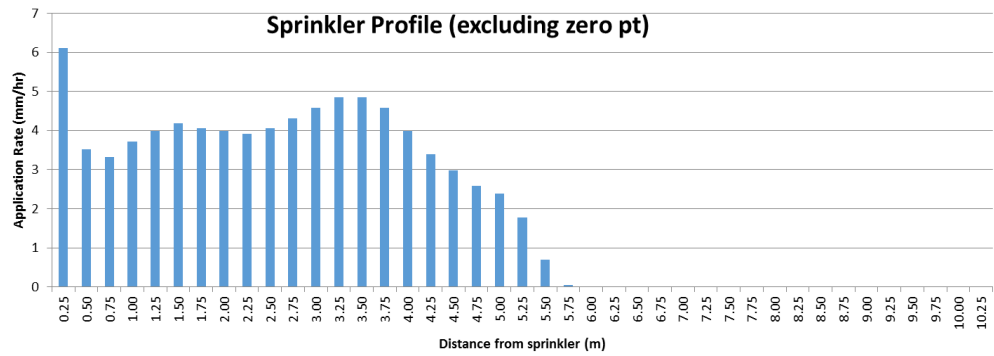
<u>Environment</u>	
Test Location?	Lab (Indoors)
Solar Irradiance?	No
Wind?	No
Wind Speed (kph)	0
Dry Bulb Air Temp (deg C)	15
Wet Bulb Air Temp (deg C)	n/a
Water Temp (deg C)	
Relative Humidity	n/a
Av. Hourly Loss to Evaporation on 10.0mL Sample in Catch-can	0

<u>Scales</u>	
Brand	Digitech
Measurement Increments	0.01g (up to 1kg)
Tolerance Checked?	Yes May 2015
Tolerance	<0.03%
Pressures	
Gauge 1 (Primary)	Wika Mechanical -100 to 250kPa
Gauge 2 (Secondary)	(0 PSI to 60 PSI)

Nelson S3000 #14 @ 20psi (red plate)

Distance (m)	Mass			Average Mass (g)	Depth (mm)	Application Rate (mm/hr)
	Can 1 (g)	Can 2 (g)	Can 3 (g)			
0.00	3808			3808	72	124
0.25	27	32	33	31	4	6
0.50	16	21	16	18	2	4
0.75	16	18	16	17	2	3
1.00	19	18	19	19	2	4
1.25	20	20	20	20	2	4
1.50	21	21		21	2	4
1.75	20	20	21	20	2	4
2.00	20	20	20	20	2	4
2.25	20	19	20	20	2	4
2.50	21	20	20	20	2	4
2.75	22	21	22	22	3	4
3.00	23	23	23	23	3	5
3.25	24	25	24	24	3	5
3.50	24	25	24	24	3	5
3.75	23			23	3	5
4.00	20			20	2	4
4.25	17			17	2	3
4.50	15			15	2	3
4.75	13			13	2	3
5.00	12			12	1	2
5.25	9			9	1	2
5.50	4			4	0	1
5.75	0			0	0	0
6.00	0			0	0	0
6.25	0			0	0	0
6.50	0			0	0	0
6.75	0			0	0	0
7.00	0			0	0	0
7.25	0			0	0	0
7.50	0			0	0	0
7.75	0			0	0	0
8.00	0			0	0	0
8.25	0			0	0	0
8.50	0			0	0	0
8.75	0			0	0	0
9.00	0			0	0	0

Nelson S3000 #14 @ 20psi (red plate)



Nelson S3000 #38 @ 20psi (red plate)

Sprinkler Settings

Nozzle	38	1/128ths	REPEAT
Pressure	20	PSI (150kPa)	Big Gauge
Sprinkler Type	S3000	(Grey Cap)	
Plate Colour	Red		
Height Sprinkler	2.54	m	
Height Catch-cans	0.1	m	
Effective Height	2.44	m	
Catch-can Diameter	105	mm	
Catch-can Lip Thickness	0.5	mm	
Zero Pot Can Diameter	260	mm	

Date & Duration

Test Date:	18/06/15	REPEAT TEST
	(hh:mm:24hr)	
Time Start		or Stopwatch Time
Time Finish		0:41:06
Total Time		(h:mm:ss)
Total Time (digital)	0.69	hrs

Flow Rates

KENT FLOWMETER

Flow Meter @ START	37.4223	m3
Flow Meter @ END	39.2524	m3
Av. Flow Rate	44.5	L/min
Av. Flow Rate	11.8	US GPM

ABB MAGMASTER ELECTROMAGNETIC FLOWMETER

Velocity	4.18	m/s	
Instantaneous Flow Rate	0.74	L/s	@ Time 0:01:00
Instantaneous Flow Rate	0.74	L/s	@ Time 0:06:00
Instantaneous Flow Rate	0.74	L/s	@ Time 0:54:00
Av. Instantaneous Flow Rate	0.740	L/s	
Equivalent Av. Flow Rate	44.4	L/min	
Equivalent Av. Flow Rate	11.73	US GPM	

NELSON SUPPLIED FLOW VALUES FOR GIVEN NOZZLE & PRESSURE

Flow Rate per TN Nozzle Chart	42.7	L/min
Flow Rate per TN Nozzle Chart	11.3	US GPM

Environment

Test Location?	Lab (Indoors)
Solar Irradiance?	No
Wind?	No
Wind Speed (kph)	0
Dry Bulb Air Temp (deg C)	16
Wet Bulb Air Temp (deg C)	n/a
Water Temp (deg C)	16
Relative Humidity	n/a
Av. Hourly Loss to Evaporation on 1.0mL Sample in Catch-can	0

Scales

Brand	Digitech
Measurement Increments	0.01g (up to 1kg)
Tolerance Checked?	Yes May 2015
Tolerance	<0.03%

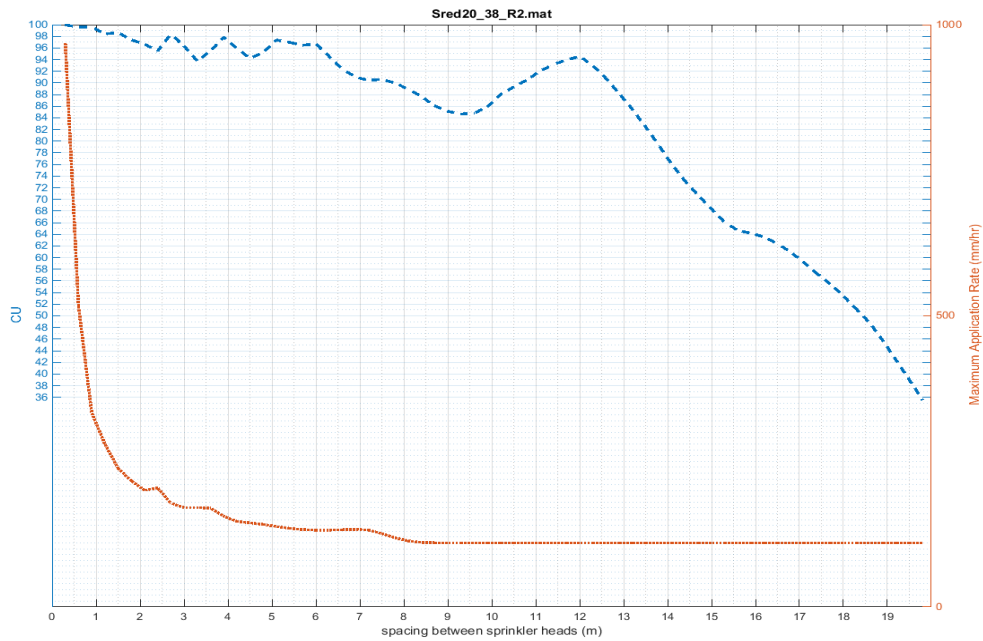
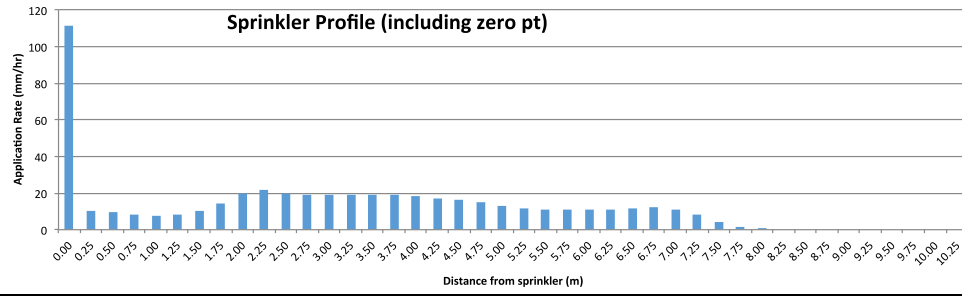
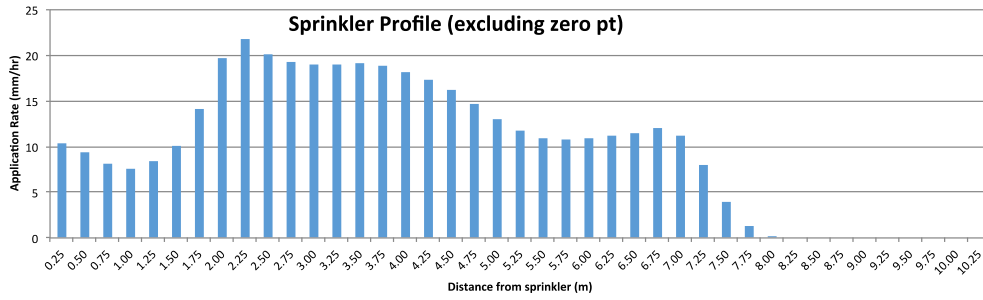
Pressures

Gauge 1 (Primary)	Wika Mechanical -100 to 250kPa
Gauge 2 (Secondary)	(0 PSI to 30 PSI)

Nelson S3000 #38 @ 20psi (red plate)

Distance (m)	Mass			Average Mass (g)	Depth (mm)	Application Rate (mm/hr)
	Can 1 (g)	Can 2 (g)	Can 3 (g)			
0.00	4059			4059	76	112
0.25	53.9	62.7	66.6	61	7	10
0.50	55.4	56.7	55.0	55.7	6.4	9.4
0.75	49.1	48.0	47.2	48.1	5.6	8.1
1.00	45.4	39.5	49.6	44.8	5.2	7.6
1.25	49.8			49.8	5.8	8.4
1.50	59.6			59.6	6.9	10.0
1.75	83.4			83.4	9.6	14.1
2.00	116.6			116.6	13.5	19.7
2.25	129.2			129.2	14.9	21.8
2.50	118.9			118.9	13.7	20.0
2.75	114.1			114.1	13.2	19.2
3.00	112.8			112.8	13.0	19.0
3.25	113.0			113.0	13.0	19.1
3.50	113.8			113.8	13.1	19.2
3.75	111.6			111.6	12.9	18.8
4.00	107.6			107.6	12.4	18.1
4.25	102.4			102.4	11.8	17.3
4.50	96.3			96.3	11.1	16.2
4.75	87.2			87.2	10.1	14.7
5.00	77.2	77.9	77.0	77.4	8.9	13.0
5.25	69.6	70.2	69.5	69.8	8.1	11.8
5.50	65.3	65.3	64.7	65.1	7.5	11.0
5.75	64.5	63.5	64.1	64.0	7.4	10.8
6.00	64.4	64.5	64.0	64.3	7.4	10.8
6.25	66.5	66.2	67.1	66.6	7.7	11.2
6.50	68.6	67.3	68.8	68.2	7.9	11.5
6.75	71.0	70.0	72.4	71.1	8.2	12.0
7.00	65.6	65.2	68.0	66.3	7.7	11.2
7.25	47.4	47.3	48.5	47.7	5.5	8.0
7.50	23.7			23.7	2.7	4.0
7.75	8.1			8.1	0.9	1.4
8.00	1.4			1.4	0.2	0.2
8.25	0.0			0.0	0.0	0.0
8.50	0.0			0.0	0.0	0.0
8.75	0.0			0.0	0.0	0.0
9.00	0.0			0.0	0.0	0.0
9.25	0.0			0.0	0.0	0.0
9.50	0.0			0.0	0.0	0.0
9.75	0.0			0.0	0.0	0.0
10.00	0.0			0.0	0.0	0.0
10.25	0.0			0.0	0.0	0.0

Nelson S3000 #38 @ 20psi (red plate)



Nelson S3000 #44 @ 25psi (red plate)

<u>Sprinkler Settings</u>		
Nozzle	44	1/128ths
Pressure	25	PSI
Sprinkler Type	S3000	(Grey Cap)
Plate Colour	Red	
Height sprinkler	2.54	m
Height catch-cans	0.1	m
Effective Height	2.44	m
Catch-can Diameter	105	mm
Catch-can Lip Thickness	0.5	mm
Zero Pot Can Diameter	260	mm

<u>Date & Duration</u>		
Test Date:	2/06/15	
	(hh:mm@24hr)	
Time Start		or Stopwatch Time
Time Finish		0:33:26
Total Time		(h:mm:ss)
Total Time (digital)	0.56	hrs

<u>Flow Rates</u>		
KENT FLOWMETER		
Flow Meter @ START	23.9887	m3
Flow Meter @ END	26.2888	m3
Av. Flow Rate	68.8	L/min
Av. Flow Rate	18.2	US GPM
ABB MAGMASTER ELECTROMAGNETIC FLOWMETER		
Velocity	6.5	m/s
Instantaneous Flow Rate	1.14	L/s @ Time
Instantaneous Flow Rate	1.14	L/s @ Time
Instantaneous Flow Rate	1.13	L/s @ Time
Av. Instantaneous Flow Rate	1.137	L/s
Equivalent Av. Flow Rate	68.2	L/min
Equivalent Av. Flow Rate	18.02	US GPM
NELSON SUPPLIED FLOW VALUES FOR GIVEN NOZZLE & PRESSURE		
Flow Rate per BTN Nozzle Chart	64.3	L/min
Flow Rate per BTN Nozzle Chart	17	US GPM

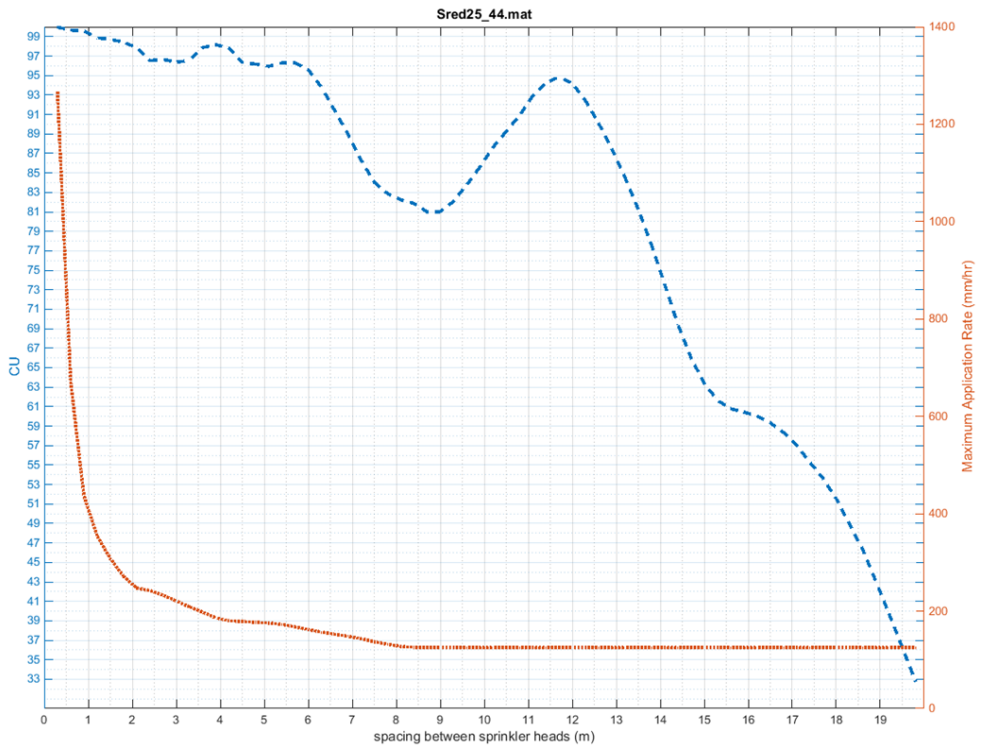
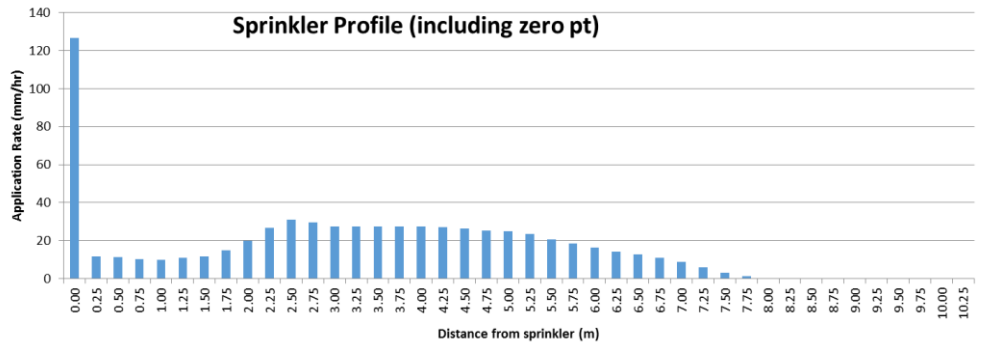
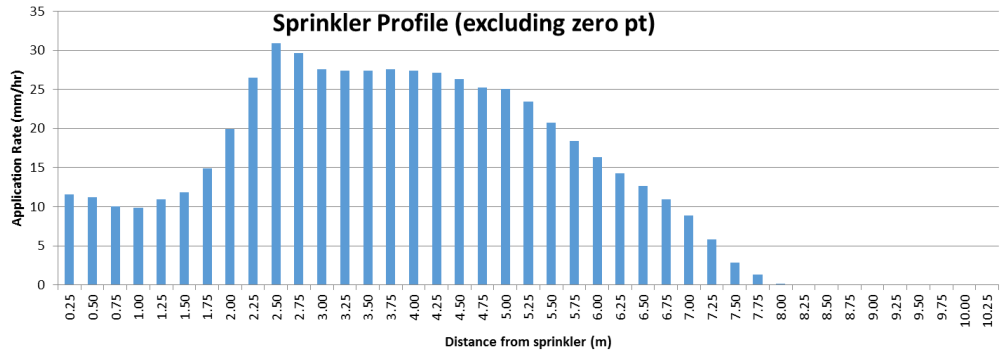
<u>Environment</u>		
Test Location?	Lab (Indoors)	
Solar Irradiance?	No	
Wind?	No	
Wind Speed (kph)	0	
Dry Bulb Air Temp (deg C)	14	
Wet Bulb Air Temp (deg C)	n/a	
Water Temp (deg C)	16	
Relative Humidity	n/a	
Av. Hourly Loss to Evaporation on 10.0mL Sample in Catch-can	0.1	ml

<u>Scales</u>		
Brand	Digitech	
Measurement Increments	0.01g (up to 1kg)	
Tolerance Checked?	Yes (May 2015)	
Tolerance	<0.03%	
Pressures		
Gauge 1 (Primary)	Wika Mechanical	100 @ 250kPa
Gauge 2 (Secondary)	(0 PSI @ 60 PSI)	

Nelson S3000 #44 @ 25psi (red plate)

Distance (m)	Mass			Average Mass (g)	Depth (mm)	Application Rate (mm/hr)
	Can 1 (g)	Can 2 (g)	Can 3 (g)			
0.00	3743			3743	70	127
0.25	45.0	68.0	55.0	56	6	12
0.50	52.0	65.0	45.0	54.0	6.2	11
0.75	48.0	38.0	60.0	48.7	5.6	10
1.00	47.0	42.0	54.0	47.7	5.5	10
1.25	53.0			53.0	6.1	11
1.50	57.0			57.0	6.6	12
1.75	72.0			72.0	8.3	15
2.00	96.0			96.0	11.1	20
2.25	128.0			128.0	14.8	27
2.50	149.0			149.0	17.2	31
2.75	143.0			143.0	16.5	30
3.00	133.0			133.0	15.4	28
3.25	132.0			132.0	15.2	27
3.50	132.0			132.0	15.2	27
3.75	133.0			133.0	15.4	28
4.00	132.0			132.0	15.2	27
4.25	131.0			131.0	15.1	27
4.50	127.0			127.0	14.7	26
4.75	122.0			122.0	14.1	25
5.00	121.0			121.0	14.0	25
5.25	113.0			113.0	13.0	23
5.50	100.0			100.0	11.5	21
5.75	89.0			89.0	10.3	18
6.00	79.0			79.0	9.1	16
6.25	69.0			69.0	8.0	14
6.50	61.0			61.0	7.0	13
6.75	53.0			53.0	6.1	11
7.00	43.0			43.0	5.0	9
7.25	28.0			28.0	3.2	6
7.50	14.0			14.0	1.6	3
7.75	6.5			6.5	0.8	1
8.00	0.7			0.7	0.1	0
8.25	0.2			0.2	0.0	0
8.50	0.0			0.0	0.0	0
8.75	0.0			0.0	0.0	0
9.00	0.0			0.0	0.0	0

Nelson S3000 #44 @ 25psi (red plate)



Nelson S3000 #38 @ 30psi (red plate)

Sprinkler Settings	
Nozzle	38 1/128ths
Pressure	30 PSI
Sprinkler Type	S3000 (Grey Cap)
Plate Colour	Red
Height Sprinkler	2.54 m
Height Catch-cans	0.1 m
Effective Height	2.44 m
Catch-can Diameter	105 mm
Catch-can Lip Thickness	0.5 mm
Zero Pot Can Diameter	260 mm

Date & Duration	
Test Date:	2/06/15 (hh:mm:24hr)
Time Start	<input type="text"/>
Time Finish	<input type="text"/>
Total Time	<input type="text"/>
or	
Stopwatch Time	0:38:53 (h:mm:ss)
Total Time (digital)	0.65 hrs

Flow Rates	
KENT FLOWMETER	
Flow Meter @ START	26.5805 m3
Flow Meter @ END	28.7072 m3
Av. Flow Rate	54.7 L/min
Av. Flow Rate	14.5 US GPM
ABB MAGMASTER ELECTROMAGNETIC FLOWMETER	
Velocity	5.1 m/s
Instantaneous Flow Rate	0.91 L/s @ Time 0:01:00
Instantaneous Flow Rate	0.91 L/s @ Time 0:17:00
Instantaneous Flow Rate	L/s @ Time <input type="text"/>
Av. Instantaneous Flow Rate	0.910 L/s
Equivalent Av. Flow Rate	54.6 L/min
Equivalent Av. Flow Rate	14.43 US GPM
NELSON SUPPLIED FLOW VALUES FOR GIVEN NOZZLE & PRESSURE	
Flow Rate per TN Nozzle Chart	52.3 L/min
Flow Rate per TN Nozzle Chart	13.8 US GPM

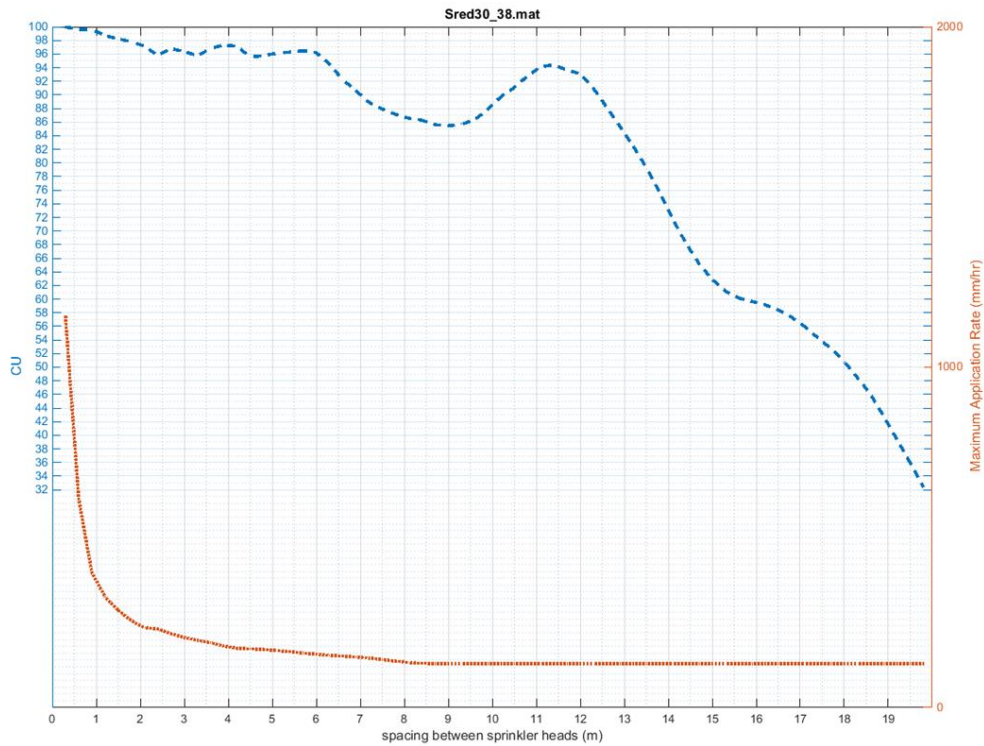
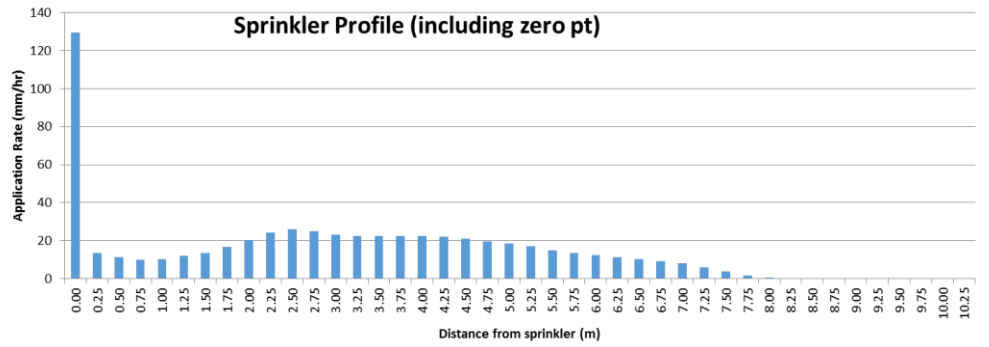
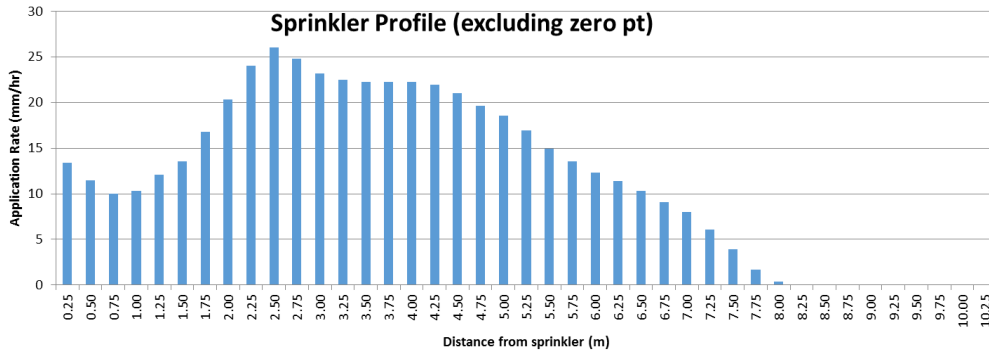
Environment	
Test Location?	Lab (Indoors)
Solar Irradiance?	No
Wind?	No
Wind Speed (kph)	0
Dry Bulb Air Temp (deg C)	15
Wet Bulb Air Temp (deg C)	n/a
Water Temp (deg C)	15
Relative Humidity	n/a
Av. Hourly Loss to Evaporation on 1.0m L Sample in Catch-can	0

Scales	
Brand	Digitech
Measurement Increments	0.01g (up to 1kg)
Tolerance Checked?	Yes (May 2015)
Tolerance	<0.03%
Pressures	
Gauge 1 (Primary)	Wika Mechanical 1-100 to 250kPa
Gauge 2 (Secondary)	(0 PSI to 30 PSI)

Nelson S3000 #38 @ 30psi (red plate)

Distance (m)	Mass			Average Mass (g)	Depth (mm)	Application Rate (mm/hr)
	Can 1 (g)	Can 2 (g)	Can 3 (g)			
0.00	4462			4462	84	130
0.25	98.0	57.0	70.0	75	9	13
0.50	85.0	58.0	50.0	64.3	7.4	11
0.75	51.0	74.0	44.0	56.3	6.5	10
1.00	56.0	52.0	65.0	57.7	6.7	10
1.25	68.0			68.0	7.9	12
1.50	76.0			76.0	8.8	14
1.75	94.0			94.0	10.9	17
2.00	114.0			114.0	13.2	20
2.25	135.0			135.0	15.6	24
2.50	146.0			146.0	16.9	26
2.75	139.0			139.0	16.1	25
3.00	130.0			130.0	15.0	23
3.25	126.0			126.0	14.6	22
3.50	125.0			125.0	14.4	22
3.75	125.0			125.0	14.4	22
4.00	125.0			125.0	14.4	22
4.25	123.0			123.0	14.2	22
4.50	118.0			118.0	13.6	21
4.75	110.0			110.0	12.7	20
5.00	104.0			104.0	12.0	19
5.25	95.0			95.0	11.0	17
5.50	84.0			84.0	9.7	15
5.75	76.0			76.0	8.8	14
6.00	69.0			69.0	8.0	12
6.25	64.0			64.0	7.4	11
6.50	58.0			58.0	6.7	10
6.75	51.0			51.0	5.9	9
7.00	45.0			45.0	5.2	8
7.25	34.0			34.0	3.9	6
7.50	22.0			22.0	2.5	4
7.75	9.4			9.4	1.1	2
8.00	2.1			2.1	0.2	0
8.25	0.0			0.0	0.0	0
8.50	0.0			0.0	0.0	0
8.75	0.0			0.0	0.0	0
9.00	0.0			0.0	0.0	0

Nelson S3000 #38 @ 30psi (red plate)



Nelson S3000 #21 @ 20psi (yellow plate)

<u>Sprinkler Settings</u>		
Nozzle	21	1/128ths
Pressure		20 PSI
Sprinkler Type		S3000 (Grey Cap)
Plate Colour	Yellow	
Height Sprinkler		2.4 m
Height Catch-cans		0.1 m
Effective Height		2.3 m
Catch-can Diameter		110 mm
Catch-can Lip Thickness		6 mm
Zero Pot Can Diameter		260 mm

<u>Date & Duration</u>		
Test Date:	11/05/15 (hh:mm@24hr)	
Time Start	11:46	or <input type="text" value="Stopwatch Time"/> (h:mm:ss)
Time Finish	12:32	
Total Time	0:46	
Total Time (digital)	0.77 hrs	

<u>Flow Rates</u>			
KENT FLOWMETER			
Flow Meter @ START	<input type="text"/>	m3	
Flow Meter @ END	<input type="text"/>	m3	
Av. Flow Rate		0.0 L/min	
Av. Flow Rate		0.0 US GPM	
ABB MAGMASTER ELECTROMAGNETIC FLOWMETER			
Velocity	<input type="text"/>	m/s	
Instantaneous Flow Rate	<input type="text"/>	L/s	@ Time <input type="text"/>
Instantaneous Flow Rate	<input type="text"/>	L/s	@ Time <input type="text"/>
Instantaneous Flow Rate	<input type="text"/>	L/s	@ Time <input type="text"/>
Av. Instantaneous Flow Rate		#DIV/0! L/s	
Equivalent Av. Flow Rate		#DIV/0! L/min	
Equivalent Av. Flow Rate		#DIV/0! US GPM	
NELSON SUPPLIED FLOW VALUES FOR GIVEN NOZZLE @ PRESSURE			
Flow Rate per BTN Nozzle Chart	12.7	L/min	
Flow Rate per BTN Nozzle Chart	<input type="text"/>	US GPM	

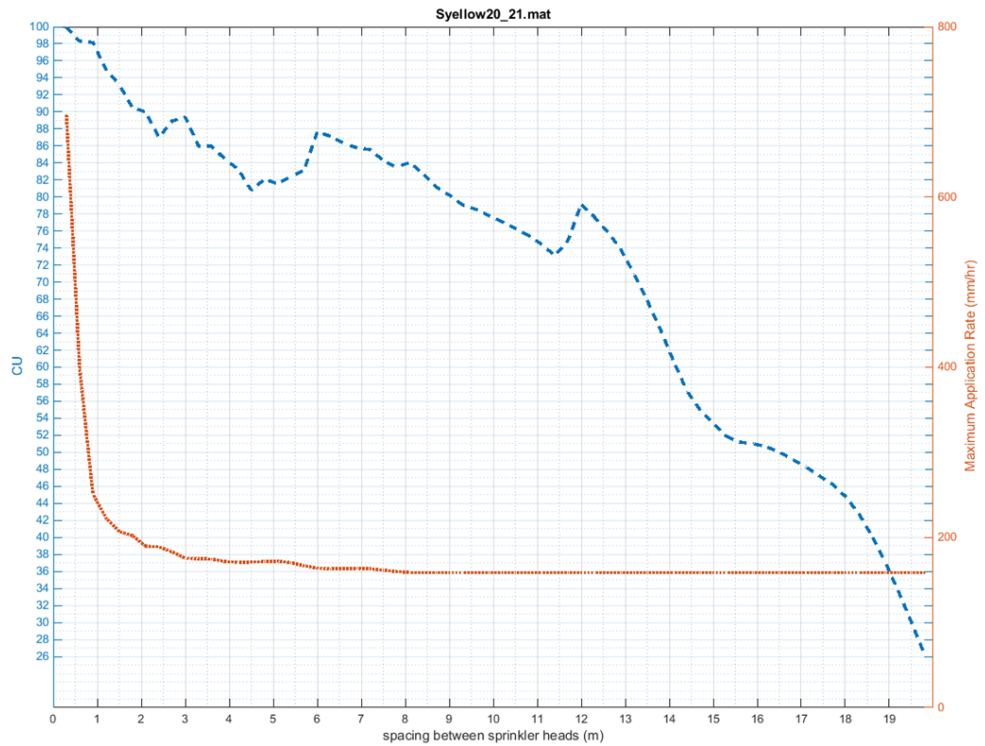
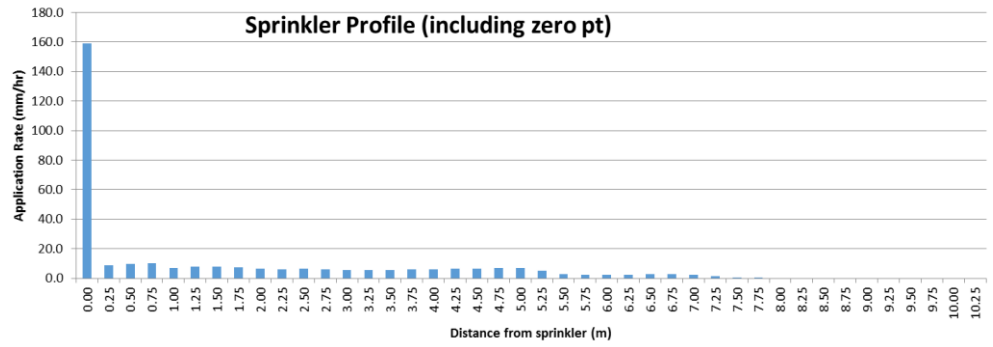
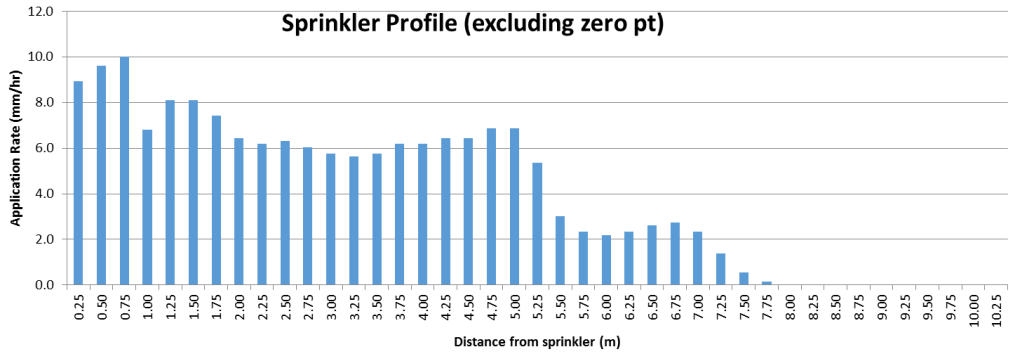
<u>Environment</u>	
Test Location?	Lab (Indoors)
Solar Irradiance?	No
Wind?	No
Wind Speed (kph)	0
Dry Bulb Air Temp (deg C)	17
Wet Bulb Air Temp (deg C)	n/a
Water Temp (deg C)	15
Relative Humidity	n/a
Av. Hourly Loss to Evaporation on 10.0mL Sample in Catch-can	0

<u>Scales</u>	
Brand	Digitech
Measurement Increments	0.01g (up to 1kg)
Tolerance Checked?	Yes (May 2015)
Tolerance	<0.03%
Pressures	
Gauge 1 (Primary)	Wika Mechanical -100 @ 250kPa
Gauge 2 (Secondary)	(0 PSI @ 60 PSI)

Nelson S3000 #21 @ 20psi (yellow plate)

Distance (m)	Mass			Average Mass (g)	Depth (mm)	Application Rate (mm/hr)
	Can 1 (g)	Can 2 (g)	Can 3 (g)			
0.00	6475			6475	122	159.1
0.25	67	65	63	65	7	8.9
0.50	70	68	72	70.0	7.4	9.6
0.75	76	73	70	73.0	7.7	10.0
1.00	48	51	50	49.7	5.2	6.8
1.25	59			59.0	6.2	8.1
1.50	59			59.0	6.2	8.1
1.75	54			54.0	5.7	7.4
2.00	47			47.0	4.9	6.5
2.25	45			45.0	4.7	6.2
2.50	46			46.0	4.8	6.3
2.75	44			44.0	4.6	6.0
3.00	42			42.0	4.4	5.8
3.25	41			41.0	4.3	5.6
3.50	42			42.0	4.4	5.8
3.75	45			45.0	4.7	6.2
4.00	45			45.0	4.7	6.2
4.25	47			47.0	4.9	6.5
4.50	47			47.0	4.9	6.5
4.75	50			50.0	5.3	6.9
5.00	50			50.0	5.3	6.9
5.25	39			39.0	4.1	5.4
5.50	22			22.0	2.3	3.0
5.75	17			17.0	1.8	2.3
6.00	16			16.0	1.7	2.2
6.25	17			17.0	1.8	2.3
6.50	19			19.0	2.0	2.6
6.75	20			20.0	2.1	2.7
7.00	17			17.0	1.8	2.3
7.25	10			10.0	1.1	1.4
7.50	4			4.0	0.4	0.5
7.75	1			1.0	0.1	0.1
8.00	0			0.0	0.0	0.0
8.25	0			0.0	0.0	0.0
8.50	0			0.0	0.0	0.0
8.75	0			0.0	0.0	0.0
9.00	0			0.0	0.0	0.0

Nelson S3000 #21 @ 20psi (yellow plate)



Appendix E: Field Data

Raw data from the nine pairs of field tests using the sprinkler infiltrometer (bucket infiltrometer) in Test A and the mobile sprinkler rig in Test B are tabled here.

Test 1A		Application Rate: 178 mm/hr			
		Plot Area: 0.0638 m ²			
t (min)	runoff for period (ml)	runoff cumulative (ml)	runoff cumulative (m³)	runoff cumulative (mm)	cumulative infiltration (mm)
0	0	0	0	0	0
3	28	28	0.00003	0.4	8.5
6	234	262	0.00026	4.1	13.7
9	250	512	0.00051	8.0	18.7
12	230	742	0.00074	11.6	24.0
15	170	912	0.00091	14.3	30.2
18	180	1092	0.00109	17.1	36.3
21	190	1282	0.00128	20.1	42.2
24	194	1476	0.00148	23.1	48.1
27	152	1628	0.00163	25.5	54.6
30	184	1812	0.00181	28.4	60.6
33	230	2042	0.00204	32.0	65.9
36	222	2264	0.00226	35.5	71.3
39	217	2481	0.00248	38.9	76.8
42	253	2734	0.00273	42.9	81.7
45	282	3016	0.00302	47.3	86.2
48	311	3327	0.00333	52.2	90.2
51	270	3597	0.00360	56.4	94.9
54	260	3857	0.00386	60.5	99.7
57	196	4053	0.00405	63.5	105.6
60	174	4227	0.00423	66.3	111.7

Test 1B					
	Total Runoff (ml)	Total Runoff (mm)	Speed of Rig (m/min)	Nozzle Size (3TN)	Pressure (psi)
	2000	3.6	0.6	44	6

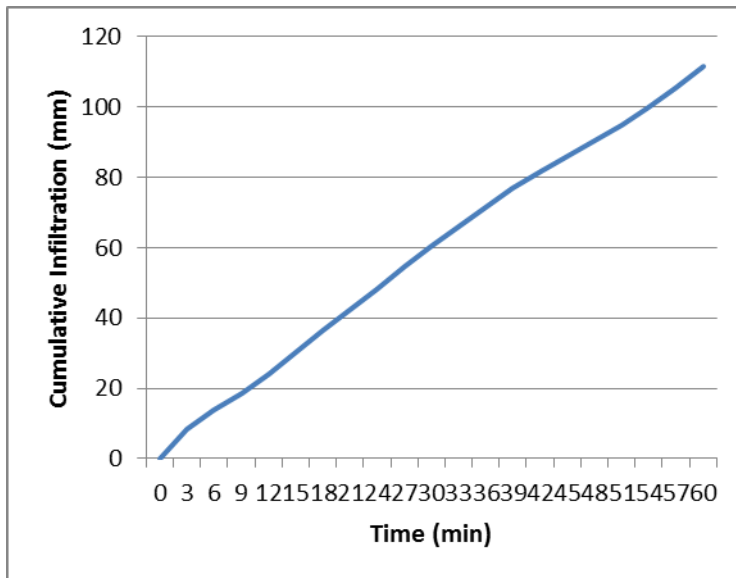


Figure E-1: I vs t plot for Test 1A.

Test 2A		Application Rate: 178 mm/hr			
		Plot Area: 0.0638 m ²			
t	runoff	runoff	runoff	runoff	cumulative
	for period	cumulative	cumulative	cumulative	infiltration
(min)	(ml)	(ml)	(m³)	(mm)	(mm)
0	0	0	0	0	0
3	26	26	0.00003	0.4	8.5
6	162	188	0.00019	2.9	14.9
9	190	378	0.00038	5.9	20.8
12	194	572	0.00057	9.0	26.6
15	211	783	0.00078	12.3	32.2
18	212	995	0.00100	15.6	37.8
21	263	1258	0.00126	19.7	42.6
24	268	1526	0.00153	23.9	47.3
27	296	1822	0.00182	28.6	51.5
30	260	2082	0.00208	32.6	56.4
33	323	2405	0.00241	37.7	60.2
36	340	2745	0.00275	43.0	63.8
39	344	3089	0.00309	48.4	67.3
42	338	3427	0.00343	53.7	70.9
45	341	3768	0.00377	59.1	74.4
48	340	4108	0.00411	64.4	78.0
51	331	4439	0.00444	69.6	81.7
54	338	4777	0.00478	74.9	85.3
57	328	5105	0.00511	80.0	89.1
60	337	5442	0.00544	85.3	92.7

Test 2B					
	Total Runoff (ml)	Total Runoff (mm)	Speed of Rig (m/min)	Nozzle Size (3TN)	Pressure (psi)
	3050	5.4	0.6	44	6

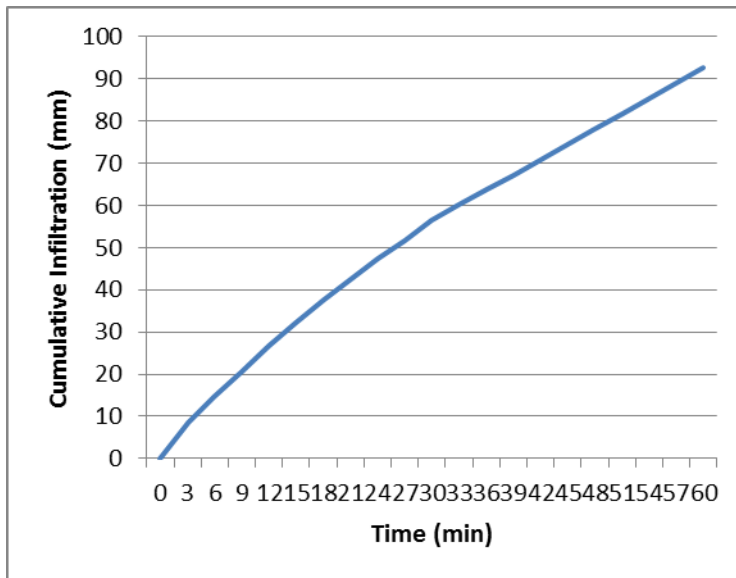


Figure E-2: I vs t plot for Test 2A.

Test 3A		Application Rate: 178 mm/hr Plot Area: 0.0638 m ²			
t	runoff	runoff	runoff	runoff	cumulative
(min)	for period	cumulative	cumulative	cumulative	infiltration
	(ml)	(ml)	(m³)	(mm)	(mm)
0	0	0	0	0	0
3	5	5	0.00001	0.1	8.8
6	130	135	0.00014	2.1	15.7
9	231	366	0.00037	5.7	21.0
12	225	591	0.00059	9.3	26.3
15	366	957	0.00096	15.0	29.5
18	274	1231	0.00123	19.3	34.1
21	275	1506	0.00151	23.6	38.7
24	280	1786	0.00179	28.0	43.2
27	285	2071	0.00207	32.5	47.6
30	315	2386	0.00239	37.4	51.6
33	278	2664	0.00266	41.8	56.1
36	311	2975	0.00298	46.6	60.2
39	300	3275	0.00328	51.3	64.4
42	291	3566	0.00357	55.9	68.7
45	284	3850	0.00385	60.4	73.1

Test 3B					
Total Runoff (ml)	Total Runoff (mm)	Speed of Rig (m/min)	Nozzle Size (3TN)	Pressure (psi)	
5200	9.2	0.6	44	6	

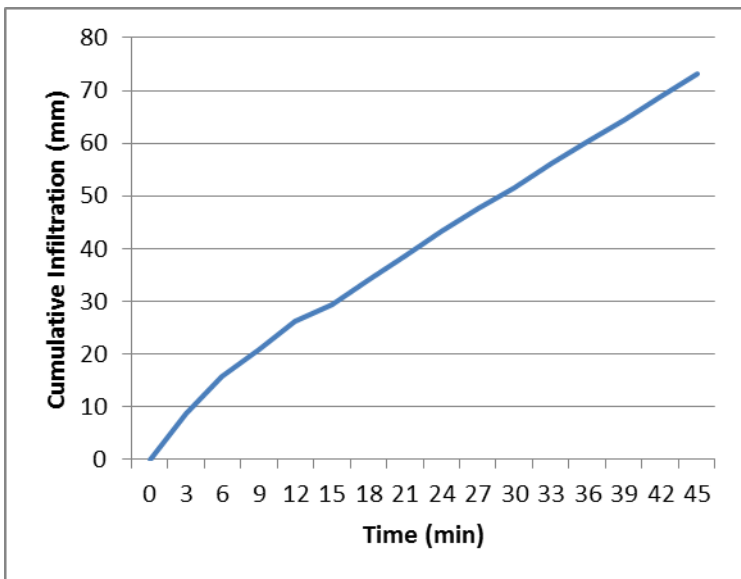


Figure E-3: I vs t plot for Test 3A.

Test 4A		Application Rate: 178 mm/hr Plot Area: 0.0638 m ²			
t	runoff for period	runoff cumulative	runoff cumulative	runoff cumulative	cumulative infiltration
(min)	(ml)	(ml)	(m ³)	(mm)	(mm)
0	0	0	0	0	0
3	76	76	0.00008	1.2	7.7
6	317	393	0.00039	6.2	11.6
9	337	730	0.00073	11.4	15.3
12	387	1117	0.00112	17.5	18.1
15	374	1491	0.00149	23.4	21.1
18	384	1875	0.00188	29.4	24.0
21	350	2225	0.00223	34.9	27.4
24	337	2562	0.00256	40.2	31.0
27	360	2922	0.00292	45.8	34.3
30	372	3294	0.00329	51.6	37.4
33	352	3646	0.00365	57.2	40.7
36	346	3992	0.00399	62.6	44.2
39	331	4323	0.00432	67.8	47.9
42	343	4666	0.00467	73.1	51.5
45	344	5010	0.00501	78.5	55.0

Test 4B					
	Total Runoff (ml)	Total Runoff (mm)	Speed of Rig (m/min)	Nozzle Size (3TN)	Pressure (psi)
	8150	14.5	0.6	44	6

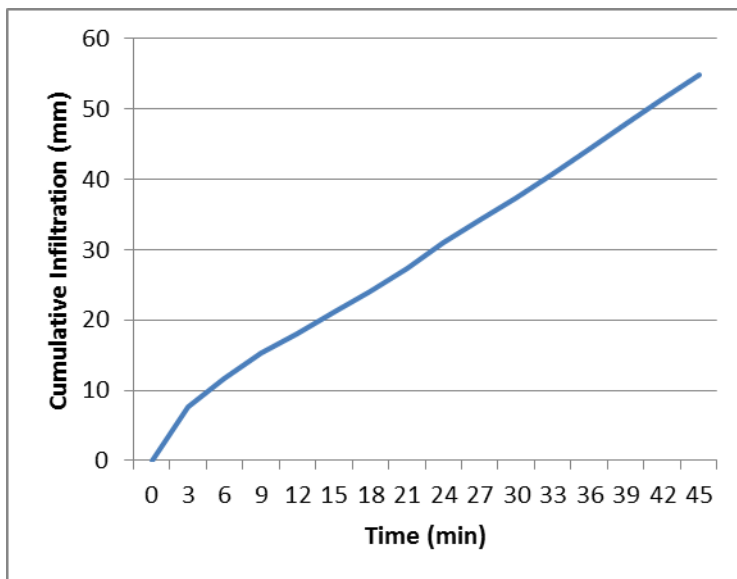


Figure E-4: I vs t plot for Test 4A.

Test 5A		Application Rate: 178 mm/hr Plot Area: 0.0638 m ²			
t	runoff for period	runoff cumulative	runoff cumulative	runoff cumulative	cumulative infiltration
(min)	(ml)	(ml)	(m ³)	(mm)	(mm)
0	0	0	0	0	0
3	50	50	0.00005	0.8	8.1
6	190	240	0.00024	3.8	14.0
9	311	551	0.00055	8.6	18.1
12	284	835	0.00084	13.1	22.5
15	275	1110	0.00111	17.4	27.1
18	260	1370	0.00137	21.5	31.9
21	267	1637	0.00164	25.7	36.6
24	256	1893	0.00189	29.7	41.5
27	214	2107	0.00211	33.0	47.1
30	250	2357	0.00236	36.9	52.1
33	253	2610	0.00261	40.9	57.0
36	253	2863	0.00286	44.9	61.9
39	253	3116	0.00312	48.8	66.9
42	293	3409	0.00341	53.4	71.2
45	251	3660	0.00366	57.4	76.1

Test 5B					
Total Runoff (ml)	Total Runoff (mm)	Speed of Rig (m/min)	Nozzle Size (3TN)	Pressure (psi)	
6100	10.8	0.6	32	6	

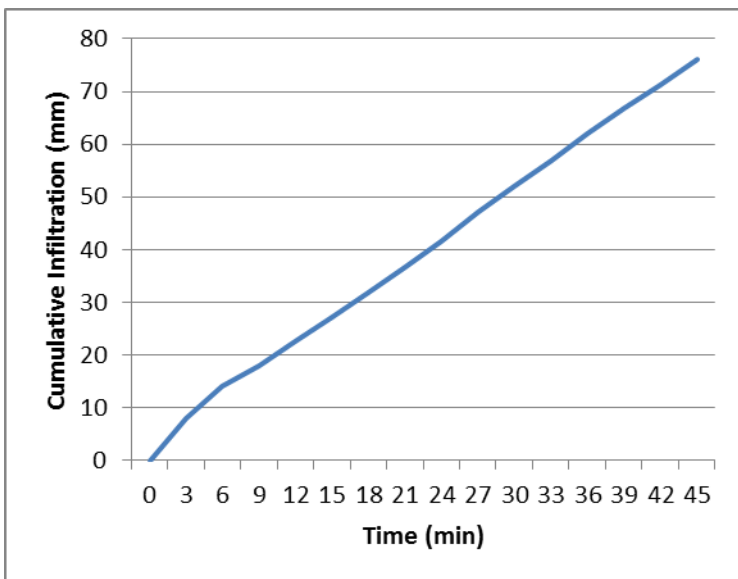


Figure E-5: I vs t plot for Test 6A.

Test 6A

Application Rate:	178 mm/hr
Plot Area:	0.0638 m ²

t (min)	runoff for period (ml)	runoff cumulative (ml)	runoff cumulative (m3)	runoff cumulative (mm)	infiltration cumulative (mm)
0	0	0	0	0	0
3	163	163	0.00016	3	6
6	182	345	0.00035	5	12
9	198	543	0.00054	9	18
12	236	779	0.00078	12	23
15	246	1025	0.00103	16	28
18	233	1258	0.00126	20	34
21	223	1481	0.00148	23	39
24	225	1706	0.00171	27	44
27	202	1908	0.00191	30	50
30	235	2143	0.00214	34	55
33	192	2335	0.00234	37	61
36	200	2535	0.00254	40	67
39	140	2675	0.00268	42	74
42	166	2841	0.00284	45	80
45	185	3026	0.00303	47	86

Test 6B

Total Runoff (ml)	Total Runoff (mm)	Speed of Rig (m/min)	Nozzle Size (3TN)	Pressure (psi)
5100	9.1	0.6	44	6

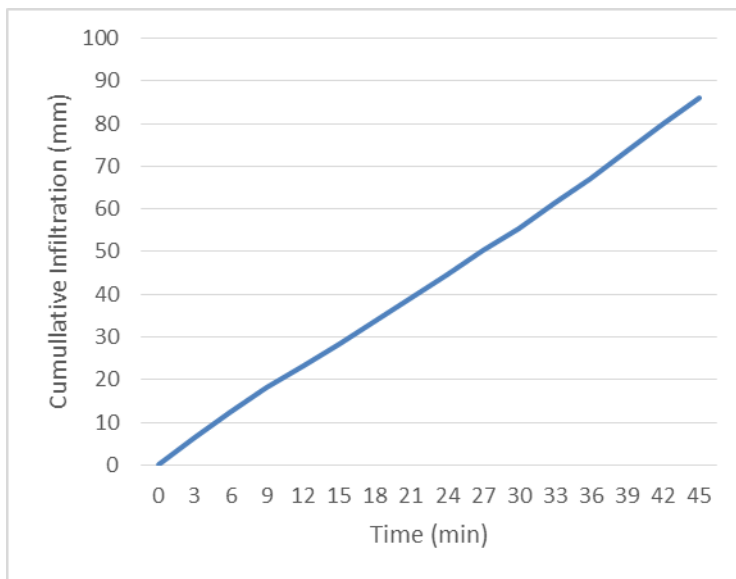


Figure E-6: I vs t plot for Test 6A.

Test 7Ae		Application Rate: 178 mm/hr			
		Plot Area: 0.0638 m ²			
t	runoff	runoff	runoff	runoff	cumulative
(min)	for period	cumulative	cumulative	cumulative	infiltration
	(ml)	(ml)	(m ³)	(mm)	(mm)
0	0	0	0	0	0
3	94	94	0.00009	1.5	7.4
6	211	305	0.00031	4.8	13.0
9	222	527	0.00053	8.3	18.4
12	217	744	0.00074	11.7	23.9
15	265	1009	0.00101	15.8	28.7
18	249	1258	0.00126	19.7	33.7
21	243	1501	0.00150	23.5	38.8
24	229	1730	0.00173	27.1	44.1
27	205	1935	0.00194	30.3	49.8
30	208	2143	0.00214	33.6	55.4
33	199	2342	0.00234	36.7	61.2
36	192	2534	0.00253	39.7	67.1
39	254	2788	0.00279	43.7	72.0
42	240	3028	0.00303	47.5	77.1
45	231	3259	0.00326	51.1	82.4

Test 7Be					
Total	Total	Speed of	Nozzle Size	Pressure	
Runoff	Runoff	Rig	(3TN)	(psi)	
(ml)	(mm)	(m/min)			
5850	10.4	0.6	44	6	

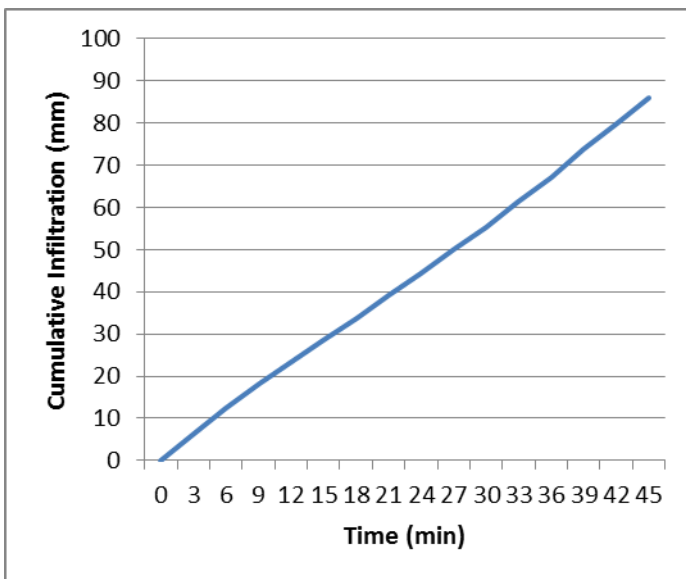


Figure E-7: I vs t plot for Test 7A.

Test 8A		Application Rate: 178 mm/hr			
		Plot Area: 0.0638 m ²			
t	runoff	runoff	runoff	runoff	cumulative
(min)	for period	cumulative	cumulative	cumulative	infiltration
	(ml)	(ml)	(m ³)	(mm)	(mm)
0	0	0	0	0	0
3	110	110	0.00011	1.7	7.2
6	119	229	0.00023	3.6	14.2
9	176	405	0.00041	6.3	20.4
12	275	680	0.00068	10.7	24.9
15	206	886	0.00089	13.9	30.6
18	233	1119	0.00112	17.5	35.9
21	197	1316	0.00132	20.6	41.7
24	218	1534	0.00153	24.0	47.2
27	230	1764	0.00176	27.7	52.4
30	185	1949	0.00195	30.6	58.4
33	172	2121	0.00212	33.2	64.7
36	205	2326	0.00233	36.5	70.3
39	248	2574	0.00257	40.3	75.4
42	246	2820	0.00282	44.2	80.4
45	251	3071	0.00307	48.1	85.4
Test 8B					
	Total	Total	Speed of	Nozzle Size	Pressure
	Runoff	Runoff	Rig	(3TN)	(psi)
	(ml)	(mm)	(m/min)		
	6000	10.7	0.61	44	6

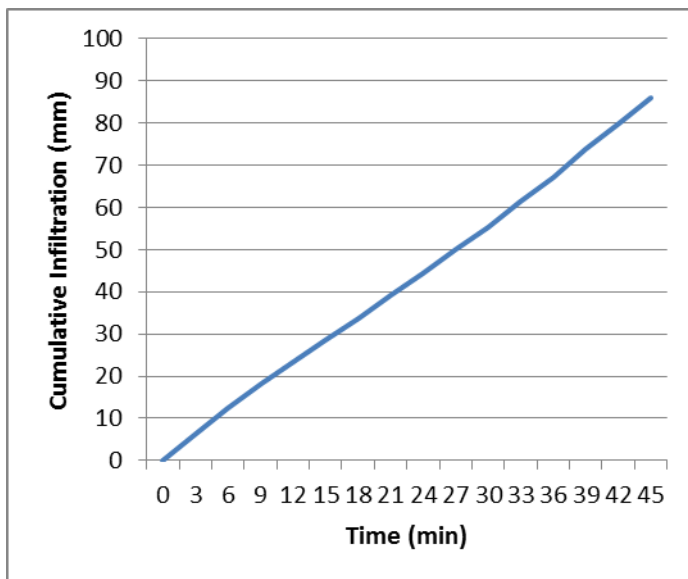


Figure E-83: I vs t plot for Test 8A.

Test 9A		Application Rate: 150 mm/hr			
		Plot Area: 0.0638 m ²			
t	runoff	runoff	runoff	runoff	cumulative
(min)	for period	cumulative	cumulative	cumulative	infiltration
	(ml)	(ml)	(m ³)	(mm)	(mm)
0	0	0	0	0	0
3	14	14	0.00001	0.2	7.3
6	81	95	0.00010	1.5	13.5
9	145	240	0.00024	3.8	18.7
12	132	372	0.00037	5.8	24.2
15	166	538	0.00054	8.4	29.1
18	187	725	0.00073	11.4	33.6
21	194	919	0.00092	14.4	38.1
24	250	1169	0.00117	18.3	41.7
27	212	1381	0.00138	21.6	45.9
30	195	1576	0.00158	24.7	50.3
33	188	1764	0.00176	27.7	54.8
36	224	1988	0.00199	31.2	58.8
39	196	2184	0.00218	34.2	63.3
42	200	2384	0.00238	37.4	67.6
45	207	2591	0.00259	40.6	71.9

Test 9B					
Total	Total	Speed of	Nozzle Size	Pressure	
Runoff	Runoff	Rig	(3TN)	(psi)	
(ml)	(mm)	(m/min)			
4950	8.8	0.61	44	6	

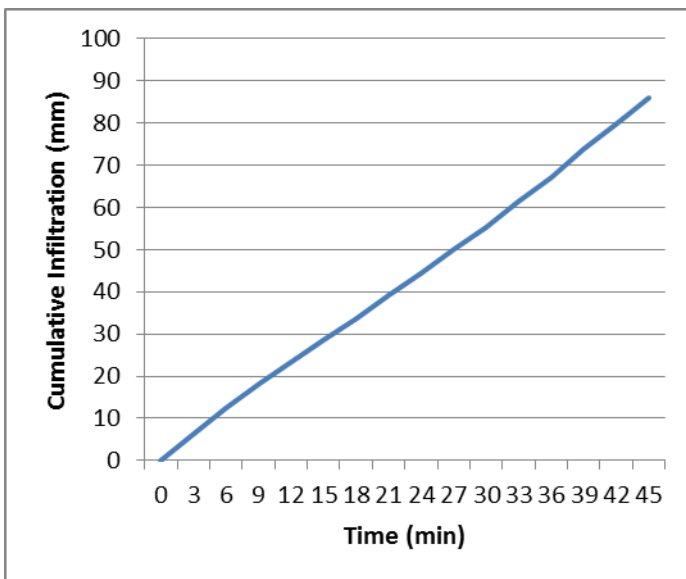


Figure E-9: I vs t plot for Test 9A.

Appendix F - Project Administration

F1. Project Risk Management

Separate risk assessments were conducted for the laboratory work and for the field work.

Z113 Hydraulics Lab Risk Assessment

Hazards

1. Wet floor: The risk of slipping was assessed as ‘possible’ with possibly minor injury from a fall. Thus the risk level was deemed MODERATE. Existing controls included built-in drainage and non-slip floor surface. Additional controls to put in place included placing ‘Wet Floor’ signage in prominent positions; wear sturdy footwear with non-slip tread; reduce size of wet area by screening off the sprinkler head; and no running.
2. Pump machinery: The risk of injury from moving pump machinery was assessed as ‘unlikely’ with possibly moderate injury. Thus the risk level was deemed LOW. Existing controls included housing the pumps in a separate pump room, or housing the smaller pump within a protective cover that prevents contact with any moving parts. Additional controls to put in place include locating the smaller pump away from trafficked areas and away from work spaces.
3. Electrical equipment: The risk of electrical injury was assessed as ‘unlikely’ with possible major or catastrophic consequences. Thus the risk level was deemed moderate. Existing controls include USQ tagged and tested electrical pumps and leads being used; IP67 switch boxes in place where electrical pumps need to be switched on/off; weather-proof powerpoint covers where leads are plugged in. Additional controls include routing power leads so that they are not lying in water at any time and are behind screens so that they are not splashed; turning off power leads which are not in use.

Field Work

Hazards

1. Pump machinery: The risk of injury from moving pump machinery was assessed as ‘unlikely’ with possibly moderate injury. Thus the risk level was deemed LOW. Existing controls include housing the pump within a protective cover that prevents contact with any moving parts. Additional controls to put in place include locating the pump behind a chain fence so that it cannot be accessed except by person’s possessing a key.
2. Electrical supply to pump: The risk of electrical injury was assessed as ‘unlikely’ with possible major or catastrophic consequences. Thus the risk level was deemed MODERATE. Existing controls include having safety switches on the power box; having the power sockets housed inside weather-proof casings that are positioned well above the ground; having the electrical box fenced off so that persons passing by cannot interact with the equipment; using USQ tagged and tested leads and pumps. Additional controls include positioning pumps well away from where water from the sprinklers will be spraying; keeping power leads and connections away from where the ground may become wet.
3. Tall test rig: The risk of falling during construction is assessed as possible with minor consequences. Thus the risk level is deemed MODERATE. There are no existing controls. Additional controls are to assemble as much of the test rig at ground level first; use a sturdy step ladder with an assistant to stabilise the ladder; design the test rig so that minimal work is required from the ladder; limit the test rig to approx. 3m total height so that the height stood on the step ladder will not need to exceed 1.6m.
4. Cold weather: The risk of hypothermia due to cold weather and getting wet from spraying sprinklers is assessed as ‘rare’ with possible insignificant injury. Thus the risk level is deemed LOW. No controls are in place. Additional controls include not performing outdoor tests in windy conditions; rain jacket and rain pants.

F2. Project Planning: Timelines, Resource Requirements

	date due	date actual finish	done?	hours planned 347	hours actual 389	resources required	cost (budg) 1310	cost (actual) 1903
PROJECT PLANNING DELIVERABLES								
Project Proposal	11-Mar	6-Mar	Y	1	1		0	0
Project Specification	18-Mar	16-Mar	Y	2	2		0	0
Project Management Plan	1-Apr	20-Mar	Y	2	2		0	0
Preliminary Report	3-Jun	3-Jun	Y	20	15		0	0
Partial Draft Dissertation	16-Sep	16-Sep	Y	15	30		0	0
DISSERTATION								
CANDIDATES CERTIFICATION	3-Jun	3-Jun	Y	1	1		0	0
ABSTRACT	29-Oct	21-Oct	Y	2	1		0	0
ACKNOWLEDGEMENTS	29-Oct	21-Oct	Y	1	1		0	0
LISTS OF FIGS, TABLES, APPENDICES, ABBREVIATIONS	29-Oct	21-Oct	Y	2	1		0	0
CHAPTER 1: INTRODUCTION	16-Sep	5-Jul	Y	5	4		0	0
CHAPTER 2: LITERATURE REVIEW	3-Jun	5-Jul	Y	40	60		0	43
CHAPTER 3: RESEARCH DESIGN & METHODOLOGY	16-Sep	16-Sep	Y					
Write computer model to compute GAML		24-Apr	Y			Matlab (student version)	60	60
Load field data		20-Apr	Y	1	1		0	0
Generate single sprinkler pattern		20-Apr	Y	8	11		0	0
Overlapping sprinklers		1-May	Y	5	5		0	0
Data extraction: i vs t , i vs l , r vs R , l vs t , i - r		20-Apr	Y	15	16		0	0
What if scenarios		n/a	N	5	0		0	0
Laboratory testing of sprinkler equipment		30-Jun	Y	15	40	various equipment, most from NCEA	200	500
Write up results		30-Jun	Y	8	8		0	0
Desktop testing of computer model		1-Sep	Y	10	6		0	0
Field testing of computer model		12-Sep	Y				0	0
Construct field test rig		10-Jul	Y	8	16	materials as per test rig design	1000	900
Ponded Ring Infiltrometer tests for comparison		n/a	N	8	0	rings from NCEA, make Mariotte bottles	50	0
Field static tests		14-Aug	Y	16	30	use field test rig	0	300
Field moving tests		14-Aug	Y	16	30	use field test rig	0	100
Write-up & proofing		10-Sep	Y	12	16		0	0
CHAPTER 4: RESULTS AND DISCUSSION	29-Oct	21-Oct	Y					
Data analysis and plotting		14-Oct	Y	16	8		0	0
Comparisons of model and field data		16-Oct	Y	8	4		0	0
What if scenarios		n/a	N	8	0		0	0
Discussion		21-Oct	Y	16	6		0	0
Write-up and Proofing		21-Oct	Y	12	10		0	0
CHAPTER 5: CONCLUSIONS & FURTHER WORK	29-Oct	19-Oct	Y	5	6		0	0
APPENDICES	29-Oct	19-Oct	Y				0	0
Chu's Method		5-Oct	Y	2	2		0	0
Risk Assessment	3-Jun	15-Mar	Y	1	1		0	0
Matlab code		3-Jun	Y	1	2		0	0
Project Specification and Project Management Plan	3-Jun	3-Jun	Y	1	3		0	0
REFERENCES	16-Sep	5-Jul	Y	2	2		0	0
PRESENTATION								
POWERPOINT PRESENTATION	21-Sep	16-Sep	Y	10	5		0	0
TRANSCRIPT / SPEAKER NOTES	21-Sep	16-Sep	Y	5	2		0	0
REHEARSAL	18-Sep	16-Sep	Y	2	1		0	0
PROJECT CONFERENCE ATTENDANCE	21-Sep	24-Sep	Y	40	40		0	0

F3. Consequential Effects of the Project

Four hypothetical scenarios are envisaged to possibly follow from the project. Whilst Scenario 1 is clearly preferred, the consequential effects of both Scenarios 1 and 3 are agreeable.

Scenario 1

The proposed model and the results and conclusions are valid and accurate AND the report is used as its purpose was intended by the author (i.e. as an educational exercise, as per the report's disclaimer).

Possible Consequences

A reader of the dissertation might well become interested in the model, results and conclusions but will understand that the production of the dissertation was an educational exercise at an undergraduate level and thus may be without the rigor or controls that should characterise published work at higher levels or in a professional context. The ideas and positive results reported in the dissertation may, however, legitimately act as an impetus for further study and research into the topic area, either by the author or by a reader.

Scenario 2

The proposed model and the results and conclusions are valid and accurate AND the report is not used as its purpose was intended by the author (i.e. as an educational exercise, as per the report's disclaimer).

Possible Consequences

The results and conclusions might end up being inappropriately applied to 'real-life' situations either directly by the author, by recommendation to another person, or through hear-say. However, a) the results and conclusions reported in the dissertation might be peculiar to the particular testing scenario; b) assumptions may have been made explicitly, implicitly or even unwittingly, that render the results and conclusions inappropriate for many 'real-life' applications; c) the dissertation probably is unlikely to feature the rigor and controls to ensure the quality and reliability of the results and conclusions. Inappropriate use of the contents of the study may end up being of little consequence, but it is conceivable that physical and financial losses and a loss of reputation to those who names have been associated with the study could result.

Scenario 3

The proposed model and the results and conclusions are not valid or accurate AND the report is used as its purpose was intended by the author (i.e. as an educational exercise, as per the report's disclaimer)

Possible Consequences

The value of this study (as an educational exercise) lies in the process learned rather than the results per se. Thus the consequence in Scenario 3 can still be positive for the author of the study. Also, in this Scenario, if the project serves to demonstrate that the proposed model does not, in fact, work then this may be of benefit to others who might be considering the same.

Scenario 4

The proposed model and the results and conclusions are not valid or accurate AND the report is not used as its purpose was intended by the author (i.e. as an educational exercise, as per the report's disclaimer).

Possible Consequences

Clearly this is the worst Scenario and would conceivably only occur as a result of poor judgement and foolishness on the part of the person using the report. The potential consequences may reflect those of Scenario 2, but could well be worse.

